



UNIVERSITAT POLITÈCNICA
DE CATALUNYA

Master Thesis

ENERGY-EFFICIENT DYNAMIC RESOURCE
ALLOCATION WITH ENERGY HARVESTING NODES

Author: Javier Rubio López

Advisor: Dr. Antonio Pascual Iserte

Array and Multichannel Processing Group
Department of Signal Theory and Communications
Universitat Politècnica de Catalunya

Barcelona, July 2012

A mis padres,

Abstract

In wireless communications, there is a trend to deploy shorter-distance networks to cope with the high demanding necessities of bit-rate that current applications require. In such networks, the power needed for transmission is considerably low, due to proximity between base station and mobile terminals. As a consequence, complex baseband algorithms for signal processing and radio frequency circuitry require an amount of power that is comparable or even higher than the power for transmission. Moreover, energy harvesting techniques, which allows user to collect energy from the environment, are being emerged as a potential solution for battery durability.

In this master thesis, the allocation of radio resources in such a scenario is addressed. Nodes are considered to be battery-powered devices with an energy harvesting source that allows them to recharge their batteries. Nodes feed back their battery status information jointly with the channel state information to the scheduler, which makes a resource allocation based on all the energy constraints of the problem and not only taking the transmitted power and the channel state information as in classical approaches.

The final objective is to carry out a design of scheduling algorithms able to provide a longer lifetime network, where lifetime is defined to be the period of time till the first node runs out of battery.

In the first part of the thesis we consider some simplifications. Flat-fading channels are assumed and the classical rate-power Shannon's formula is used. As a result, continuous bandwidth and power assignment as well as Gaussian constellations are considered. Resource allocation problems are reformulated as convex optimization problems, which are solved using powerful software packages, or algorithms based on Lagrange duality developed in this master thesis

In the second part of the thesis, a more practical approach is carried out. Now, finite-size constellations, such as QAM constellations are considered. Therefore, a discrete rate-

power function based on BER requirements is proposed. Generally, these allocation problems are integer combinatorial and thus non-convex. Optimum solutions are computationally prohibited due to brute force search time consuming techniques. We propose greedy-like algorithms to cope this problem, where subcarriers, bit allocation and power are assigned dynamically, according to a given objective and energy constraints.

From simulation results, we conclude that by using the techniques proposed in the master thesis, not only it is possible to enhance the network lifetime, but also the average bit-rate achieved by the network terminals compared with classical approaches.

Resumen

Existe una tendencia en comunicaciones sin cables a desplegar redes para cubrir distancias más cortas, con el objetivo de cubrir las necesidades de bit-rate que requieren las actuales aplicaciones. Sin embargo, en tales redes, la potencia necesaria en la transmisión es considerablemente baja, debido a la proximidad entre la estación base y los terminales móviles. Como consecuencia, los complejos algoritmos de procesamiento de señal de banda base y los circuitos de radio frecuencia requieren un consumo energético comparable o incluso mayor que el necesario en transmisión. Además, técnicas de *harvesting* están siendo desarrolladas como soluciones potenciales a incrementar la durabilidad de las baterías.

En esta tesis de máster, se lleva a cabo el diseño de asignación de recursos radio en el escenario planteado anteriormente. Los terminales se consideran dispositivos con batería finita, previstos de una fuente de *harvesting* de energía que les permite recargar las baterías cada cierto tiempo. Los terminales envían sus estados de las baterías junto con la estimación del canal al *scheduler*. Éste realiza una asignación de recursos teniendo en cuenta todo el gasto energético, tanto de los algoritmos de procesamiento de señal como de la circuitería de radio frecuencia además de la potencia en transmisión, y no sólo de ésta última junto con la estimación del canal, como sucede en diseños clásicos.

El objetivo final es llevar a cabo el diseño de algoritmos de *scheduling* que sean capaces de alargar la vida útil de la red, donde vida útil se define como el periodo de tiempo transcurrido hasta que el primer terminal se queda sin batería.

En la primera parte de la tesis se asumen algunas simplificaciones. Canales planos en frecuencia y la función continua de Shannon que relaciona bit-rate y potencia son utilizados. Como resultado, asignación continua de ancho de banda y potencia, además de constelaciones Gaussianas, son consideradas. Los problemas de asignación de recursos son reformulados como problemas de optimización convexa, los cuales son resueltos mediante paquetes de software o algoritmos basados en dualidad de Lagrange desarrollados en esta tesis de máster.

En la segunda parte de la tesis se llevan a cabo diseños más realistas y prácticos. Ahora se consideran constelaciones de dimensión finita, como por ejemplo modulaciones del tipo QAM. Ello hace que la función rate-potencia pase a ser discreta y esté basada en requerimientos de BER. Generalmente, estos problemas de asignación de recursos son combinatorios y por lo tanto no son convexos. Las soluciones óptimas suelen ser computacionalmente prohibitivas debido a la extensa búsqueda que se tiene que realizar. Es por ello que se proponen algoritmos de tipo *greedy* para solucionar el problema de la búsqueda exhaustiva, donde portadoras, asignación de bits y potencia son asignadas de forma dinámica, en función de un objetivo y de las restricciones de energía.

Mediante los datos obtenidos en las simulaciones, podemos concluir que usando las técnicas propuestas en esta tesis, no sólo es posible incrementar el tiempo de vida de la red, sino que además es posible incrementar el bit-rate medio conseguido por los terminales de la red comparado con técnicas clásicas de asignación de recursos.

Acknowledgements

En estas líneas de la tesis, quiero agradecer a todos aquellos que de algún modo u otro me han apoyado y han estado a mi lado durante mucho tiempo.

En primer lugar quiero agradecer la ayuda incondicional de mi director de tesis Antonio Pascual Iserte. Quiero darte las gracias por todo el apoyo recibido y por la confianza depositada en mí desde buen comienzo de nuestra relación, además de todo el soporte técnico siempre que lo he necesitado.

Me gustaría agradecer a mis padres todo lo que han hecho por mí durante todos estos años. Siempre han hecho todo lo posible para que yo llegue justo donde estoy ahora. Desde buen comienzo, siempre me apoyaron para que yo estudiara y me ayudaron en todo lo que hiciera falta sin dudarlo. Ahora que ya he acabado mi carrera, esta tesis va por vosotros.

Finalmente, me gustaría dar las gracias a todas las personas, amigos y compañeros de universidad, que me han acompañado en esta etapa de mi vida. En especial tengo que nombrar a Carlos R., Carlos S., Israel D., Roser F., Victor M., David I., Arnau R. y a mi amigo y compañero de máster, Avinash A. Con ellos he compartido los mejores momentos de mi vida últimamente. Espero que nuestra amistad perdure para siempre.

Javier Rubio López

Barcelona, julio 2012.

Table of Contents

List of Figures	xvii
List of Tables	xix
Acronyms	xxi
1 Introduction	1
1.1 Motivation	1
1.2 Objectives of the Thesis	5
1.3 Outline of Thesis	6
2 Fundamentals of Radio Resource Allocation in Wireless Communications	7
2.1 Mathematical Preliminaries	7
2.1.1 Convex Optimization	7
2.1.2 Convex Sets and Convex Functions	8
2.1.3 Definition of Convex Problems	10
2.1.4 Duality Theory and Karush-Kuhn-Tucker Conditions	12
2.1.5 Multicriterion Optimization	14

2.1.6	Solving Convex Problems	16
2.2	Overview of Radio Resource Management for OFDMA Systems	16
2.2.1	Introduction to Orthogonal Frequency Division Multiplexing	17
2.2.2	OFDM-based Multiple Access Technologies	18
2.2.3	Radio Resource Management Techniques for OFDMA Systems	20
2.2.4	Solving Radio Resource Allocation Problems	24
3	Energy Efficient Resource Allocation with Energy Harvesting Nodes and QoS Constraints over Flat-Fading Channels	27
3.1	Introduction	27
3.2	System Model	27
3.2.1	Power Consumption Models	29
3.3	Energy Efficient Sum-Rate Maximization with QoS Constraints	33
3.3.1	Energy Allocation at Each Iteration	36
3.3.2	Sub-Optimal Case: Fixed Transmission Bandwidth	37
3.3.3	Simulation Results	40
3.4	Energy Efficient Maximin with QoS Constraints	46
3.5	Sum-Rate - Maximin Trade-off	49
3.6	Sum-Rate - Sum-Residual Trade-off	52
3.6.1	Sub-Optimal Case: Fixed Transmission Bandwidth	55
3.7	Chapter Summary and Conclusions	60
3.A	Appendix: Proof of Lemma 3.1	61
3.B	Appendix: Proof of Lemma 3.2	61

3.C	Appendix: KKT Conditions of Problem (3.15)	62
3.D	Appendix: Proof of Lemma 3.3	63
3.E	Appendix: KKT Conditions of Problem (3.17)	64
3.F	Appendix: Proof of Lemma 3.4	65
3.G	Appendix: KKT Conditions of Problem (3.22)	66
3.H	Appendix: KKT Conditions of Problem (3.25)	67
3.I	Appendix: Proof of Lemma 3.5	68
3.J	Appendix: Proof of Lemma 3.6	68
3.K	Appendix: Proof of Lemma 3.7	69
4	Practical Energy Efficient Resource Allocation with Energy Harvesting Nodes over Frequency-Selective Channels	71
4.1	Introduction	71
4.2	System Model	73
4.3	Energy Adaptive Schemes with Battery Constraints	75
4.4	Rate Adaptive Schemes with Battery Constraints	78
4.4.1	Single Modulation Type	79
4.4.2	Adaptive Modulation	80
4.5	Simulation Results	82
4.6	Chapter Summary and Conclusions	90
4.A	Appendix: System and Simulation Modeling	92
4.A.1	User Distribution	92
4.A.2	Propagation	92

4.A.3 Channel Gain Calculation	94
5 Conclusions and Future Work	95
5.1 Conclusions	95
5.2 Future Work	96
Bibliography	97

List of Figures

1.1	The required transmit power for two short-distance bands of interest. Most applications today lie somewhere between the two curves.	2
1.2	A broadcast OFDM scenario, consisting of one transmitter (base station) and several receivers.	4
1.3	Multiple parallel relay channel, consisting of one transmitter (S), several intermediate nodes (R), and a destination node (D).	4
2.1	(a) Example of a convex set. (b) Example of a nonconvex set.	8
2.2	(a) Example of a convex function. (b) Example of a concave function.	9
2.3	Example of a Pareto region of two functions.	15
2.4	OFDM modulator and demodulator	18
3.1	Time slot structure and energy arrivals	29
3.2	Transceiver circuit blocks	31
3.3	Modified water-filling algorithm	39
3.4	Battery evolution of 4 nodes with different approaches: (a) maximization of the sum rate and no energy constraints. (b) maximin rate approach and no energy constraints. (c) maximization of the sum rate with energy constraint and parameter $\alpha = 0.1$. (d) maximization of the sum rate with energy constraint and parameter $\alpha = 0.01$	43

3.5	Battery evolution of 16 nodes with different approaches: (a) maximization of the sum rate and no energy constraints. (b) maximin rate approach and no energy constraints. (c) maximization of the sum rate with energy constraint and parameter $\alpha = 0.1$. (d) maximization of the sum rate with energy constraint and parameter $\alpha = 0.01$	44
3.6	(a) Average battery evolution of 4 nodes. (b) Average battery evolution of 12 nodes	45
3.7	(a) Average data-rate evolution of 4 nodes. (b) Average data-rate evolution of 12 nodes.	45
3.8	(a) Sum rate evolution. (b) Average percentage of battery level spent by users (a negative percentage means a gain in battery level).	46
3.9	Sum-Rate comparison between optimal and suboptimal approaches.	46
3.10	Trade-off between sum-rate and worst residual battery level	49
3.11	Trade-off curve between sum-rate and energy consumption using a exponential model for the decoding consumption model.	51
3.12	Trade-off curve between sum-rate and energy consumption using a linear model for the decoding consumption model.	51
3.13	Trade-off between sum-rate and energy consumption	53
3.14	Trade-off between sum-rate and energy consumption	55
4.1	Power spectral density of two realizations of Rayleigh frequency-selective channels used in this chapter.	74
4.2	Battery evolution of the maximin problem.	85
4.3	Sum-rate evolution of the maximin problem.	86
4.4	Example of resource allocation of the adaptive modulation greedy algorithm.	87
4.5	(a) Sum rate evolution. (b) Average percentage of battery level spent by users (a negative percentage means a gain in battery level).	87

4.6	Battery evolution of single modulation greedy-SREE scheme (a) System with 10 users and $\alpha = 0.1$. (b) System with 10 users and $\alpha = 0.01$. (c) System with 50 users and $\alpha = 0.1$. Only ten random users are depicted. (d) System with 50 users and $\alpha = 0.01$. Only ten random users are depicted.	88
4.7	Battery evolution of adaptive modulation greedy-SREE scheme (a) System with 10 users and $\alpha = 0.1$. (b) System with 10 users and $\alpha = 0.01$. (c) System with 50 users and $\alpha = 0.1$. Only ten random users are depicted. (d) System with 50 users and $\alpha = 0.01$. Only ten random users are depicted.	89
4.8	Uniformly distributed users	92
4.9	(a) Path loss. (b) Path loss + shadowing.	93

List of Tables

3.1	Simulation parameters	41
4.2	Simulation parameters	84
4.3	Time of execution of optimum and greedy algorithms with single modulation	90
4.4	Time of execution of optimum and greedy algorithms with adaptive modulation	90

Acronyms

ADSL	Asynchronous Digital Subscriber Line
AMC	Adaptive Modulation and Coding
APA	Adaptive Power Allocation
BER	Bit Error Rate
BS	Base Station
CDMA	Code Division Multiple Access
CP	Cyclic Prefix
CSI	Channel State Information
DMT	Discrete Multi Tone
DS	Delay Spread
DSA	Dynamic Spectrum Allocation
FDMA	Frequency Division Multiple Access
FFT	Fast Fourier Transform
GP	Geometric Programming
IFFT	Inverse Fast Fourier Transform
J	Joules
KKT	Karush-Kuhn-Tucker
LOS	Line of Sight
LP	Linear Programming
MAC	Medium Access Control
mAh	milli-Ampere hour
MCS	Modulation and Coding Scheme
MIMO	Multiple Input Multiple Output
MOP	Multi-objective Optimization Problem
OFDM	Orthogonal Frequency Division Multiplexing
OFDMA	Orthogonal Frequency Division Multiple Access
PA	Power Amplifier
PAPR	Peak to Average Power Ratio

PDP	Power Delay Profile
PHY	Physical
QAM	Quadrature Amplitude Modulation
QoS	Quality of Service
QP	Quadratic Programming
RF	Radio Frequency
RRA	Radio Resource Allocation
RRM	Radio Resource Management
SINR	Signal to Interference Noise Ratio
SNR	Signal to Noise Ratio
TDMA	Time Division Multiple Access

Chapter 1

Introduction

1.1 Motivation

In the last years, there has been a considerable expansion of wireless networks. With the evolution and improvement of wireless standards, more and more users are introduced in the systems every day. This expansion, and the fact that newer applications require higher data-rates, involves a need for a substantial increase of system capacity. In wireless networks, the resources are shared between users and they are limited. As a consequence, there must be an entity that manages the radio resources in a suitable way. In order to be more efficient, networks are becoming smaller in terms of distance between the central node and the intermediate nodes (in case of a sensor network) or the base station and users (in case of a cellular network). For instance, in cellular networks the trend is to deploy small cells called femtocells [9], [30], in order to provide high data-rates with a good performance to many users simultaneously. Due to the short distances between transmitter and receiver, the radiated power associated with the Power Amplifier (PA) can be compared or even lower than the power consumed by the Radio Frequency (RF) chain and the baseband signal processing algorithms [24], [13], [14] (see Fig. 1.1). Moreover, the high data-rate needed by the terminals entails situations where the users run out of battery noteworthy fast. All this matters, jointly with the idea that new energy harvesting technologies¹ are being emerged [51], [25], makes that new strategies for allocation the radio resources have to be developed.

In classical Radio Resource Allocation (RRA) policies, a given objective function is maximized or minimized (usually the data-rate or the transmit power) but without considering

¹These technologies are able to collect energy from the environment and to recharge the batteries of the nodes.

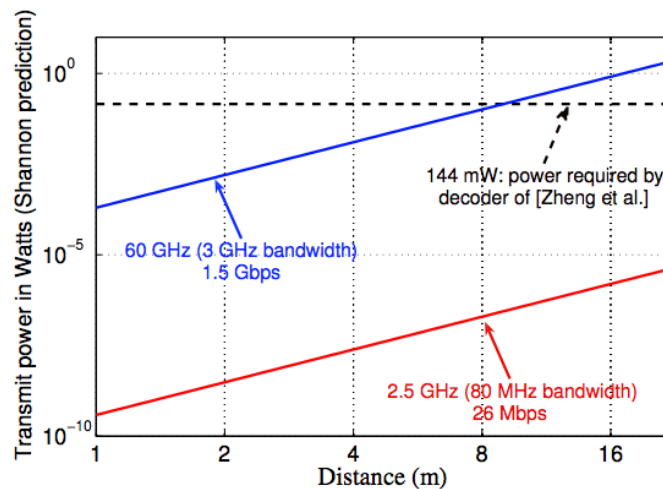


Figure 1.1: The required transmit power for two short-distance bands of interest. Most applications today lie somewhere between the two curves.

the energy spent in the whole communication process, only the radiated power transmitted by the PA. The main goal of this thesis is to design and develop strategies of RRA procedures where the nodes are battery-powered devices and are provided with a energy harvesting source. Thus, the information concerning the status of the battery level will play explicitly a role in the allocation decision.

There is a new line of research, being currently developed, concerning the concept of *Green Communications*² [33], [4], [40]. Particularizing to the area of RRA strategies for wireless networks, there have been some works so far, but to the best of our knowledge, none of them have included the information of the battery level in the allocation.

In [12], [13] authors developed strategies to optimize the modulation type based on a global energy minimization while satisfying a given throughput and delay requirements. They showed an 80% energy savings in uncoded systems. For coded systems, they showed that the benefit of coding varies with the transmission distance and the underlying modulation schemes. In [14] authors presented an approach for a joint design of the physical (PHY), Medium Access Control (MAC), and routing layers to minimize network energy consumption. They minimized the total network energy that included both transmission and circuit energy consumptions. They optimized the routing flow, Time Division Multiple Access (TDMA) slot assignment, and Quadrature Amplitude Modulation (QAM) modulation rate and power on each link. However, most of the works found in the literature based on energy efficient approaches are based on the quotient metric of bits over Joules that was first introduced by Verdu in [47]. Miao et al. developed resource allocation strategies based on this quotient

²Green Communications deals with energy-aware and energy-efficient schemes and strategies in order to reduce the emitted CO₂ and to increase the lifetime of the network

in many works [35], [34], [36], [?]. The main problem associated with this approach is that the bit-rate obtained by the optimization problem is very small and may not be enough for some applications. There have also been some tries to incorporate the energy efficiency in Multiple Input Multiple Output (MIMO) schemes [40]. For example, in [3] authors presented a precoder design based on the maximization of the quotient metric of bits over Joules. They concluded that to maximize the metric they should transmit with very low power, which turns in very small bit-rate. In [28] authors considered an energy-efficient multiuser MIMO beamforming algorithm that maximized the minimum energy efficiency among all the users with individual Signal to Interference Noise Ratio (SINR) constraints. The metric used was based on bits over Joules but SINR constraints made the bit-rate be controlled by this quality parameter. MIMO cooperation under energy efficiency was addressed in [44]. They considered individual single-antenna nodes that cooperate to form multiple-antenna transmitters or receivers. By transmitting and/or receiving information jointly, they showed that tremendous energy saving was possible for transmission distances larger than a given threshold, even when they took into account the local energy cost necessary for joint information transmission and reception. They also showed that over some distance ranges, cooperative MIMO transmission and reception could simultaneously achieved both energy savings and delay reduction. In [45] an energy-efficient cooperative relay selection scheme that utilized the transmission power more efficiently in cooperative relaying systems was proposed. Based on a suboptimal solution, the energy-efficient relay selection scheme was given, which selected the relay stations with the best energy efficiency and decided the optimal number of cooperative relay stations. Compared with the fixed relay cooperation, the simulation results showed that the proposed scheme could improve the energy efficiency as well as the system capacity, irrespective of the channel state conditions. Finally, other works considered the potential game theory frame to come up with new design strategies for the resource allocation problem from an energy-efficiency perspective [21], [17].

In this thesis, we consider a broadcast scenario. The reason for choosing to study this scenario is because the scientific community assumed in the wireless research area that most of the data traffic in networks is transmitted in the downlink link. This is so, since the data generation of multimedia services like audio and video streaming, web browsing is highly asymmetric.

The broadcast allocation has two potential scenarios of applicability. First, we have the usual downlink scenario of a cellular network, depicted in Fig. 1.2. In this case, we are experiencing every day a constant change of technology, making the applications higher and higher computationally cost demanding. This, turns in a battery short lifetime and a decrease of user happiness.

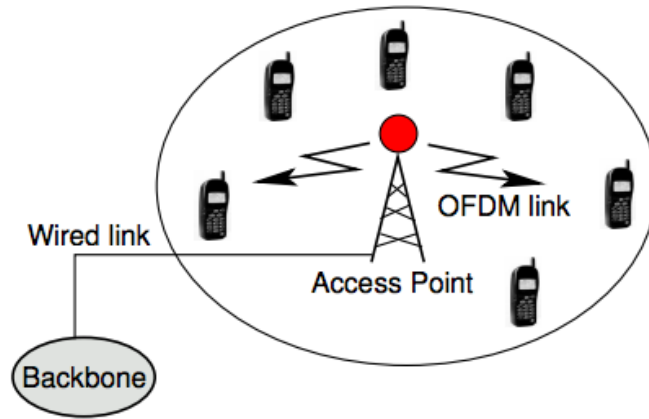


Figure 1.2: A broadcast OFDM scenario, consisting of one transmitter (base station) and several receivers.

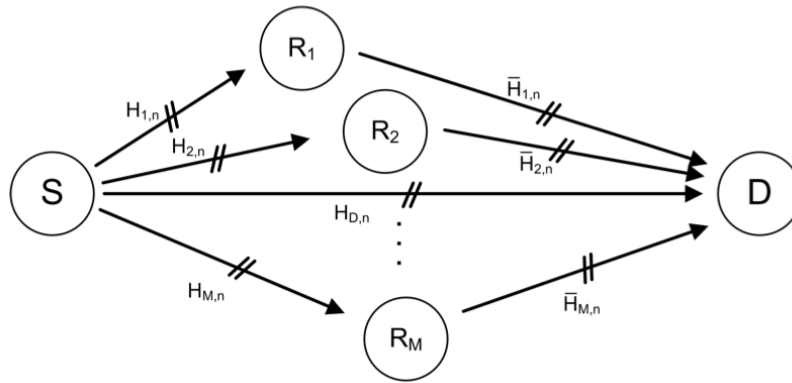


Figure 1.3: Multiple parallel relay channel, consisting of one transmitter (S), several intermediate nodes (R), and a destination node (D).

The second potential scenario is the multiple parallel relay channel [2], where a set of intermediate battery-constrained wireless nodes retransmit data from a source transmitter to a given receiver. Fig. 1.3 depicts the proposed scenario. As a general framework, we have included a direct link between the transmitter and the receiver. For the sake of simplicity, we will not consider direct link, so that both problems, the cellular scenario and the multiple parallel relay channel are mutually equivalent. In these wireless networks, the replacement of the battery of the intermediate nodes may be very difficult, costly or even impossible. In such a case, there is a crucial need for incorporating the battery status in the allocation policy in order to minimize the network cost and to maximize the network operation.

1.2 Objectives of the Thesis

The concepts that will be treated throughout this thesis stand in the forefront of future broadband wireless systems. The general objective of this work is to contribute with the state-of-the-art by settling critical and original knowledge about RRM for wireless networks in the ambit of the PHY and MAC layer where nodes are battery-constrained and have harvesting capabilities. The main objectives of this thesis are summarized below:

1. Theoretically conceive and evaluate, using link-level simulations, adaptive Radio Resource Management (RRM) solutions for the downlink of Orthogonal Frequency Division Multiple Access (OFDMA) -based networks, mainly focusing on the optimization of sub-carrier assignment, data-rate (bit loading) and power allocation.
2. Conceptually study the fundamental trade-off between capacity/throughput and energy efficiency in wireless networks and propose ways to manage this trade-off using RRM.
3. Formulate and evaluate RRM policies with different optimization objectives, such as maximization of system capacity, minimization of the energy consumed by the network players or a compromise between these factors.
4. Find techniques that contribute to the optimization of the battery lifetime of users, and therefore, the lifetime of the network itself.

General system assumptions:

- The Base Station (BS) has perfect knowledge of the Channel State Information (CSI) of all mobile terminals in all sub-carriers.
- The channel coefficients are assumed to be constant during the whole frame. However, different channels realizations are generated in each simulation.
- In Chapter 4, users experience frequency-selective Rayleigh channel. However, sub-carriers are considered to have smaller bandwidth than the coherence channel bandwidth, and thus, it makes the sub-carriers to experience flat-fading.

- The mobile terminals are static, i.e., there is no mobility. However, in each realization of the simulation (at the end of one frame), a different user distribution is simulated in order to capture the system performance in different coverage situations.
- It is not considered any signaling information to be sent or received by the users within the allocated channels. Allocation information transmission procedures are omitted in our models. As a consequence, the data-rate allocated to a given channel is fully used by the user to receive useful information.

1.3 Outline of Thesis

The organization of the thesis is as follows. In chapter 2 the fundamentals of radio resource allocation strategies applied to wireless communications will be presented. We will provide a mathematical framework able to solve the resource allocation problems. Then, the basic idea of resource allocation will be introduced. In chapter 3 the resource allocation problem when the channels are considered flat-fading will be studied. Hardware models will be presented to characterize the energy dissipated by the receivers when decoding the received data. Afterwards, different resource allocation problems will be addressed and, when possible, sub-optimal approaches with semi-analytical solutions will be provided. In chapter 4 a more realistic scenario is considered. Channels are considered to be frequency-selective. Moreover, a set of finite-size constellations will be considered which yields to bit and power loading algorithms. Chapter 6 will present the conclusions of the thesis and propose some further research works.

Chapter 2

Fundamentals of Radio Resource Allocation in Wireless Communications

2.1 Mathematical Preliminaries

In this section, a mathematical framework based on *convex optimization* theory is presented. This section is a brief summary of [7] that aims to provide a self-contained document which will give a broad understanding of the basic ideas to the reader that is not familiar with this theory. In order to find the mathematical foundations in a more depth, the interested reader is referred to [7]. These mathematical preliminaries will be useful in some chapters of the thesis where nonlinear constrained convex optimization problems must be solved.

2.1.1 Convex Optimization

Convex optimization theory provides a framework for solving a variety of constrained optimization problems. There is in general no analytical formula for the solution of convex optimization problems. However, in some cases, it is possible to obtain a closed-form solution, or at least a semi-analytical solution¹ based on the application of the Karush-Kuhn-Tucker (KKT) conditions under some mild conditions, as it will be shown later on this section. Besides, there exists a great variety of very effective numerical methods for solving the problems

¹A semi-analytical solution means a solution that is achieved with an iterative algorithm.

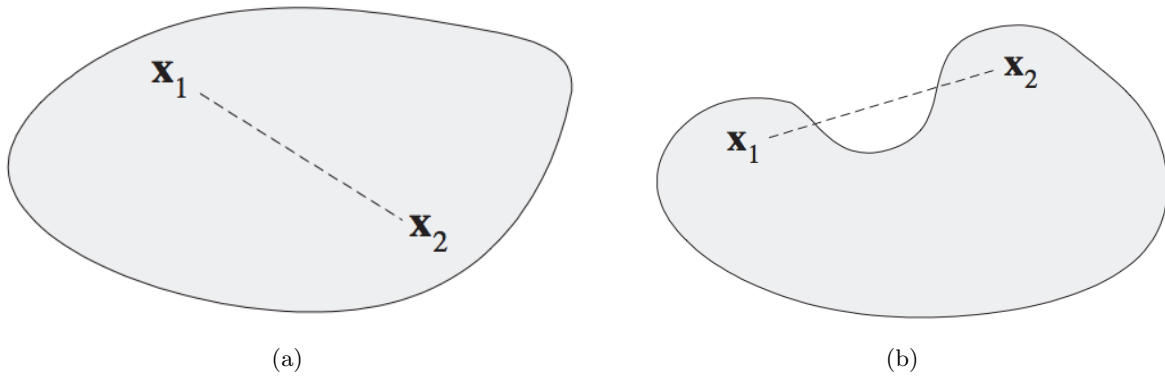


Figure 2.1: (a) Example of a convex set. (b) Example of a nonconvex set.

with no analytical solution, such as for example *interior point methods*. It is out of the scope of this thesis to present such methods, for a formal description the reader is referred to [7].

2.1.2 Convex Sets and Convex Functions

Suppose $x_1 \neq x_2$ are two points in \mathbf{R}^n . Points of the form

$$y = \theta x_1 + (1 - \theta)x_2,$$

where $\theta \in \mathbf{R}$, form the *line* passing through x_1 and x_2 . The parameter value $\theta = 0$ corresponds to $y = x_2$, and the parameter value $\theta = 1$ corresponds to $y = x_1$. Values of the parameter θ between 0 and 1 correspond to the (closed) *line segment* between x_1 and x_2 .

A set \mathcal{A} is a *convex set* if the line segment between any two points in \mathcal{A} lies in \mathcal{A} . This can be expressed mathematically as

$$\theta \mathbf{x}_1 + (1 - \theta)\mathbf{x}_2 \in \mathcal{A}, \quad \forall \mathbf{x}_1, \mathbf{x}_2 \in \mathcal{A}, \quad \forall \theta \in [0, 1].$$

Fig. 2.1 depicts a simple example of a convex and nonconvex sets in \mathbf{R}^2 . Basically, a set is convex if every point in the set can be reached by any other point in the set through a straight line that must also lie in the set. There are many examples of convex sets. The most important ones are cones, hyperplanes and halfspaces, Euclidean balls and ellipsoids, among others. There exists a variety of properties and mathematical operations that preserve convexity concerning convex sets. For instance, the intersection of an infinite number of convex sets is convex, i.e., if S_α is convex for every $\alpha \in \mathcal{A}$, then $\bigcap_{\alpha \in \mathcal{A}} S_\alpha$ is convex. A important property of a convex function is that the associated *sublevel set* is convex, where

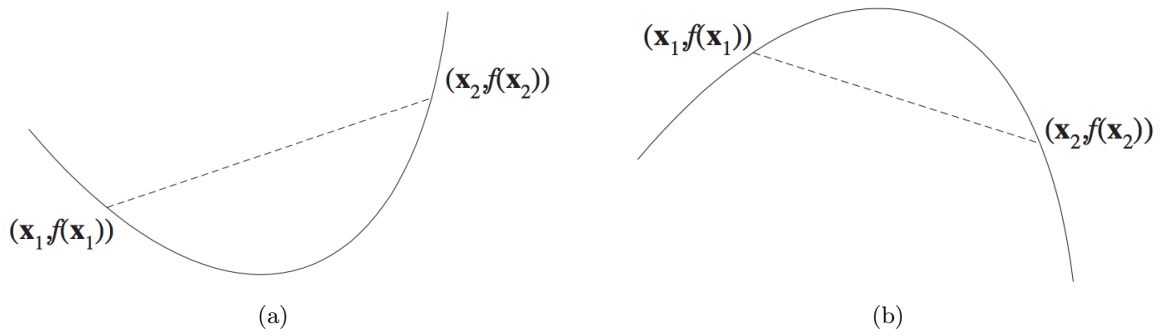


Figure 2.2: (a) Example of a convex function. (b) Example of a concave function.

the α -sublevel set $S_\alpha f$ is defined as

$$S_\alpha f \triangleq \{\mathbf{x} \in \text{dom } f : f(\mathbf{x}) \leq \alpha\}.$$

See [7] for a more complete list of properties and examples of convex sets.

A function $f : \mathbf{R}^n \rightarrow \mathbf{R}$ is a *convex function* if $\text{dom } f$ is a convex set and if $\forall \mathbf{x}_1, \mathbf{x}_2 \in \text{dom } f$ and $\forall \theta \in [0, 1]$, we have

$$f(\theta \mathbf{x}_1 + (1 - \theta) \mathbf{x}_2) \leq \theta f(\mathbf{x}_1) + (1 - \theta) f(\mathbf{x}_2). \quad (2.1)$$

Geometrically, the previous inequality means that the line segment between $(\mathbf{x}_1, f(\mathbf{x}_1))$ and $(\mathbf{x}_2, f(\mathbf{x}_2))$ lies above the graph of f . The simplest example of a convex function is the set of affine functions which have the form $f(\mathbf{x}) = \mathbf{a}^T \mathbf{x} + b$. A function f is *concave* if $-f$ is convex. Examples of convex and concave functions are exponential functions, powers, logarithms, etc. We say f is *strictly convex* if strict inequality holds in (2.1) whenever $x \neq y$ and $0 < \theta < 1$ (strictly concave if $-f$ is strictly convex). See Fig. 2.2 for a representation of a convex and a concave function.

In order to verify the convexity of a function, two conditions must hold. Let us start with the so-called *first-order condition*. Suppose f is differentiable and its domain is convex. Then, f is convex if, and only if,

$$f(\mathbf{x}_2) \leq f(\mathbf{x}_1) + \nabla f(\mathbf{x}_1)^T (\mathbf{x}_2 - \mathbf{x}_1)$$

holds for all $\mathbf{x}_1, \mathbf{x}_2 \in \text{dom } f$. On the other hand, the *second-order condition* states that if f is twice differentiable, i.e., its Hessian $\nabla^2 f$ exists at each point in $\text{dom } f$, then f is convex if and only if its domain is convex and

$$\nabla^2 f(\mathbf{x}) \succeq 0,$$

that is, its Hessian matrix is positive semidefinite.

2.1.3 Definition of Convex Problems

The general notation to describe a constrained optimization problem is as follows:

$$\begin{aligned} & \underset{\mathbf{x}}{\text{minimize}} && f_0(\mathbf{x}) && (2.2) \\ & \text{subject to} && f_i(\mathbf{x}) \leq 0, && i = 1, \dots, m, \\ & && h_i(\mathbf{x}) = 0, && i = 1, \dots, p. \end{aligned}$$

This notation represents the problem of finding an \mathbf{x} that minimizes $f_0(\mathbf{x})$ (called the *objective* or *cost function*) among all \mathbf{x} that satisfy the conditions $f_i(\mathbf{x}) \leq 0, i = 1, \dots, m$ and $h_i(\mathbf{x}) = 0, i = 1, \dots, p$. The variable \mathbf{x} is called the *primal optimization variable*. The inequalities $f_i(\mathbf{x}) \leq 0$ and their corresponding functions $f_i : \mathbf{R}^n \rightarrow \mathbf{R}$ are called the *inequality constraints* and *inequality constraint functions*, respectively. Conversely, the equations $h_i(\mathbf{x}) = 0$ and their corresponding functions $h_i : \mathbf{R}^n \rightarrow \mathbf{R}$ are called the *equality constraints* and *equality constraint functions* respectively. If there are no constraints, the problem is called *unconstrained optimization problem*.

The set of points for which the objective and all constraint functions are defined,

$$\mathcal{D} = \bigcap_{i=0}^m \text{dom } f_i \cap \bigcap_{i=1}^p \text{dom } h_i,$$

is called the *domain* of the optimization problem (2.2). A point $\mathbf{x} \in \mathcal{D}$ is *feasible* if it satisfies the constraints $f_i(\mathbf{x}) \leq 0, i = 1, \dots, m$ and $h_i(\mathbf{x}) = 0, i = 1, \dots, p$ simultaneously. If there exists at least one feasible point in the problem (2.2), then the problem is said to be *feasible*, and *infeasible* otherwise. The set of all feasible points is called the *feasible set* or the *constraint set*.

The *optimal value* p^* of the problem (2.2) is defined as

$$p^* = \inf \{f_0(\mathbf{x}) \mid f_i(\mathbf{x}) \leq 0, i = 1, \dots, m, h_i(\mathbf{x}) = 0, i = 1, \dots, p\}.$$

The optimal value p^* is allowed to have values within the range $\pm\infty$. If the optimal value is $p^* = \infty$, then the problem is *infeasible*, whereas the problem is said to be *unbounded below* if $p^* = -\infty$.

If \mathbf{x}^* is feasible and $f_0(\mathbf{x}^*) = p^*$, then we say \mathbf{x}^* is an *optimal point* or *optimal solution*.

The set of all optimal points is called the *optimal set*, which is expressed

$$\mathcal{X} = \{\mathbf{x} \mid f_i(\mathbf{x}) \leq 0, i = 1, \dots, m, h_i(\mathbf{x}) = 0, i = 1, \dots, p, f_0(\mathbf{x}) = p^*\}.$$

It is said that the optimum value is *attained* or *achieved* if there exists an optimal point for the problem (2.2). Accordingly, if \mathcal{X} is empty, it is said that the optimal value is not attained or not achieved.

A feasible point \mathbf{x} is *locally optimal* if there is an $R > 0$ such that

$$f_0(\mathbf{x}) = \inf \{f_0(\mathbf{z}) \mid f_i(\mathbf{z}) \leq 0, i = 1, \dots, m, h_i(\mathbf{z}) = 0, i = 1, \dots, p, \|\mathbf{z} - \mathbf{x}\|_2 \leq R\}.$$

All optimal points are also locally optimal, but the converse is not always true. There may exist some locally values which do not yield to optimal solutions (i.e., globally optimal).

The problem (2.2) is said to be a *convex optimization problem* if the objective function is convex, if the inequality constraint functions $f_i(\mathbf{x}) \leq 0, i = 1, \dots, m$ are all convex, and if the equality constraint functions $h_i(\mathbf{x}) = \mathbf{a}_i^T \mathbf{x} - b_i, i = 1, \dots, m$ are affine. Based on the definition of the domain of the optimization problem, it is easy to realize that the domain of a convex optimization convex is also convex, since it is the intersection of the set of domains of all the functions, which are convex. Additionally, the constraint set is also convex since it is the intersection of m convex sublevel sets, and p hyperplanes. A fundamental property of convex optimization problems is that any locally optimal point is at the same time globally optimal [7]. Sometimes it is useful to transform the original problem into an equivalent problem. This is done mostly when the original problem is not convex. These tricks may include a change of variables or the introduction of slack variables. Some of these techniques will be used and commented along this thesis whenever needed.

The most common convex optimization problems are Linear Programming (LP) problems, *quadratic programming* (QP)² and *geometric programming* (GP)³. For a large descriptions of convex optimization problems see [7].

A *concave optimization problem* is a problem where the objective function, concave in this case, is to be maximized, and the inequality constraint functions $f_i(\mathbf{x}) \leq 0, i = 1, \dots, m$ are convex, the equality constraint functions $h_i(\mathbf{x}) = 0, i = 1, \dots, p$ are affine. This problem can be easily transformed to a standard convex optimization problem by just minimizing the convex function $-f_0(\mathbf{x})$ subject to the same original constraints.

²An optimization problem is said to be QP if the objective function is quadratic and the constraint functions are affine.

³An optimization problem is said to be GP if the objective function and the inequality constraint functions are posynomials, and the equality constraint functions are monomials.

2.1.4 Duality Theory and Karush-Kuhn-Tucker Conditions

Given the optimization problem in standard form (2.2), and assuming its domain is not empty, the *Lagrangian* of the problem can be defined as

$$L(\mathbf{x}; \boldsymbol{\lambda}, \boldsymbol{\nu}) \triangleq f_0(\mathbf{x}) + \sum_{i=1}^m \lambda_i f_i(\mathbf{x}) + \sum_{i=1}^p \nu_i h_i(\mathbf{x}),$$

where $\boldsymbol{\lambda} = [\lambda_1 \dots \lambda_m]^T$ and $\boldsymbol{\nu} = [\nu_1 \dots \nu_p]^T$ are the vector of *Lagrange multipliers* associated to the i th inequality and equality constraint functions respectively. The Lagrangian multipliers are commonly referred to as *dual variables*. We define the *Lagrange dual function* (or just *dual function*) as the infimum of the Lagrangian over \mathbf{x}

$$g(\boldsymbol{\lambda}, \boldsymbol{\nu}) = \inf_{\mathbf{x} \in \mathcal{D}} L(\mathbf{x}; \boldsymbol{\lambda}, \boldsymbol{\nu}) = \inf_{\mathbf{x} \in \mathcal{D}} \left(f_0(\mathbf{x}) + \sum_{i=1}^m \lambda_i f_i(\mathbf{x}) + \sum_{i=1}^p \nu_i h_i(\mathbf{x}) \right)$$

such that $\boldsymbol{\lambda} \in \mathbf{R}^m, \boldsymbol{\nu} \in \mathbf{R}^p$ and \mathcal{D} is the domain of the original problem (2.2). When the Lagrangian is unbounded below, the dual function takes on the value $-\infty$. Since the dual function $g(\boldsymbol{\lambda}, \boldsymbol{\nu})$ is the pointwise infimum of a family of affine functions of $(\boldsymbol{\lambda}, \boldsymbol{\nu})$, it is concave even when the problem (2.2) is not convex [7]. A point $(\boldsymbol{\lambda}, \boldsymbol{\nu})$ is said to be *dual feasible* if $\boldsymbol{\lambda} \succeq 0$ and $(\boldsymbol{\lambda}, \boldsymbol{\nu}) \in \mathbf{dom} g$. An important statement is that the dual function evaluated at any dual feasible point yields a lower bound on the optimal value p^* of the original problem (2.2). The proof is as follows

$$\begin{aligned} p^* = f_0(\mathbf{x}^*) &\geq f_0(\mathbf{x}^*) + \sum_{i=1}^m \lambda_i f_i(\mathbf{x}^*) + \sum_{i=1}^p \nu_i h_i(\mathbf{x}^*) & (2.3) \\ &\geq \inf_{\mathbf{z} \in \mathcal{D}} \left(f_0(\mathbf{z}) + \sum_{i=1}^m \lambda_i f_i(\mathbf{z}) + \sum_{i=1}^p \nu_i h_i(\mathbf{z}) \right) \\ &= g(\boldsymbol{\lambda}, \boldsymbol{\nu}) \end{aligned}$$

The best lower bound that can be obtained from the Lagrange dual function may be found by solving the following optimization problem:

$$\underset{\boldsymbol{\lambda}, \boldsymbol{\nu}}{\text{maximize}} \quad g(\boldsymbol{\lambda}, \boldsymbol{\nu}) \quad (2.4)$$

$$\text{subject to} \quad \boldsymbol{\lambda} \succeq 0. \quad (2.5)$$

This problem is called the *Lagrange dual problem* associated with the problem (2.2). The optimal value achieved by this problem is d^* and it is attained at the dual variables $(\boldsymbol{\lambda}^*, \boldsymbol{\nu}^*)$. As it was mentioned before, it is by definition the best lower bound on p^* :

$$d^* \leq p^*.$$

The previous inequality always holds, even if the original problem is not convex. This property is known as *weak duality*. On the other hand, if the equality

$$d^* = p^*$$

holds, then it is said that *strong duality* holds (or the optimal duality gap is zero). This shows that under certain conditions, the bound obtained from the Lagrange dual problem is tight. However, strong duality does not always hold. In order to assure strong duality, for convex problems it is only needed to prove that some mild technical conditions are satisfied. These conditions are called *constraint qualifications*. An example of a constraint qualification is the *Slater's condition*. It states that strong duality holds if there exists a point \mathbf{x} such that $f_i(\mathbf{x}) < 0$, $i = 1, \dots, m$ and $\mathbf{Ax} = \mathbf{b}$ (this point is commonly referred as *strictly feasible point*).

If we assume strong duality holds, for a given primal optimal \mathbf{x}^* and dual optimal $(\boldsymbol{\lambda}^*, \boldsymbol{\nu}^*)$ variables, the following expression holds

$$\begin{aligned} f_0(\mathbf{x}^*) &= g(\boldsymbol{\lambda}^*, \boldsymbol{\nu}^*) & (2.6) \\ &= \inf_{\mathbf{x} \in \mathcal{D}} \left(f_0(\mathbf{x}) + \sum_{i=1}^m \lambda_i^* f_i(\mathbf{x}) + \sum_{i=1}^p \nu_i^* h_i(\mathbf{x}) \right) \\ &\leq f_0(\mathbf{x}^*) + \sum_{i=1}^m \lambda_i^* f_i(\mathbf{x}^*) + \sum_{i=1}^p \nu_i^* h_i(\mathbf{x}^*) \\ &\leq f_0(\mathbf{x}^*). \end{aligned}$$

An important conclusion can be drawn from the previous statement. Notice that, from the fourth line, we have that the inequality must be an equality, that is,

$$\sum_{i=1}^m \lambda_i^* f_i(\mathbf{x}^*) = 0.$$

Since each term in this sum is nonpositive, it can be concluded that

$$\lambda_i^* f_i(\mathbf{x}^*) = 0, \quad i = 1, \dots, m.$$

This condition is known as *complementary slackness*, and it holds for any primal and any

dual optimal variables. As a consequence, the complementary slackness implies that

$$\lambda_i^* > 0 \implies f_i(\mathbf{x}^*) = 0,$$

or,

$$f_i(\mathbf{x}^*) < 0 \implies \lambda_i^* = 0.$$

Using all the previous statements and assuming that all the functions $(f_0, \dots, f_m, h_1, \dots, h_p)$ are differentiable, we are able to conclude that the following equations must be fulfilled for any primal and dual optimal variables

$$\begin{aligned} f_i(\mathbf{x}^*) &\leq 0, & i = 1, \dots, m, \\ h_i(\mathbf{x}^*) &= 0, & i = 1, \dots, p, \\ \lambda_i^* &\geq 0, & i = 1, \dots, m, \\ \lambda_i^* f_i^*(\mathbf{x}^*) &= 0, & i = 1, \dots, m, \\ \nabla f_0(\mathbf{x}^*) + \sum_{i=1}^m \lambda_i^* \nabla f_i(\mathbf{x}^*) + \sum_{i=1}^p \nu_i^* \nabla h_i(\mathbf{x}^*) &= 0, \end{aligned} \tag{2.7}$$

which are called the *Karush-Kuhn-Tucker* conditions.

To summarize, for *any* optimization problem with differentiable objective and constraint functions for which strong duality holds, any pair of primal and dual optimal points must satisfy the KKT conditions (2.8). This means that KKT conditions are always necessary conditions for optimality. If, moreover, the problem is *convex*, KKT conditions are also sufficient for optimality. In other words, if the points \mathbf{x} and $(\boldsymbol{\lambda}, \boldsymbol{\nu})$ satisfy the KKT conditions, then these points are primal and dual optimal, with zero duality gap.

2.1.5 Multicriterion Optimization

Multicriterion optimization [7], [16] is a specific case of vector optimization. Vector optimization extends the standard form problem to include vector-valued objective and constraint functions. Now, instead of having only one objective function, we deal with several objectives. Still, our goal is to maximize or minimize all the objectives at the same time. It may seem reasonable that, under some conditions, we will not be able to maximize/minimize everything. In these optimization problems, the optimal solutions are called *Pareto optimal points*. Let us show an example with only two objectives to understand this concept. Imagine that we want to maximize two objectives, let us say $F_1(\mathbf{x})$ and $F_2(\mathbf{x})$. The space of feasible points are represented in Fig. 2.3, which, for this case, the feasible points are inside of what is called the *Pareto region* (i.e., the boundary line). Thus, the boundary defines the Pareto

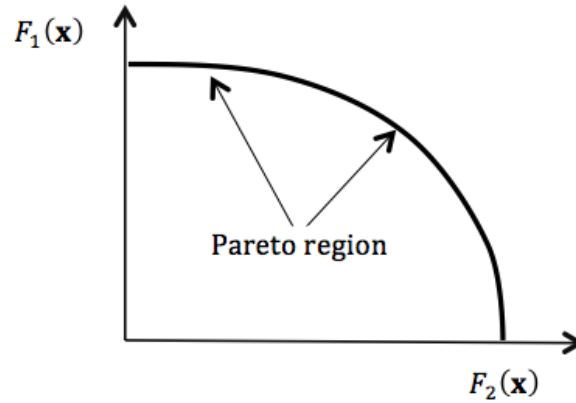


Figure 2.3: Example of a Pareto region of two functions.

optimal points of the two objectives. As a simple explanation, we can say that a Pareto optimal point is a point such that if one of the objectives improves, the other gets worse. It is easy to see graphically with the two objective example. If a Pareto point moves towards the right (along the boundary), $F_2(\mathbf{x})$ improves (increases), but in contrast $F_1(\mathbf{x})$ decreases.

Let us define the components of f_0 as F_1, \dots, F_q , to be interpreted as q different scalar objectives, each of which it is desired to be minimized. Then, in a vector optimization problem, an optimal point \mathbf{x}_1^* satisfies

$$F_i(\mathbf{x}_1^*) \leq F_i(\mathbf{x}_2), \quad i = 1, \dots, q,$$

for every feasible value \mathbf{x}_2 .

The mathematics behind this problem involves a proper cone. This is so, since now, we need to compare vector-valued objectives. The explanation made before about the Pareto points is only valid when the cone is $K = \mathbf{R}_+^q$. In this case, the problem is called *Multicriteria Optimization Problem* (MOP) (also multi-objective optimization problem). However, we could generalize the mathematical formulation including a general cone. We only need to consider the fact that each cone induces a distinct multivariate order relation. Now, we can provide a more formal definition of the Pareto optimal region. The Pareto optimal region is formed by Pareto optimal points which can be defined as the set of feasible points that makes $f_0(\mathbf{x})$ to be a minimal element of the set of achievable values. In other words, a point \mathbf{x}_1 is Pareto optimal if it is feasible and, for any feasible \mathbf{x}_2 , $f_0(\mathbf{x}_2) \preceq_K f_0(\mathbf{x}_1)$ implies $f_0(\mathbf{x}_2) = f_0(\mathbf{x}_1)$.

There are several methods for finding the Pareto points of a MOP, most of them based

on scalarization techniques. The simplest technique (and the used along this thesis) is called the *weighted sum method*, which collapses the vector objective into a single objective sum component

$$\underset{x}{\text{minimize}} \quad \sum_{k=1}^q \mu_k F_k(\mathbf{x}) \quad (2.8)$$

Thus, for a given set of μ 's, an optimal solution is obtained, that is, if we change the values of the weight, different Pareto solutions are found. In order to guarantee that the optimal solutions achieved by (2.8) are indeed the Pareto optimal points of the original problem, all the objective functions F_1, \dots, F_q must be convex and so does the constraint set [16].

2.1.6 Solving Convex Problems

As commented before, there is no general analytical formula to solve convex optimization problems. However, in cases where the objective and constraint functions are differentiable, and where the KKT holds, being able to solve the KKT equations may yield to a closed-form solution of the problem due to the fact that KKT conditions are necessary and sufficient for optimality.

Notice, nevertheless, that even if not closed-form solutions are obtained, an efficient numerical algorithm can always be implemented to achieve the optimal value thanks to the fundamental property that states that any locally optimal point is also a globally solution. This motivates the search for very fast algorithms to solve convex optimization problems. Indeed, almost real-time algorithms for solving convex problems can be found today. Among the most famous, the *interior point methods* (also called *barrier methods*) must be emphasized. These algorithms reach the optimal solution by solving a sequence of smooth unconstrained problems, usually using the Newton's method [7]. Generally, the interior-point based methods are able to provide not only the optimal primal variables, but also the optimal dual ones (that is the Lagrange multipliers). These techniques are called *primal-dual interior point methods*.

2.2 Overview of Radio Resource Management for OFDMA Systems

RRM techniques are responsible for the utilization and allocation of the radio resources of the air interface of a given wireless network. Traditionally, RRM functionalities were decisive for the guarantee of Quality of Service (QoS) requirements of different services, the maximization of the spectral efficiency, the optimization of coverage in cellular networks, or the provision

of adequate fairness in the resource distribution among the network nodes. Nowadays, with the impact of green communications in all the system levels of any communication system, RRM techniques are also crucial for providing a long network lifetime in terms of battery duration.

2.2.1 Introduction to Orthogonal Frequency Division Multiplexing

Orthogonal Frequency Division Multiplexing (OFDM) is a multicarrier transmission scheme, where a high-rate serial data stream is split up into a set of N low-rate substreams, each of which is modulated on a separate orthogonal sub-carrier [5], [48], [10]. Thereby, the bandwidth of the sub-carriers becomes small compared with the coherence bandwidth of the channel, i.e., the individual sub-carriers experience flat fading, which allows for simple equalization. This implies that the symbol period of the substreams is made long compared to the delay spread of the time-dispersive radio channel.

The OFDM transmission scheme has the following key advantages:

- Easy adaptation to severe channel conditions without complex time-domain equalization.
- Robustness against narrowband interference because such interference affects only a small percentage of the sub-carriers.
- High spectral efficiency as compared to conventional modulation schemes.
- Low sensitivity to time synchronization errors

On the other hand, OFDM also has some drawbacks compared with single-carrier modulation:

- Sensitivity to Doppler shift.
- Sensitivity to frequency synchronization problems.
- High Peak-to-Average-Power Ratio (PAPR), requiring linear transmitter circuitry, which suffers from poor power efficiency.
- Loss of efficiency caused by cyclic prefix/guard interval.

In the following, the mathematical and block description of the modulation will be presented. Each OFDM symbol is composed of two parts: the useful information part, with N samples,

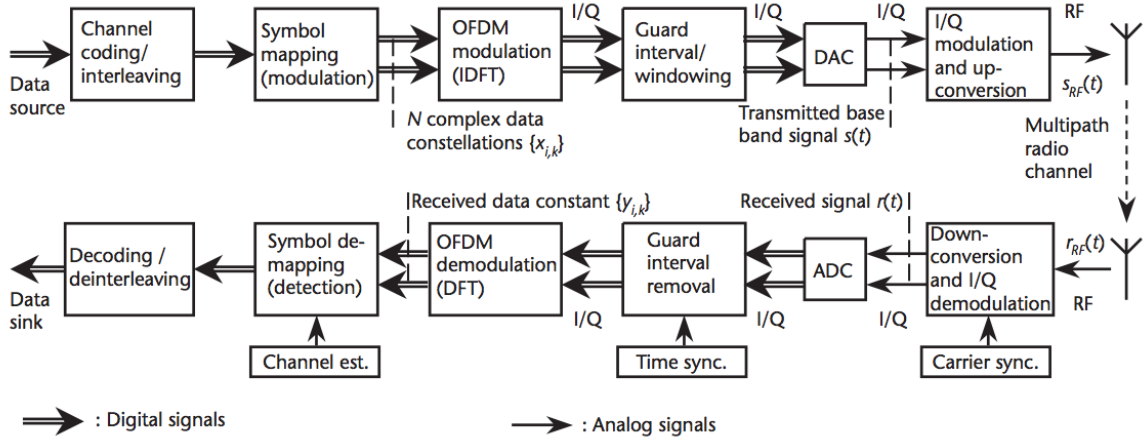


Figure 2.4: OFDM modulator and demodulator

and the Cyclic Prefix (CP), with D samples. The CP is typically added at the beginning of the OFDM symbol, and its samples are equal to the last samples D samples of the useful information. The time domain representation of an OFDM symbol at m -th time slot can be expressed as

$$x(m, n) \triangleq \frac{1}{\sqrt{N}} \sum_{k=0}^{N-1} s_k(m) e^{j2\pi f_k \frac{n}{f_s}}, \quad -D \leq n < N, \quad (2.9)$$

where f_k corresponds to the base-band frequency corresponding, f_s is the sampling frequency, $s_k(m)$ is the QAM symbol and n is the time index. Notice that, the generation of the samples in (2.9) can be easily implemented using a N -point inverse Fast Fourier Transform (IFFT). The block diagram of a point-to-point transmission using OFDM modulation is depicted in Fig. 2.4. As shown, the data stream is mapped into symbols belonging to a constellation, then converted from a serial to a parallel stream in order to assign each symbol to a specific sub-carrier using the IFFT. After that, all IFFT samples are converted back from parallel to serial and the CP is added at the beginning of the symbol. Finally, the OFDM symbol is I/Q modulated. The structure of the receiver is symmetric to the transmitter scheme. The signal is first baseband converted and then the CP is removed. OFDM demodulation is achieved now using the Fast Fourier Transform (FFT) and finally symbols are decoded.

For a more elaborate introduction to OFDM, the reader may refer to [38], [39].

2.2.2 OFDM-based Multiple Access Technologies

OFDM combined with multiple access techniques allows to exploit new sources of diversity that jointly with the classical ones must be well explored by the RRM algorithms. These diversities are:

- **Time:** The time diversity comes from the time-varying nature of the wireless radio channel. The velocity in which the state of the channel changes can be estimated by the channel coherence time.
- **Frequency:** Frequency diversity concerns the fact that different sub-carriers of a wireless system may have a strongly varying attenuation, due to the frequency selectivity of the wireless channel.
- **Space:** In systems with multiple antennas, it is also possible to enumerate space diversity. Space offers a new dimension to be explored by the fact that antennas placed at a certain distance provide a different wireless channel.
- **Multi-user:** As several terminals are located in a given position, sub-carriers are likely to be in different quality states for different network nodes, i.e., a certain node may experience some carriers in a deep fade while others could take profit of them. This is true since, in general, the fading process is statistically independent for different nodes.

In order to fully exploit the flexibility offered by OFDM efficient RRM techniques are of utmost importance. Assuming that the transmitter knows the CSI of the different users, adaptive allocation mechanisms can be used to allocate the limited resources, e.g., bandwidth and power, in an intelligent way in order to maximize some performance metric. Therefore, the problem of allocating time slots, sub-carriers, rates, and power to the different users in an OFDM system has been an area of active research. Based on everything exposed before, there exists a set of different multiple access schemes that take profit of the advantages of the digital modulation OFDM. There are studies that show the performance comparison between them [42]. These multiple access schemes are:

- **OFDM-Frequency Division Multiple Access (FDMA):** Network nodes are pre-assigned a set of sub-carriers. It is considered static resource allocation. With this scheme, multi-user diversity cannot be explored since carriers in a deep fade for a given user are wasted and probably not used.
- **OFDM-TDMA:** All the sub-carriers are available for a given node and a certain time-slot. Normally, this is also considered static resource allocation, since the assignment of frames are pre-established at the beginning of the communication. As happened in previous scheme, OFDM-TDMA is not able to fully explore the multi-user diversity due to the time-varying nature of the wireless channel. It may happen that in a given time instant, a user find most of the sub-carriers in a deep fade, having wasted one frame of the communication.

- **OFDM-Code Division Multiple Access (CDMA):** There exists also multiple versions where multi-carrier systems are combined with CDMA. OFDM symbols are pre-multiplied by their user-dependent chip code, allowing different users to share the same sub-carriers at the same time.
- **Adaptive-OFDMA:** There is no a unique name to represent this multiple access technique. Sometimes it is known as multi-user adaptive OFDM (MAO) in the community research. This multiple access technique resolves the main problems presented in previous ones: it entirely exploits the *multi-user diversity*. In order to address such a problem, multiple access is achieved in OFDM by assigning subsets of sub-carriers to different users at each OFDM symbol. This technique is known as OFDMA. On the contrary, the resources needed for signaling and the highly computational cost required by the resource algorithms makes it often impossible to implement. One must be aware that, the algorithm needs the channel state information of all users in all time-slots. If channel is almost static, the feedback information of the channel could be relaxed, but in general it is very signaling demanding in scenarios where channels are extremely time-varying, with the consequences of reducing the throughput of the network.

Apart from the previous presented techniques, others can be found in the literature. They basically present slightly modifications or combinations of the exposed ones.

2.2.3 Radio Resource Management Techniques for OFDMA Systems

The goal of any resource allocation algorithm is to explore as many diversities as possible offered by the varying nature of the wireless channel. While exploring diversity, the scheduling algorithm must make a properly usage of the different existing resources in an OFDMA-based system among the network players. There exists a wide variety of radio resources to be managed, but the most important can be summarized as follows [32]:

- **Frequency sub-carrier:** Frequency domain adaptation achieves large performance gains in cases where the channel varies significantly over the system bandwidth. Thus, frequency domain adaptation becomes increasingly important with an increasing system bandwidth. OFDM transmission straightforwardly supports such frequency-domain scheduling by the dynamic allocation of different sets of sub-carriers.
- **Time slot / frame:** Exploiting channel variations in the time domain through channel dependent scheduling provides a substantial increase in spectral efficiency. Multiplexing

can also be performed in the time dimension of OFDM-based systems, as long as it occurs between time slots (usually difficult in real-time applications) or between frames.

- **Modulation and Coding Scheme (MCS):** Using adaptive modulation and coding, the transmitter can send higher data rates over the sub-carriers with better channel conditions to improve throughput and simultaneously ensure an acceptable Bit Error Rate (BER) in all sub-carriers. The MCS used for each sub-carrier can also be changed at each time slot or frame.
- **Transmission power:** Due to the frequency-selective attenuation of the wireless channel, the transmit power per sub-carrier can be adapted in order to increase the spectral efficiency. The capacity can be maximized if more transmit power is applied to frequency areas with a low attenuation relative to the other frequencies. As different sub-carriers experience different fades and transmit different number of bits, the transmit power levels must be changed accordingly.

The allocation of resources in OFDMA-based systems corresponds to a multi-dimensional problem, since time, frequency, and spatial (in case of MIMO systems) domains should be efficiently used and combined. Therefore, significant performance improvement can be achieved by means of an efficient resource allocation strategy. RRM techniques essential provide considerable gains in energy-efficiency, capacity, fairness or QoS. From a commercial point of point, it is important to improve coverage, capacity or QoS, since it represents better monetary gains and better radio services for the final client.

However, it is also very important to reduce the network consumption of the devices plugged into the electrical network. Hence, it seems reasonable to come up with new allocation strategies that consider the energy to be spent by the network nodes in the design. On the other hand, from a customer point of view, allocation strategies should yield to better services, higher fairness, and enhanced QoS levels. Here again, it is very important to consider the energy-efficiency in the allocation procedure. This is also beneficial for the customer since with the high demanding download of fast streams, devices run out of battery considerably fast, producing a bad customer experience. In case of wireless sensor nodes, this may also be even more important, since nodes can be placed at locations where battery replacement may be even impossible, or very costly. Moreover, in these kind of networks, or in multi-hop wireless networks, the "death" of a node not only means its uselessness, sometimes it may even affect the entire network functionality.

There are many RRA algorithms available for OFDMA-based systems. In the following, we present a list containing the most researched techniques in the literature:

- **Dynamic Sub-carrier Assignment (DSA):** The spatial selectivity of the sub-carriers, which is related to the multi-user diversity, gives rise to the opportunity of assigning different sub-carriers to different users. The DSA algorithm explores this flexibility of the OFDMA system and determines the pairs users/sub-carriers according to a given RRA policy [37].
- **Adaptive Power Allocation (APA):** This algorithm is also called power loading in the literature. Each sub-carrier may face a different channel gain depending on which frequency it is related to (frequency diversity), when it is allocated (time diversity), and for which user it is assigned (multi-user diversity). Taking this into account, it is advantageous to dynamically adapt the power of each sub-carrier [20].
- **Adaptive Modulation and Coding (AMC):** This technique is also known as bit loading [8]. It exploits the time and frequency diversities in order to allocate the most suitable MCS to each sub-carrier according to its Signal-to-Noise Ratio (SNR) or BER.
- **Interference avoidance/coordination:** In systems where the interference between close networks is an issue, some interference avoidance techniques must be developed. In general, this class of RRM strategies are considered in multi-cell scenarios, where interference reduces the cell throughput.

Resource allocation for wireless communications systems may have different aims. The traditional ones include the maximization of system throughput, user QoS, or fairness in the resource distribution. The objective of this thesis is to develop a framework where battery-powered harvesting devices inform its battery status and harvesting rates to the scheduler, making this information available in the allocation and trying to optimize the lifetime of the battery-driven nodes and devices. As a consequence, energy-efficiency schemes arise naturally from this new scenario. Unfortunately, in general, these objectives cannot be attained all together simultaneously. There exists a natural trade-off between most of them. In the following, we provide some fundamental compromises that appear in wireless networks:

- **Capacity vs QoS:** A clear compromise between system capacity and user QoS is the fact that the existence of more users in the system decreases the QoS per user.
- **Fairness vs QoS:** Since the wireless resources are limited, the QoS of the users cannot be improved indefinitely. If the QoS of few users is maximized, the others will feel the lack of resources. This imbalance is translated into a fairness decrease. On the other hand, if a high fairness is assured, then the maximum achievable QoS in this situation is upper-bounded.

- **Capacity vs Fairness:** In order to maximize system capacity, the wireless resources must be allocated in the most efficient way possible. A possible way to accomplish this is by using opportunistic resource allocation algorithms, which assign the resources to the users who have the best channel conditions. As introduced before, wireless channel suffers high variability in time and frequency domain. In order to maximize capacity, the opportunistic RRM algorithm will inevitably concentrate the resources to the best users. In general, this situation is characterized by low fairness. On the other hand, if a high fairness level is required, the system is forced to cope with the bad channel conditions of the worst users and allocate resources to them.
- **Throughput vs energy-efficiency:** As commented before, in order to maximize throughput, the system will allocate resources to the users that experience the best channel condition. This could lead to a situation where users with the best conditions run out of battery, making the system non-efficient in terms of energy, whereas other users may have enough battery to be used at this time instant. However, selecting users with higher battery level may lead to situations where the system capacity is degraded. As a consequence, it is not clear what users must be selected in order to cope with this trade-off.
- **QoS vs energy-efficiency:** The compromise also arises between user QoS and network energy-efficiency. If the minimum QoS is considerably high even in situations where it is not needed, this would decrease the energy-efficiency performance of the network. From the energy-efficiency point of view, users with better harvesting rate or battery capacity could experience better QoS. But, since these parameters change along time, the scheduler may adapt the user QoS by taking into account their energy status.

Apart from the ones exposed in this thesis, in the particular case of cellular communications, compromises with coverage also appear. For example, the trade-off between coverage and QoS is evident. The higher the minimum QoS requirement is, the smaller the cell coverage will be. Another example is the trade-off between the coverage and the capacity of the cell. base stations with high power provide good coverage, but also generate excessive interference to the neighbor cells, which can decrease the overall system capacity.

Note that the compromises described above are fundamental trade-offs found in any wireless communication network. System design, the use of specific technologies, and the use of suitable RRM techniques can diminish the gap of the compromises. Adaptive RRM strategies are very useful in cases where the trade-offs cannot be solved in a 'win-win' approach.

2.2.4 Solving Radio Resource Allocation Problems

Generally a RRA problem is formulated as an optimization problem. A proper objective function to be maximized or minimized must be defined, and a set of constraints have to make the resource problem affordable. Often, the constraints are physical limitations of the network itself or QoS demands. As an example of RRA problem we have the classical maximization of the sum of all user rates subject to a power budget constraint or the minimization of the transmitter power with data rate constraints. In order to solve these problems, some optimization tools are more suitable than others. The powerful framework based on convex optimization presented in previous section is one of the most common tools used to propose RRA techniques for OFDMA systems. For instance, the Lagrangian's method of multipliers and the KKT conditions are classical tools for nonlinear constrained convex optimization problems.

When the optimum solution of the optimization problem is too difficult to be found, for example when the problem is not convex (due to the combinatorial nature of the problem itself), some sub-optimum approaches need to be used. Three of the most common approaches found in the literature are listed below [23]:

- **Relaxation of constraints:** The idea is to relax some optimization constraints in order to ease the solution of the problem. Usually the constraints are nonconvex sets, and by applying the relaxation they become convex. In RRA techniques usually appear an univocal assignment of sub-carrier that is an integer constraint. This integrity makes the whole problem nonconvex and very difficult to be solved. The key point is to relax the univocal assignment so that each sub-carrier can be assigned to multiple users simultaneously. The same problem arises with the bit loading algorithm. By doing this, the optimization problems may become linear programming problems, which can be solved efficiently. However, one must have in mind that after solving the relaxed problem, the relaxed solution has to be re-evaluated because only integer solutions are feasible from the network's point of view. Further detail will be presented in future chapters/sections of this thesis.
- **Problem splitting:** This approach uses the concept of splitting the complex problem into two or more simpler steps so that a sub-optimum solution close enough to the optimum can be found. Generally, when there are QoS constraints, the scheduler needs to assign a set of minimum resources to each user in order to guarantee that the QoS level will be achieved. Problem splitting helps facing this problem, assigning in a first step, the minimum resources, and then assigning the specific resources in order to maximize or minimize the objective function. This approach will be used in the RRA

techniques proposed in this thesis.

- **Heuristics:** It refers to experience-based techniques for problem solving, which are used to find sub-optimum solutions hopefully close to the optimum with much less complexity than other conventional combinatorial optimization techniques. It has been widely used by many works in the literature. This approach will be used in the RRA techniques proposed in this thesis.

Chapter 3

Energy Efficient Resource Allocation with Energy Harvesting Nodes and QoS Constraints over Flat-Fading Channels

3.1 Introduction

In this chapter we face the problem of RRA strategies in a downlink scenario where the receivers are battery-powered devices. Hence, the energy information of each user, that is, the knowledge about their battery status will be available at the transmitter for a suitable efficient resource allocation. Nodes are provided with energy harvesting sources that allows them to recharge their batteries at a given time instants. For simplicity, Rayleigh flat-fading channels are considered in this chapter. Therefore, there will not be subcarrier assignment. Only power allocation, bit-rate and bandwidth will be assigned by the scheduler. Energy consumption models for the transmitter and receiver will be presented. These models will be used throughout the whole thesis.

3.2 System Model

Let us consider a set of users indexed by $k \in \mathcal{K} \triangleq \{1, \dots, K\}$ with a finite battery capacity, C_{max}^k . As mentioned in the introduction, we focus on a broadcast scenario where K single-

antenna receivers are served by a single-antenna transmitter. This scenario has two potential applications, namely the downlink in a cellular network and the first phase or hop of a multiple parallel relay channel (see Fig. 1.2 and 1.3). We index time by the slot $t \in \mathcal{T} \triangleq \{1, \dots, T\}$ with a duration of T_l seconds per time-slot. Receivers are provided with an energy harvesting source that allows them to recollect energy dynamically from the environment to be used in the transmission or reception. We follow a discretized model for energy arrivals where energy is collected by the receiver at known time instants. For simplicity in the notation, we consider that the receivers are only allowed to collect energy between time slots, being $E_k(t)$ the energy harvested in Joules by the k -th user at the t -th time slot, but it is easy to generalize it having different harvesting sources. Therefore, energy harvested at time slot t is available at time slot $t + 1$. For the sake of simplicity, we assume that all users are provided with the same energy harvesting sources and therefore, the energy packets contain the same amount of Joules for all users, whenever the harvesting source is able to collect energy. Hence, $E_k(t) \in \{0, E\}$, where E is the amount of Joules contained in an energy packet. Receivers feed back their current battery status at the beginning of the allocation, that is, at $t = 1$, and then for the next T time-slots, it is only necessary to feed back whether there is energy available at the harvester at the end of each time slot. This can be implemented with a single bit feedback channel whenever energy is available. That makes the resource allocation very efficient in terms of feedback channel usage. BS can estimate the energy spent by the receivers at each time slot using the models presented in further sections of this chapter.

At the allocation stage, bandwidths are assigned disjointly to the users. For the sake of simplicity, the frequency band for a given user is considered to be flat fading. Assume there is a total bandwidth W_T to be scheduled at each time slot. The channel gains between the BS and the receivers during the t -th time slot $g_k(t) \in \mathbb{C}$ are modeled by a i.i.d. random complex Gaussian variables $\sim \mathcal{CN}(0, \sigma_{h_k}^2)$, being $\sigma_{h_k}^2$ the channel variance and k the receiver index. We also assume that at the beginning of each allocation all the receivers feed back their channel informations and, thus, BS is provided with CSI. To better describe the model, we provide the following definitions:

Definition 1 (Battery without harvesting). *The battery of the k -th user, denoted by $C_k(t)$, corresponds to the amount of available energy at the end of the t -th time slot, just before any potential harvesting. As commented before, we consider receivers with finite battery capacity, C_{max}^k . Hence, $C_k(t)$ must always fulfilled that $0 \leq C_k(t) \leq C_{max}^k, \forall t, k$.*

Definition 2 (Battery with harvesting). *The battery of the k -th user after adding the energy collected by the harvesting source, is denoted as $\tilde{C}_k(t) = \max\{C_{max}^k, C_k(t) + E_k(t - 1)\}$.*

Due to the harvest source, overflows of the battery may be produced. Thus, the energy lost due to overflow at t -th time slot by k -th receiver, denoted as $O_k(t)$ is $O_k(t) = \max\{0, C_k(t) +$

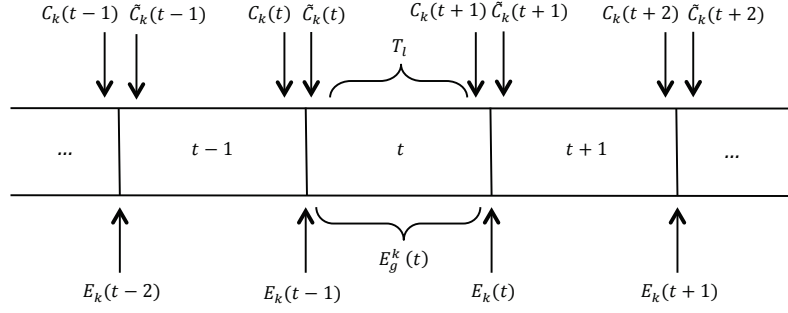


Figure 3.1: Time slot structure and energy arrivals

$E_k(t-1) - C_{max}^k$. Notice that overflow assures that the battery level will never be above the maximum battery capacity. Also note that battery level has units of capacity, whereas energy has units of Joules. Capacity and energy are related through the voltage consumption of the circuit. For simplicity, we consider the voltage of the circuit to be 1 volt, and thus, the relation between the battery level and the energy stored in the battery in units of milliAmpere-hour (mAh) and Joules (J) is $1 \text{ mAh} \equiv 3.6 \text{ J}$. Thanks to that, we can operate directly with energy and capacity units.

Definition 3 (Energy available for scheduling). *The energy available for the scheduling algorithm at the BS of the k -th user at the t -th time slot is denoted by $E_g^k(t)$.*

Notice that $E_g^k(t)$ is different from the current battery level $\tilde{C}_k(t)$, since as it will be shown later, in most of the cases not all the battery level is allowed to be used at the scheduling stage, but only a fraction of $\tilde{C}_k(t)$ will be used in order to restrict the energy spent by the receiver when decoding the information.

Fig. 3.1 depicts the time slot structure and at what time instants energies are collected and are available for allocation at BS.

3.2.1 Power Consumption Models

In this section we present the models of the energy consumed by the receiver and the transmitter. As presented before, in order to minimize the total energy consumption, all RF and signal processing blocks should be considered in the optimization model and not only the radiated power, as done classically. The energy consumed by the transceiver can be separated into two groups: the energy consumed by the RF components and the energy consumed by the baseband signal processing algorithms. Thus, the power consumed by the transceiver is

$$P_{c,tot} = P_{bb} + P_c, \quad (3.1)$$

where P_{bb} is the power consumed by the baseband signal processing algorithms and P_c models the power consumed by RF subsystems. In [Marcu "a 90 nm"], authors show that for high data rate communication, the power required for decoding dominates other sinks of power, such as other baseband signal processing techniques or even RF components. As we focus on a downlink scenario, P_{bb} corresponds to the power consumed by the receivers at the decoding stage, that is, $P_{bb}^{rx} = P_{dec}^{rx}$. On the other hand, we assume no complicated baseband signal processing techniques at the transmitter side, so $P_{bb}^{tx} = 0$. This is true since the complexity of signal processing algorithms at transmission is considerably low compared with the processing needed at the receiver side. Usually, decoding algorithms are highly demanding in terms of computational requirements.

RF Components

The RF model proposed in this thesis is based on [13], which is shown in Fig. 3.2. It presents the RF blocks of the transmitter and the receiver. On the transmitter side, the signal is first converted to an analog signal by using a digital-to-analog converter (DAC). Then it is filtered by a conventional filter and modulated with the local oscillator (LO) and the mixer. Finally it is amplified by the power amplifier (PA) and transmitted to the channel through the antenna. The receiver model is using a reverse architecture based on the transmitter. These architectures are very generic and a different architecture could be easily adapted. We assume all blocks at both sides are always in active mode, even though there is no signal to transmit or the receive. Another possible strategy could be to take into account the time the transceiver is active and inactive and include such times in the optimization problem. In classical approaches, i.e., large distances between nodes, the power consumed by the PA was highly dominant, and it made no sense to include other parts of RF chain. This is not so for short distances, where the path losses are low, and therefore the power needed in the PA is also low.

Taking all this into account, the total power consumption by the transmitter RF blocks can be modeled as:

$$P_c^{tx} = P_{mix} + P_{syn} + P_{filt} + P_{DAC}, \quad (3.2)$$

where P_{mix} is the mixer power consumption, P_{syn} is the frequency synthesizer power consumption and, P_{DAC} is the power consumed by the DAC block. In the same manner we can define the power consumption at the receiver system:

$$P_c^{rx} = P_{mix} + P_{syn} + P_{LNA} + P_{filr} + P_{IFA} + P_{ADC}, \quad (3.3)$$

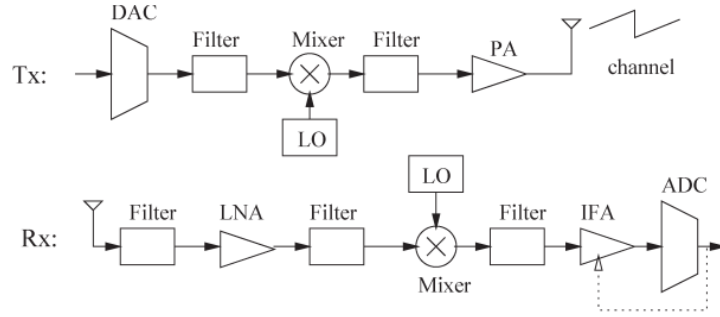


Figure 3.2: Transceiver circuit blocks

where P_{LNA} and P_{IFA} are the power consumed by the Low Noise Amplifier (LNA) and Intermediate Frequency Amplifier (IFA) and P_{ADC} is the analog-to-digital converter consumed power. The specific consumption model of each of the components can be found in [13]. If sleep mode is used, as for example in wireless sensor networks, minor changes must be applied to the models proposed. For further details see [13].

Baseband Signal Processing Consumption

As mentioned before, we assume no complicated models of signal processing are applied at the transmitter side. Transmitted signals are orthogonal to different users and there is no need to include any pre-cancellation techniques such as dirty paper coding. Therefore, the energy consumed by the baseband signal processing algorithms at the transmitter is considered negligible and, thus, it will be omitted in the design. Moreover, we are dealing with a downlink scenario, where the BS is connected to a energy source and in this case, BS is not energy-limited. On the other hand, the energy consumed by the receivers should be taken into account since the users are considered battery-powered devices closely placed to the BS. Even though we focus on a broadcast scenario, it is clear to see that all these ideas also apply to the first phase of a multiple parallel relay channel. It is shown in [24], [13], [44] that operating in short ranges, the transmit power can be significantly smaller than the power consumed in decoding. Hence, it seems reasonable to include decoding power in the downlink scenario. From now on, we omit the upper-index rx to refer to power of decoding at the receiver.

There are different models for P_{dec} in the literature. In [?] authors claim that P_{dec} is linearly related with the data rate at reception. The proposed model is

$$P_{dec} = \frac{\xi_D E_{node} m l R_{dec}}{R_{ch}}. \quad (3.4)$$

The data rate is proportional to R_{dec} which it affects linearly the power consumed by decoding stage.

Authors in [11] propose a power estimation model for Viterbi decoding algorithms. They also claim that the consumed power by the Viterbi algorithm grows linearly with the data rate. The model proposed in this case is,

$$P_{dec} \approx (P_v)_{ref} \frac{R/kB_r V_{dd}^2 L_D N_s (L_m + L_w + 104)}{1.38 \times 10^6}. \quad (3.5)$$

Most of the variables given in previous model are decoder specific and a full analysis of it is out of the scope of the thesis and can be found in [11].

However, there are other models in the literature. In [43] authors propose an exponential model for the decoding complexity. They claim that the state space and the number of possible state transitions in the decoder-trellis expands exponentially with the data rate. In fact, they say that the computation power can be expressed as,

$$P_{dec} = c_1 c_2^{c_3 R}, \quad (3.6)$$

where the constants c_j are decoder specific and R is the data rate. In fact, in order to be more general, all the constants c_j should be user-dependent, since in real scenarios, users may have different implementations of the Viterbi algorithm. Then, the computation power of the k -th user is modeled as,

$$P_{dec,k} = c_{1k} c_{2k}^{c_{3k} R}. \quad (3.7)$$

Also, let us denote for convenience, $c_1 c_2^{c_3 R}$ as $c_1 e^{c_4 R}$, where $c_4 = c_3 \ln(c_2)$. The previous model may be the object of some criticism due to the fact that the computation power is not zero when the rate assigned to the user is zero. A possible interpretation of this phenomenon can be considered to be RF power consumption, such as for instance the power consumption of the electronics of the decoder itself when it is in idle state. However, a more accurate model would be

$$P_{dec,k} = c_{1k} (e^{c_{4k} R} - 1). \quad (3.8)$$

Therefore, the total power consumption of the receiver is modeled as

$$P_{c,tot,k}^{rx} = P_{dec,k}(R) + P_c^{rx}, \quad (3.9)$$

and the energy consumed by the whole receiver is described as

$$T_l \cdot (P_{dec,k}(R) + P_c^{rx}) \leq E_g^k(t), \quad (3.10)$$

where T_l is the duration of the time-slot in seconds. As it is expressed, the energy consumed by the receiver must be lower than the energy allowed by the scheduling algorithm, $E_g^k(t)$ for the k -th user, that is a fraction of the current battery level of the user as it will be seen in further sections. This is, in fact, a constraint to be added in the resource allocation algorithm. This will be presented and commented with more details in §3.3. The previous constraint can also be thought as an upper bound on the maximum data-rate to be attained by the k -th user at the t -th time slot,

$$R_{max,k}(t) \geq R_k(t), \quad (3.11)$$

which provides a general framework regardless the model of the baseband signal processing consumption used. The relation between the $R_{max,k}(t)$ and the energy allowed by the scheduling is

$$R_{max,k}(t) = P_{dec,k}^{-1} \left(\frac{E_g^k(t)}{T_l} - P_c^{rx} \right). \quad (3.12)$$

For the particular case of the exponential model, the relation between the maximum data-rate and energy is as follows

$$R_{max,k}(t) = \frac{1}{c_{4k}} \ln \left(\frac{E_g^k(t) - P_c^{rx} T_l}{T_l c_{1k}} \right). \quad (3.13)$$

If we consider the case of linear model of power consumption, the relation between the maximum data-rate and energy is now

$$R_{max,k}(t) = \frac{1}{\nu} \left(\frac{E_g^k(t) - P_c^{rx} T_l}{T_l} \right), \quad (3.14)$$

where ν is a constant that incorporates all the decoder parameters presented in (3.4) and (3.5).

Therefore, at each time slot, the BS will allocate a given $E_g^k(t)$ and thus, the rate obtained by the allocation algorithm must fulfilled $R_k(t) \leq R_{max,k}(t)$.

3.3 Energy Efficient Sum-Rate Maximization with QoS Constraints

In this section, we consider the problem of sum-rate maximization under constraints in the maximum energy spent per receiver. This problem was studied long time ago in terms of resource allocation, but to the best of our knowledge, no one has included any information regarding the battery status of the terminals nor the harvesting capabilities of the receivers.

There are other works in the literature, such as [15], [1] that considered other objective functions. For instance, it is well known that taking the geometric mean of the receiver rates as a objective function provides fairness between users in terms of similar data-rates. Other techniques such as the maximization of the minimum user data-rate (*maximin* approaches) may also be considered. We study different approaches in further sections that will be compared with the one presented in this section based on the maximization of the sum-rate. Given all that, the problem of resource allocation with QoS constraints is formulated as follows:

$$\begin{aligned}
& \underset{\{R_i, p_i, B_i\}_{i=1}^K}{\text{maximize}} && \sum_{i=1}^K R_i && (3.15) \\
& \text{subject to} && C1 : \sum_{i=1}^K p_i + P_c^{tx} \leq P_{max} \\
& && C2 : \sum_{i=1}^K B_i \leq W_T \\
& && C3 : -B_i \log\left(1 + \frac{p_i |g_i(t)|^2}{B_i N_0}\right) + R_i \leq 0, \quad i = 1, \dots, K, \\
& && C4 : R_{max,i} \geq R_i, \quad i = 1, \dots, K, \\
& && C5 : R_i \geq \text{qos}_i, \quad i = 1, \dots, K, \\
& && C6 : p_i \geq 0, \quad i = 1, \dots, K, \\
& && C7 : B_i \geq 0, \quad i = 1, \dots, K,
\end{aligned}$$

where p_i and B_i are the power allocated and the bandwidth assigned to the i -th user. R_i is the data-rate of i th user, and the objective function to be optimized is what is called the sum-rate, i.e., the sum of all receiver rates. qos_i represents a minimum data-rate to be assigned to i -th user, and P_{max} the maximum transmit power available at the BS. Constraint $C4$ considers the limitation of energy to be spent by receivers (it is a general model, where the data-rate is constrained to have a maximum value, see (3.13) and (3.14)). Notice that, the model of energy consumption does not affect the solution of the problem.

In current mobile standard communications, the bandwidth assignment is implemented through sub-carriers using the modulation OFDM based on the access technology OFDMA [50], [18]. OFDMA assigns a set of sub-carriers to each user and loads a given number of bits per carrier in order to fulfill the requirements of QoS. Sub-carriers do not necessarily have to be adjacent. In order to formulate our bandwidth allocation problem in terms of sub-carrier allocation, an integrity constraint must be added in order to guarantee univocal assignment of the sub-carrier. However, if the number of sub-carriers is high enough with a small frequency inter-carrier separation and considering flat-fading conditions, the proposed problem in this section, (3.15), would yield to almost the same results.

The previous problem is a convex optimization problem where the objective function and the constraints are easily verified to be convex. The objective function is a sum of piece-wise linear functions of R , and thus convex. $C1$ is affine since we have a linear sum over p_i 's and a constant and hence convex. The same reasoning can be applied for $C2$. $C4 - C7$ are all linear on the design variables, and hence convex. Convexity of $C3$ is provided in the following lemma:

Lemma 3.1. *Constraint $C3$ of problem (3.15) is jointly convex on B_i and p_i .*

Proof. See Appendix 3.A. ■

This implies that the solution to the problem can be obtained by using one of the multiple efficient algorithms such as the interior point methods [7]. The key point of the design is to provide a framework that maximizes the time-of-live of all terminals providing at the same time a certain QoS. In order to achieve that, the variable $E_g^k(t)$ plays an important role. This variable, which is user and time-dependent, controls the maximum rate assigned to a given user and provides the total energy available to be spent by the k -th user at t -th time slot. When trying to optimize the sum-rate, there exists a trade-off between the associated rate and the energy spent by the receiver. The higher the rate assigned, the more energy spent and the lower the battery level will be. By contrast, thanks to the harvesting property of receivers, the scheduler could increase the time-of-live of receivers and at the same time obtain a considerably gain in average sum-rate with respect to traditional sum-rate schedulers that do not consider energy constraints and allow to have big peak rates, which most of the times are unnecessary, and will cause the user to quickly run out of battery.

Optimality Conditions

Let R_i^* , p_i^* , and B_i^* be any primal optimal points. The previous problem has infinite possible optimal solutions ¹ that will be achieved depending on the algorithm. One solution is to attain the maximum transmitter power, $\sum_{i=1}^K p_i^* + P_c^{tx} = P_{max}$ and have $\sum_{i=1}^K B_i^* \leq W_T$ whereas the other solution minimizes the power, having fixed the sub-carrier assignment, $\sum_{i=1}^K B_i^* = W_T$ and varying the powers $\sum_{i=1}^K p_i^* + P_c^{tx} \leq P_{max}$. If a general solver is used, this cannot be controlled in principle. If a customized algorithm is developed, one of the two solutions must be chosen. The following lemma follows easily:

Lemma 3.2. *The data-rate function $R_i = B_i \log\left(1 + \frac{p_i |g_i(t)|^2}{B_i N_0}\right)$ is monotonically increasing in p_i and B_i .*

¹i.e., infinite different solutions that achieve the optimum value of the objective function and that fulfill the constraints.

Proof. See Appendix 3.B. ■

Due to previous lemma, we are able to claim that constraint C3 is tight at the optimum value, i.e., $R_i^* = B_i^* \log\left(1 + \frac{p_i^* |g_i(t)|^2}{B_i^* N_0}\right)$, since if $R_i^* < B_i^* \log\left(1 + \frac{p_i^* |g_i(t)|^2}{B_i^* N_0}\right)$ we can decrease p_i^* or B_i^* and still fulfill all the constraints. As a consequence of that, it is easily verified that if $p_i^* = 0 \implies B_i^* = 0$ and $R_i^* = 0$. The converse is also true for all variables, that is, if $B_i^* = 0 \implies p_i^* = 0$ and if $R_i^* = 0 \implies B_i^* = 0$ and $p_i^* = 0$.

Slater's constraint qualification holds for this problem and, thus, the KKT are necessary and sufficient conditions for optimality (see Appendix 3.C). Therefore, when the primal problem is convex any primal and dual points that satisfy the KKT conditions are in fact the optimal points.

3.3.1 Energy Allocation at Each Iteration

The scheduler must assign the value of $E_g^k(t)$ for all users at the beginning of the t -th time-slot. As mentioned before, this value represents a given portion of the current battery $\tilde{C}_k(t)$ of the receiver that is allowed to be spent. This $\tilde{C}_k(t)$ already includes the harvested energy, thus $\tilde{C}_k(t) = \max\{C_{max}^k, C_k(t) + E_k(t-1)\}$. A possible solution is to assign constantly a fixed percentage amount of the $\tilde{C}_k(t)$ to be the available energy to spend by the receiver, i.e., $E_g^k(t)$. Hence, $E_g^k(t) = \alpha \tilde{C}_k(t)$, such as for example a given percentage of the current battery level. The impact of α in the design lies on the fact that higher values of α will allow to achieve high data-rates but the battery level will decrease considerably. If, on the other hand, α is relatively small, it will constraint a lot the maximum data-rate, increasing notably the life-time of this user due to small energy consumption. Notice then, that α controls the trade-off between the data-rate and the life-time of the user. For the sake of simplicity, we consider all users to have the same implemented Viterbi decoder. The scheduling algorithm considering assignment of energies is as follows:

Algorithm 1: Battery update and energy allocation

1: **set** minimum rates (qos_k) and initial energies:

$$E_g^k(t) = \alpha \tilde{C}_k(t) \text{ for } k = 1, \dots, K$$

2: **solve** optimization problem (3.15) and obtain:

$$R_k^*, p_k^*, B_k^* \text{ for } k = 1, \dots, K$$

3: **set** battery level according to data-rate used:

$$C_k(t+1) = \tilde{C}_k(t) - T_l (P_{dec}(R_k(t)) + P_c^{tx}) \text{ for } k = 1, \dots, K$$

4: **update** battery level according to harvesting:

$$\tilde{C}_k(t+1) = \max\{C_{max}^k, C_k(t+1) + E_k(t)\} \text{ for } k = 1, \dots, K$$

5: **updates** energies to users:

$$E_g^k(t+1) = \alpha \tilde{C}_k(t+1)$$

6: **go** to step 2

3.3.2 Sub-Optimal Case: Fixed Transmission Bandwidth

In this section we consider a sub-optimal case based on the previous optimization problem. Now, the bandwidths are fixed for all users and only the powers and the data-rates are available in the design. For this sub-optimal problem we are able to develop an analytical solution for the problem from the KKT optimality conditions.

Let us start by defining the problem:

$$\begin{aligned}
 & \underset{\{R_i, p_i\}_{i=1}^K}{\text{maximize}} && \sum_{i=1}^K R_i && (3.16) \\
 & \text{subject to} && C1 : \sum_{i=1}^K p_i + P_c^{tx} \leq P_{max} \\
 & && C2 : -B \log(1 + p_i \lambda_i) + R_i \leq 0, \quad i = 1, \dots, K, \\
 & && C3 : R_{max,i} \geq R_i, \quad i = 1, \dots, K, \\
 & && C4 : R_i \geq qos_i, \quad i = 1, \dots, K, \\
 & && C5 : p_i \geq 0, \quad i = 1, \dots, K,
 \end{aligned}$$

where λ_i represents $\frac{|g_i(t)|^2}{N_0}$. In order to simplify the problem and reduce one constraint so that one Lagrange multiplier is avoided, we transform the previous QoS-constrained problem into an equivalent unconstrained QoS problem.

Lemma 3.3. *The convex optimization problem (3.16) with QoS constraints is equivalent to the convex optimization problem defined in (3.17) without QoS constraints.*

Proof. See Appendix 3.D. ■

$$\begin{aligned}
& \underset{\{R_i, \tilde{p}_i\}_{i=1}^K}{\text{maximize}} && \sum_{i=1}^K R_i && (3.17) \\
& \text{subject to} && C1 : \sum_{i=1}^K \tilde{p}_i + P_c^{tx} \leq \tilde{P}_{max} \\
& && C2 : -B \log(\theta_i + \tilde{p}_i \lambda_i) + R_i \leq 0, \quad i = 1, \dots, K, \\
& && C3 : R_{max,i} \geq R_i, \quad i = 1, \dots, K, \\
& && C4 : R_i \geq 0, \quad i = 1, \dots, K, \\
& && C5 : \tilde{p}_i \geq 0, \quad i = 1, \dots, K.
\end{aligned}$$

Slater's constraint qualification also holds for this problem and thus, KKT conditions are necessary and sufficient for optimality. Hence, by solving the KKT condition (see Appendix 3.E) we are able to provide an analytical solution. The power allocation for the i -th user becomes,

$$\tilde{p}_i^* = \left[\frac{(1 - \alpha_i^*)B}{\sigma^* \ln(2)} - \frac{\theta_i}{\lambda_i} \right]^+, \quad (3.18)$$

where $f[x]^+ = \max(0, x)$, and α_i^* and σ^* are Lagrange multipliers. If i -th user is not saturated in C3, i.e., $R_{max,i} > R_i^* \implies \alpha_i^* = 0$ by the complementary slackness. Thus, $\tilde{p}_i^* = \left[\frac{B}{\sigma^* \ln(2)} - \frac{\theta_i}{\lambda_i} \right]^+$, which is a classical water-filling solution with activation order given by $\frac{1}{\sigma^*} > \frac{\theta_i \ln(2)}{\lambda_i}$. On the other hand, if user is saturated, i.e., $R_{max,i} = R_i^*$, then $\tilde{p}_i^* = \frac{R_{max,i} - \theta_i}{\lambda_i}$. By inspection, we are also able to find a saturation order, according to C3, that will help us to develop an efficient algorithm that attains the optimum value. The condition for the i -th user to be saturated is $\frac{1}{\sigma^*} \geq \frac{\ln(2)2^{\frac{R_{max,i}}{B}}}{\lambda_i}$. The converse is also true, that is, if for i -th user $\frac{1}{\sigma^*} \geq \frac{\ln(2)2^{\frac{R_{max,i}}{B}}}{\lambda_i}$ holds, then the user is saturated. It may seem that by having a small value of λ_i and also small value of $R_{max,i}$ the user could be saturated and at the same time no active, which makes no sense. The following trivial lemma follows:

Lemma 3.4. *If a user is not active it cannot be saturated regardless the value of R_{max} and λ that it has.*

Proof. See Appendix 3.F. ■

Let us denote $s(i)$ as the index of the i -th saturated user and let also $c = \frac{B}{\sigma^* \ln(2)}$. The developed algorithm that attains the optimum value is presented below.

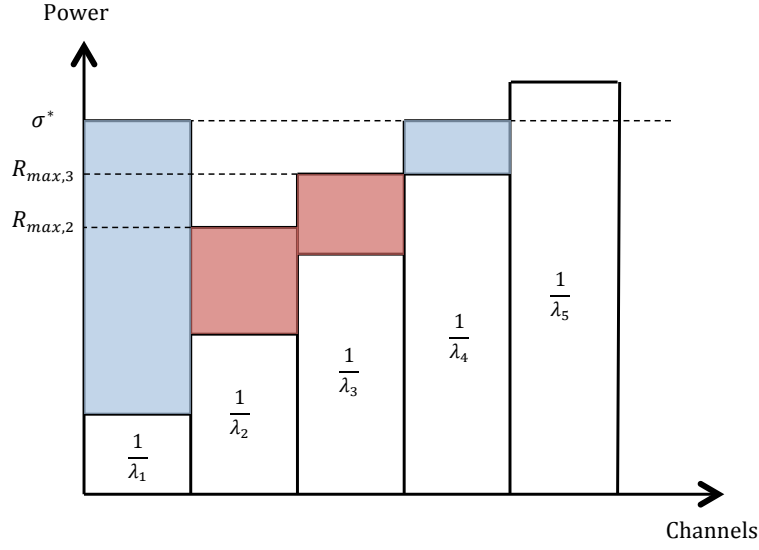


Figure 3.3: Modified water-filling algorithm

Algorithm 2: Rate and power allocation with fixed bandwidth

- 1: **set** $\zeta_j = \frac{2 \frac{R_{max,j}}{B}}{\lambda_j} \rightarrow$ order increasingly
 - 2: $\mathcal{A} = \{1, 2, \dots, K\}; k = 1$
 - 3: **solve** $c : \sum_{j \in \mathcal{A}} \left(c - \frac{\theta_j}{\lambda_i} \right)^+ = \tilde{P}_{max}$
 - 4: **if** $c \geq \zeta_k$ **then**
 - 5: $P_k = \frac{2 \frac{R_{max,k}}{B} - \theta_k}{\lambda_k}$
 - 6: $\tilde{P}_{max} \leftarrow \tilde{P}_{max} - \sum_{j=1}^k P_k$
 - 7: $\mathcal{A} \leftarrow \mathcal{A} - \{s(k)\}$
 - 8: $k \leftarrow k + 1$
 - 9: **go to** 2
 - 10: **end if**
 - 11: **assign** $\tilde{p}_i^* = \min\left(c - \frac{\theta_i}{\lambda_i}, \zeta_k\right) \rightarrow p_i^* = \tilde{p}_i^* + p_{min,i}$
 - 12: $R_i^* = B \log\left(1 + p_i^* \lambda_i\right)$
 - 13: **end algorithm**
-

Fig. 3.3 depicts the results of the modified water-filling algorithm presented before. For the sake of simplicity users are ordered increasingly. In the Fig., users two and three are battery-limited and therefore they cannot achieve the water-level. Users one and four are not yet energy-limited, whereas user five has no allocated power.

3.3.3 Simulation Results

In this section we present simulation results related to the previous resource allocation problems. For the optimal case with variable bandwidth assignment, we performed the simulations using the commercial build-in function of MATLAB *fmincon*. *fmincon* allows to find a minimum of a constrained nonlinear multivariable optimization problem, regardless of its convexity. However, since the problem (3.15) was proved to be convex, we assure to achieve the global optimum using *fmincon*. Nevertheless, results presented for the sub-optimal case were obtained by means of the greedy-like algorithm developed in the thesis and described at the end of §3.3.2.

In order to evaluate our algorithms, we compare them with other traditional resource allocation strategies. Two techniques were considered in the simulations: the maximization of the sum-rate without energy constraints (SR) and the maximization of the minimum user data rate (*maximin* approach). From now on, we will refer as SREE to the problem (3.15).

Table 3.1 depicts all the simulation parameters considered in the model. The values of the parameters concerning the RF blocks were extracted from [CUI]. We consider an exponential model for energy consumption of baseband signal processing algorithms where all users have the same algorithms implemented, although similar results could have been obtained following other consumption models. Additionally, simulations using a different value of the parameter α are shown. Initial level of batteries are assigned randomly between a minimum value, 1000mAh, and a maximum value, 15000mAh. This means that some users may have the same initial battery. Besides, we assume the maximum capacity level C_{max}^k is two times the initial value, thus, users start the reception with half of its total battery capacity.

We must say that the results are conditioned to the values of constants c_1 and c_4 . These constants control the relation between the data-rate and the energy consumption. In order to be able to see the performance of our algorithm in a short period of time, we assigned a sufficiently high values to these constants. However, by assigning them smaller values, more realistic data would be obtained, but longer simulations in time would be needed. The results are also conditioned to the size of the energy packet, which is assigned to be 100mAh. The harvesting allocation per time slot among users was implemented by assigning randomly to each user at each time slot two possible values, 0 or E (see Table 3.1). Thus, packets of energy of different time slots are independent. A more realistic case would take into account a bursty energy packet collection, since the source harvests energy under some conditions. For example if the node is static and the harvesting source is based on kinetic energy, no energy could be stored for a period of time. QoS is omitted in the SR approach since sometimes the battery level of the users do not allow to guarantee it, making the optimization problem

Table 3.1: Simulation parameters

Parameter	Value
Central frequency	2 GHz
Bandwidth	20 MHz
Number of users	up to 20
Frame duration	125 μ s
Time slot duration T_l	5 μ s
Maximum BS transmission power	1 W
P_{mix}	30 mW
$P_{filt} = P_{filtr}$	2.5 mW
P_{LNA}	20 mW
P_{syn}	50 mW
P_{IFA}	3 mW
$P_{ADC} = P_{DAC}$	60 mW
Energy packet size E	100 mAh
Battery capacity level	$1000 \leq C_{max}^k \leq 15000$ [mAh]
Channel model	Rayleigh flat-fading
Noise spectral density N_0	-174 dBm/Hz
Decoder constant c_1	200000
Decoder constant c_4	4.83×10^{-6}
Energy allocation parameter α	0.1 and 0.01
Mobile terminal speed	static
QoS	200 kbits/s
Number of channel realizations	500

infeasible.

All the plots shown in this section are averaged over 500 different channel realizations. Fig. 3.4 shows the evolution of the battery level of a system with four users for all models. As it was expected, the battery levels of the SR (3.4 (a)) decrease very fast making some users to run out of battery almost instantly. This is so, because the system does not limit the data-rate. A user can get a data-rate proportionally to the whole current battery level, even if he does not need it. This is the main drawback of SR approaches. On the contrary, the maximin approach (3.4 (b)) assigns (more or less) the same data-rate to all the users and it turns out to be the minimum required data-rate. If the required data-rate is low enough, users are able to improve its battery level due to the harvesting source. Finally we have the results for two different values of battery assignment parameter α (3.4 (c-d)) of the proposed model SREE. It can be seen that higher values of α makes the battery level to decrease faster than if smaller values are assigned to it. It is possible to find a balance where users do not spend more battery than the one they are using and collecting from the harvesting source. This is the case of (3.4 (d)).

Notice that, if the number of users is increased (see Fig. 3.5), there are some users that even in the SR approach are able to maintain its battery level quite high. This is due to the fact that, in order to maximize the sum-rate, there may be some users that are not served by the BS. This is the case where some users are far from the location of the BS. In order to compare the energy consumption with the assigned data-rate we provide with two figures. Fig. 3.6 shows the average between users under the four models with different number of users in the system. Fig. 3.7 presents the average data-rate distribution for the same models and number of users. Surprisingly, the SREE outperforms, in term of average data-rate, the case where no energy constraints are included. This is so because the SR model provides high peaks of data-rate to the users that translates in big amounts of energy consumed, yielding to users without battery for the future time-slots.

Fig. 3.8(a) depicts the evolution of the sum-rate when the number of users increases. Note that, the SREE with $\alpha = 0.1$ is better than the SR up to 16 users. Looking at Fig. 3.8(b) it is clear the improvement in terms of battery usage of SREE against SR. By assigning a higher value of α (for example $\alpha = 0.2$) we could assure a better sum-rate than SR regardless the number of users and still offer an improvement on the battery level.

Finally, Fig. 3.9 shows the comparison between the optimal bandwidth algorithm (3.15) and the fixed and equal bandwidth allocation case (3.17), where the transmission bandwidths were considered fixed among users. There exists a small difference in terms of the sum-rate between the optimal and sub-optimal models, but, on the other hand, the complexity of the

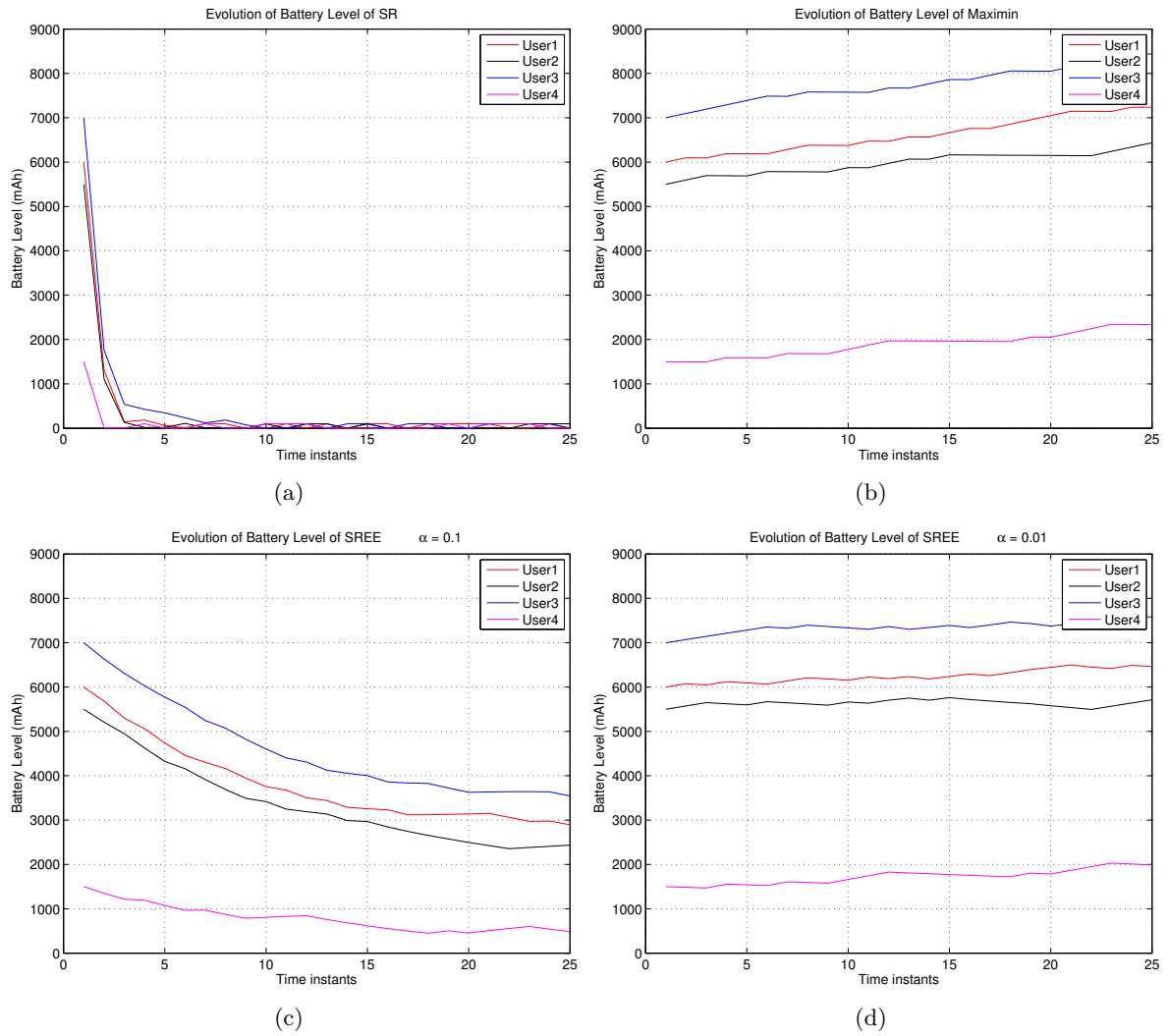


Figure 3.4: Battery evolution of 4 nodes with different approaches: (a) maximization of the sum rate and no energy constraints. (b) maximin rate approach and no energy constraints. (c) maximization of the sum rate with energy constraint and parameter $\alpha = 0.1$. (d) maximization of the sum rate with energy constraint and parameter $\alpha = 0.01$.

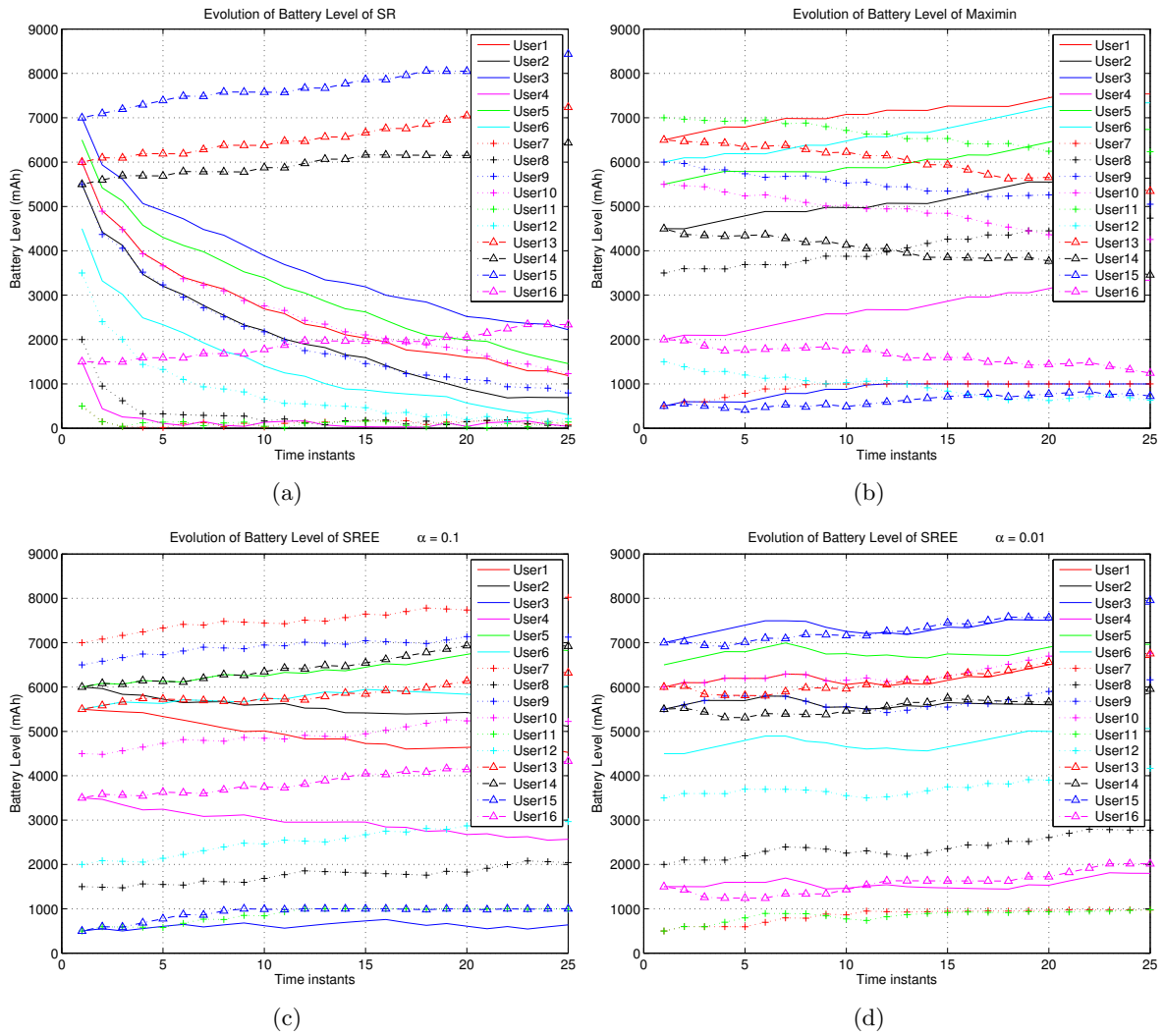


Figure 3.5: Battery evolution of 16 nodes with different approaches: (a) maximization of the sum rate and no energy constraints. (b) maximin rate approach and no energy constraints. (c) maximization of the sum rate with energy constraint and parameter $\alpha = 0.1$. (d) maximization of the sum rate with energy constraint and parameter $\alpha = 0.01$.

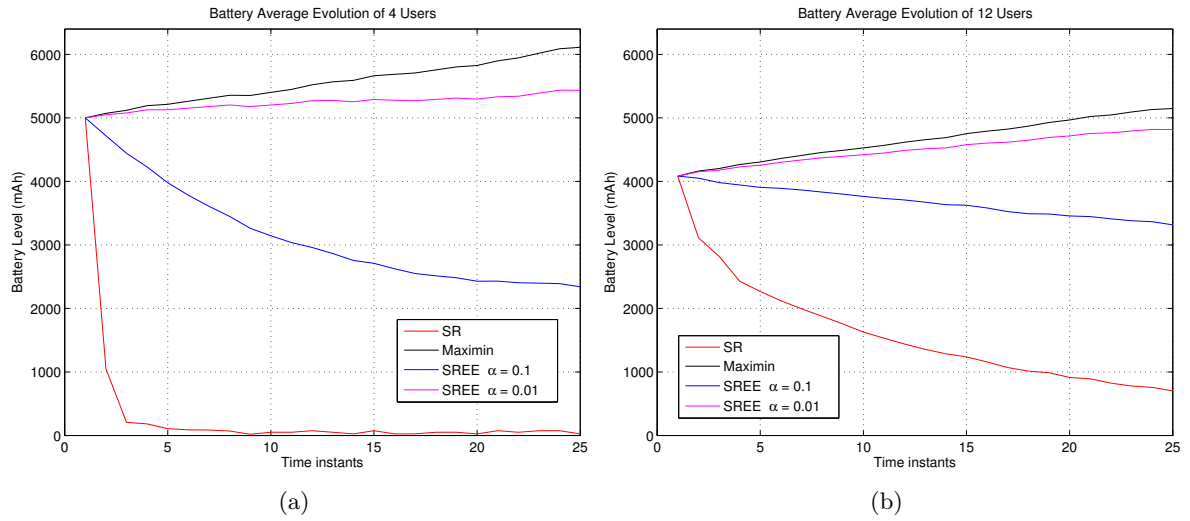


Figure 3.6: (a) Average battery evolution of 4 nodes. (b) Average battery evolution of 12 nodes

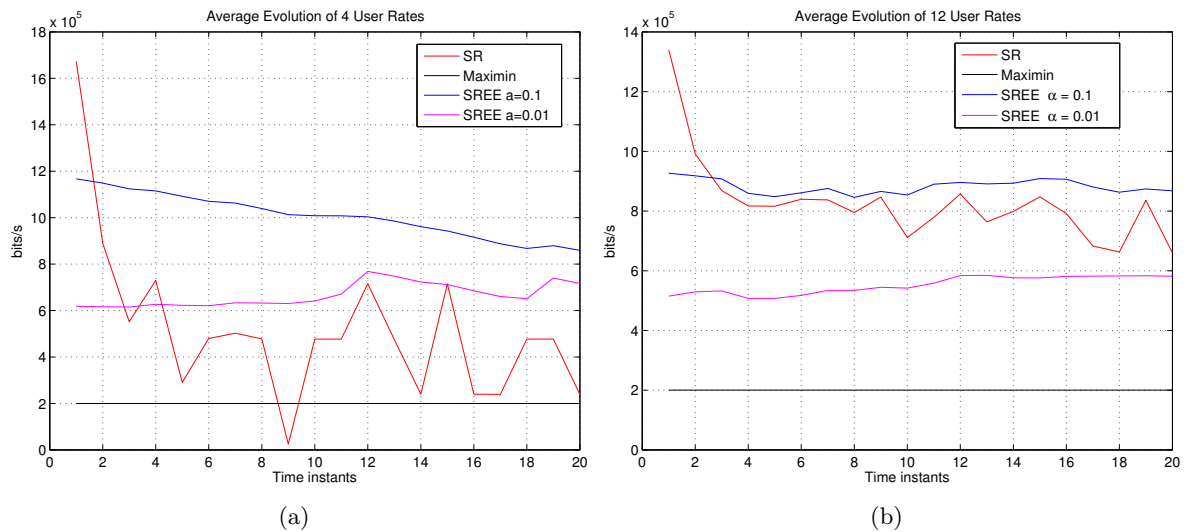


Figure 3.7: (a) Average data-rate evolution of 4 nodes. (b) Average data-rate evolution of 12 nodes.

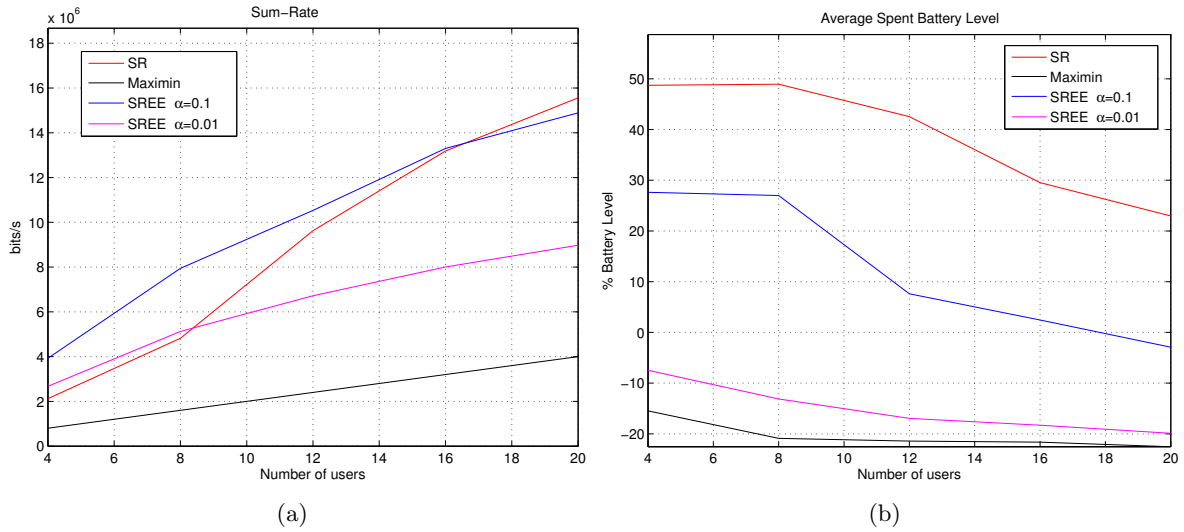


Figure 3.8: (a) Sum rate evolution. (b) Average percentage of battery level spent by users (a negative percentage means a gain in battery level).

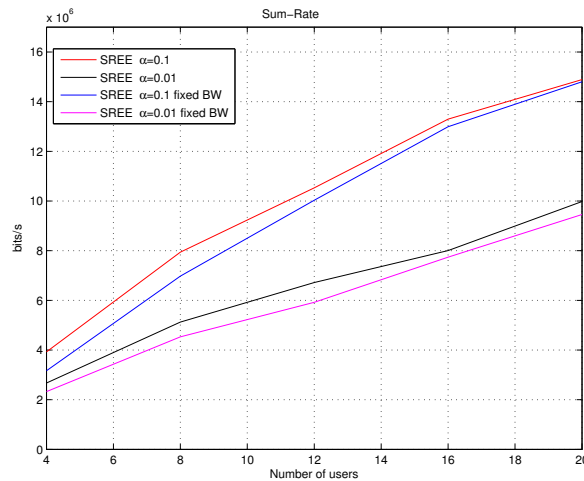


Figure 3.9: Sum-Rate comparison between optimal and suboptimal approaches.

sub-optimal case is reduced notably in front of the optimal one.

3.4 Energy Efficient Maximin with QoS Constraints

The classical maximin approach in resource allocation considered the problem of maximizing the minimum or worst user rate assignment. By means of this technique, fairness in terms of throughput between users was introduced. This problem has been studied in the literature in many different scenarios [1], [41]. In this section we propose a different maximin approach. Instead of considering to maximize the minimum user rate assignment, we maximize the minimum residual battery level after the allocation. For simplicity, we allow all users in the

system to have the same decoder algorithm, letting us remove the user-dependence of the decoding power P_{dec} . Thus, the optimization problem can be formulated as:

$$\begin{aligned}
 & \underset{\{R_i, p_i, B_i\}_{i=1}^K}{\text{maximize}} && \min_{i=1, \dots, K} \left(\tilde{C}_i(t) - T_l \cdot P_{dec}(R_i) - T_l \cdot P_c^{R_x} \right) && (3.19) \\
 & \text{subject to} && C1 : \sum_{i=1}^K p_i + P_c^{T_x} \leq P_{max} \\
 & && C2 : \sum_{i=1}^K B_i \leq W_T \\
 & && C3 : -B_i \log \left(1 + \frac{p_i |g_i(t)|^2}{B_i N_0} \right) + R_i \leq 0, && i = 1, \dots, K, \\
 & && C4 : T_l \cdot P_{dec}(R_i) + T_l \cdot P_c^{R_x} - \tilde{C}_i(t) \leq 0, && i = 1, \dots, K, \\
 & && C5 : R_i \geq \text{qos}_i, && i = 1, \dots, K, \\
 & && C6 : p_i \geq 0, && i = 1, \dots, K, \\
 & && C7 : B_i \geq 0, && i = 1, \dots, K.
 \end{aligned}$$

The previous optimization problem can be easily verified to be convex. Constraints $C1 - C3, C5 - C7$ were commented in §3.3. The objective function to be maximized is the minimum of a set of concave functions in R_i and thus, it is concave. $C4$ is easily verified to be convex on R_i . Note also that $C4$ assures that no more energy than the current battery level is spent for a given user. The direct way to solve the previous maximin problem is to first minimize the inner optimization problem, and then solve the outer maximization, either numerically or analytically. Most of the times, however, this approach is difficult because it is not possible to find analytically the inner solution, and therefore it requires a numerical solution that needs to be evaluated at each iteration of the outer maximization, which turns out to be required to solve the inner minimization numerically as many times as needed to achieve convergence. As a consequence, facing the problem directly requires a high computational cost to be solved. Fortunately, there are different ways to transform the original problem into an equivalent convex optimization problem.

Hence, we can reformulate the original problem into the following transformed convex

optimization problem:

$$\begin{aligned}
& \underset{t, \{R_i, p_i, B_i\}_{i=1}^K}{\text{maximize}} && t && (3.20) \\
& \text{subject to} && C1 : t \leq \tilde{C}_i(t) - T_l \cdot P_{dec}(R_i) - T_l \cdot P_c^{Rx} \\
& && C2 : \sum_{i=1}^K p_i + P_c^{Tx} \leq P_{max} \\
& && C3 : \sum_{i=1}^K B_i \leq W_T \\
& && C4 : -B_i \log\left(1 + \frac{p_i |g_i(t)|^2}{B_i N_0}\right) + R_i \leq 0, \quad i = 1, \dots, K, \\
& && C5 : T_l \cdot P_{dec}(R_i) + T_l \cdot P_c^{Rx} - \tilde{C}_i(t) \leq 0, \quad i = 1, \dots, K, \\
& && C6 : R_i \geq \text{qos}_i, \quad i = 1, \dots, K, \\
& && C7 : p_i \geq 0, \quad i = 1, \dots, K, \\
& && C8 : B_i \geq 0, \quad i = 1, \dots, K,
\end{aligned}$$

where a slack variable t has been introduced and the inner minimization has been transformed into a new set of constraints. The problem remains convex since the objective function is linear and $C1$ is convex in R_i . Therefore, the KKT conditions are necessary and sufficient for optimality since Slater's constraint qualification holds. Notice that now, all the available battery is available to the scheduler instead of a fraction of it. Note also that for this case, it is still needed the one-bit feedback channel to transmit the harvesting updates since problem (3.20) must be solved at each time slot and between time slots the scheduler has to update the value of $\tilde{C}_i(t)$ according to the harvesting. It is easy to realize that the previous problem has infinite number of solutions. This is so since the problem will only force the users associated with t^* (see constraint C1) to have a certain bit-rate, power and bandwidth to meet the constraint. What happens with the power, bandwidth and rates of the rest of users is not explicitly determined by the optimization problem. Different bit-rates assigned to the same users may lead to the same optimal value for the objective function as long as the bit-rates meet the other constraints (C2-C8). Let us put an example to make it clear. Let us imagine that, due to initial configuration (battery level, channel gain etc), there is only one user that achieves C1 with equality. This user is the one that after the allocation procedure yielded with the least residual battery level. The other users fulfill constraint C1 with inequality (their residual battery levels were higher). Then, there is no other constraint to assign power, bandwidth and bit-rates to the these users. Any rate, power and bandwidth configuration that fulfills constraints C2-C8 is valid. The final configuration will depend on how the specific solver faces the problem and, in general, we cannot choose the configuration. This is why we claim that there exists an infinite number of possible solutions. However, the

optimum solution that minimizes the energy is the one that assigns the value of ‘qos’ to the optimum rate for all users.

Another way to understand the resolution of the problem is by looking at it graphically. Imagine we are interested in observing what happens with the bit-rate configuration for all the users in terms of its sum, i.e., the sum-rate. The plot will represent the optimal objective value respect to the sum-rate. When two variables are traded-off we have a curve that is called the Pareto curve (see §2.1.5). Fig. 3.10 depicts a possible curve that represents the trade-off between the sum-rate and the optimal value of the problem (that is the least residual battery level). We can see that, having a solution called t_{sol}^* , there is an infinite number of possible sum-rates, which turns into individual rates, represented with the dotted red line.

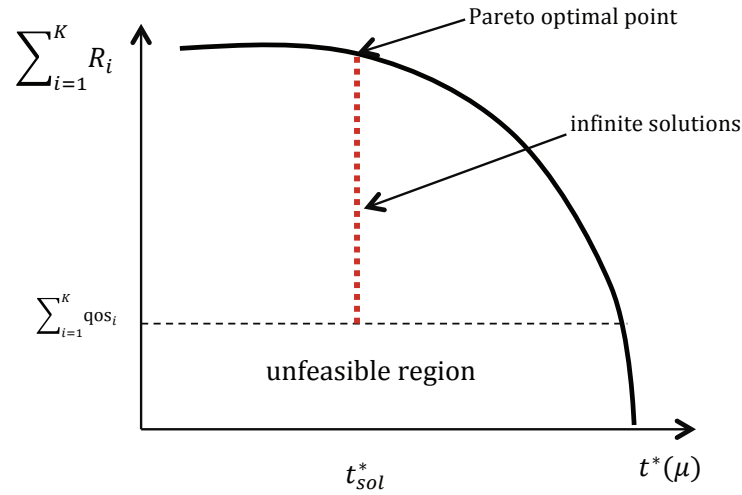


Figure 3.10: Trade-off between sum-rate and worst residual battery level

If we are interested in the solution that is Pareto optimal, that is the solution that maximizes the sum-rate for a given optimal objective value (in the graph is represented by the cross-point between the dotted red line and the Pareto curve), we need to redefine the problem introducing an extra objective function: we need the current objective function, (maximization of the minimum residual battery levels) and, on the other hand, we need the maximization of the sum-rate as another objective function. As a result, we end up with a problem with two objective functions (see §2.1.5). This problem will be addressed in next section.

3.5 Sum-Rate - Maximin Trade-off

We conclude in previous section that the maximin approach yielded to a convex optimization problem with infinite number of solutions. In this section we face a different problem where

the trade-off between the previous maximin problem and the sum-rate are both incorporated into the objective function. The problem, thus, becomes a multi-criterion optimization problem. We provide the Pareto-optimal points accounting for the solution of the maximin problem that maximizes the sum-rate. Therefore, a unique solution is obtained now.

There are several methods for finding the Pareto points of a multi-objective optimization problem. In this section, we follow the scalarization technique based on the weighted sum method [7], [16]. This method collapses the vector objective (bi-objective in this case) into a single objective component sum. According to the scalarization technique for multi-criterion problems, the allocation problem can therefore be stated as:

$$\begin{aligned}
& \underset{t, \{R_i, p_i, B_i\}_{i=1}^K}{\text{maximize}} && \sum_{i=1}^K R_i + \mu t && (3.21) \\
& \text{subject to} && C1 : t \leq \tilde{C}_i(t) - T_l P_{dec}(R_i) - T_l P_c^{R_x} \\
& && C2 : \sum_{i=1}^K p_i + P_c^{T_x} \leq P_{max} \\
& && C3 : \sum_{i=1}^K B_i \leq W_T \\
& && C4 : -B_i \log\left(1 + \frac{p_i |g_i(t)|^2}{B_i N_0}\right) + R_i \leq 0, \quad i = 1, \dots, K, \\
& && C5 : T_l \cdot P_{dec}(R_i) + T_l \cdot P_c^{R_x} - \tilde{C}_i(t) \leq 0, \quad i = 1, \dots, K \\
& && C6 : R_i \geq \text{qos}_i, \quad i = 1, \dots, K, \\
& && C7 : p_i \geq 0, \quad i = 1, \dots, K, \\
& && C8 : B_i \geq 0, \quad i = 1, \dots, K.
\end{aligned}$$

The Pareto-optimal curve can be computed by varying the value of μ within the interval $[0, \infty)$. Specifically, when μ approaches 0, all the emphasis is put on the sum-rate, which leads to the classical sum-rate maximization with no energy constraint, but the largest consumption. On the contrary, when μ increases, all the emphasis is put on the maximization of the minimum residual battery capacity, that is, the maximization of energy, all this achieving a certain QoS constraint.

The Pareto-optimal curves for a scenario with four users are shown in Fig. 3.11 and 3.12.

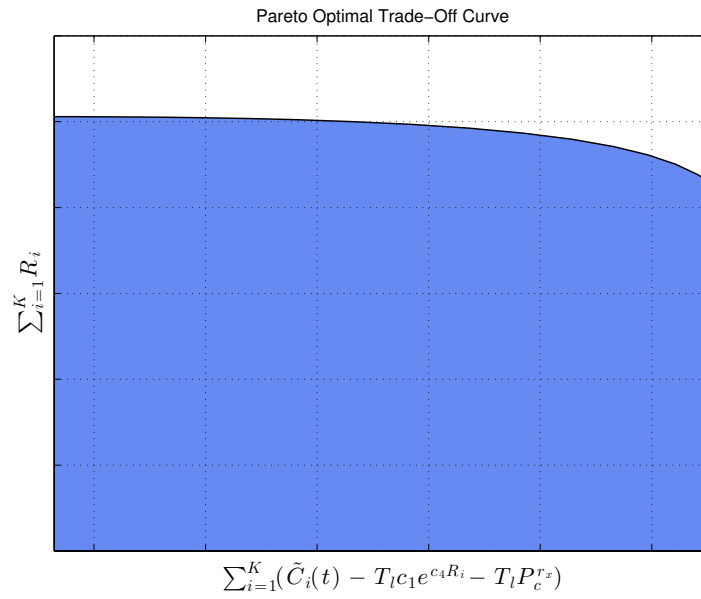


Figure 3.11: Trade-off curve between sum-rate and energy consumption using a exponential model for the decoding consumption model.

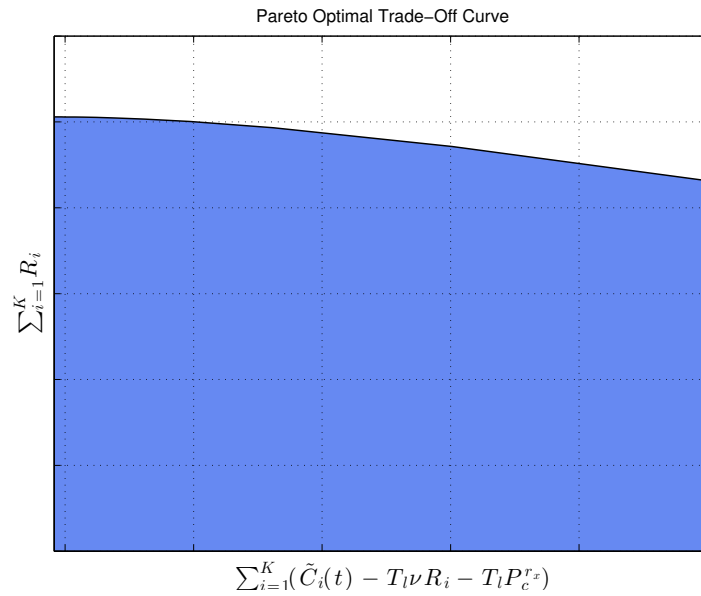


Figure 3.12: Trade-off curve between sum-rate and energy consumption using a linear model for the decoding consumption model.

3.6 Sum-Rate - Sum-Residual Trade-off

Motivated by the fact that we were not able to develop customized efficient algorithms to solve the previous optimization problem, we came up with a different optimization problem. Now, instead of maximizing the minimum of the battery level residuals, we include the sum of all the battery residuals of all users in the optimization, being the residual battery level, the level of battery after the allocation procedures. We propose a multi-criterion resource allocation problem where sum-rate and sum-residuals are to be traded off. First, we present the complete problem, where power, bandwidth, and data-rate are to be assigned. Then, we propose a sub-optimal allocation strategy based on fixed bandwidth assignment that reaches the optimal value by means of an iterative algorithm.

Exponential Model of Decoding Power

The optimization problem can be modeled as:

$$\begin{aligned}
& \underset{\{R_i, p_i, B_i\}_{i=1}^K}{\text{maximize}} && \sum_{i=1}^K R_i + \mu \sum_{i=1}^K \left(\tilde{C}_i(t) - T_l c_1 e^{c_4 R_i} - T_l P_c^{R_x} \right) && (3.22) \\
& \text{subject to} && C1 : \sum_{i=1}^K p_i + P_c^{T_x} \leq P_{max} \\
& && C2 : \sum_{i=1}^K B_i \leq W_T \\
& && C3 : -B_i \log \left(1 + \frac{p_i |g_i(t)|^2}{B_i N_0} \right) + R_i \leq 0, && i = 1, \dots, K, \\
& && C4 : R_{max,i} \geq R_i, && i = 1, \dots, K, \\
& && C5 : R_i \geq \text{qos}_i, && i = 1, \dots, K, \\
& && C6 : p_i \geq 0, && i = 1, \dots, K, \\
& && C7 : B_i \geq 0, && i = 1, \dots, K,
\end{aligned}$$

where $R_{max,i} = \frac{1}{c_4} \ln \left(\frac{\tilde{C}_i(t) - T_l P_c^{R_x}}{T_l c_1} \right)$ which assures that no more energy than the current available battery level is spent at the allocation. For this case we have that if μ approaches 0, all the emphasis is put on the sum-rate, which leads to the classical sum-rate maximization with no energy constraint, but the largest consumption. On the contrary, when μ increases, all the emphasis is put on the maximization of residual levels, that is, the maximization of energy, all this achieving a certain QoS constraint. The Pareto-optimal curve for a scenario with four users is shown in Fig. 3.13. Based on KKT observation (see Appendix 3.G), we are able to provide two upper-bounds in the following lemmas:

Lemma 3.5. *There exists a maximum value of weight μ , such that above this upper-bound*

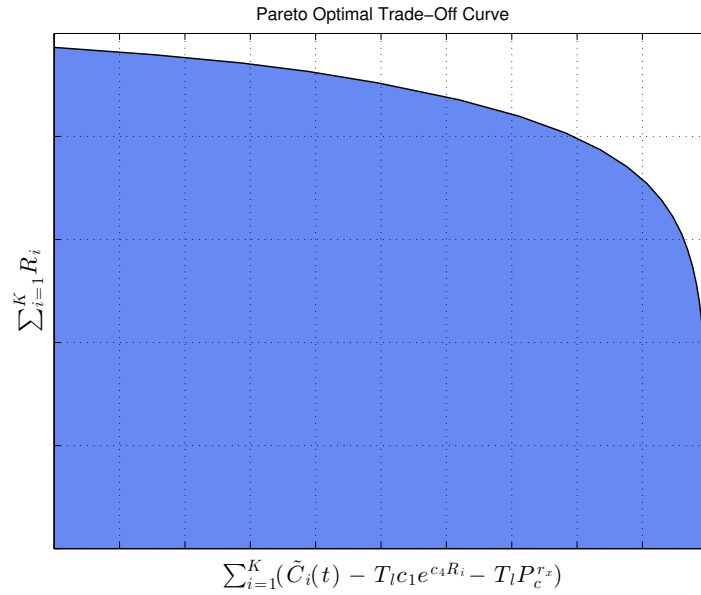


Figure 3.13: Trade-off between sum-rate and energy consumption

the data-rate optimum solution is always zero. The value of the maximum μ is:

$$\mu_{\max} = \frac{1}{T_l c_1 c_4 e^{c_4 \text{qos}_i}}. \quad (3.23)$$

Proof. See Appendix 3.I. ■

Lemma 3.5 provides an upper-bound on the value of μ . Hence the trade-off is only experienced when μ is within the interval $[0, \mu_{\max}]$.

Lemma 3.6. For a given μ, c_1 and, c_4 there is a maximum rate R_m to be attained by the receivers which is:

$$R_m = \frac{1}{c_4} \ln \left(\frac{1}{\mu T_l c_1 c_4} \right). \quad (3.24)$$

Proof. See Appendix 3.J. ■

Due to the nature of the problem, and the trade-off between maximizing the data-rate and maximizing the residuals, it appears this maximum data-rate which is of course independent of R_{\max} . Therefore, the problem has two upper bounds on the data-rates. If R_{\max} is higher than R_m then the upper bound that dominates is the lowest one, R_m in that case, and thus the user will never be saturated through $C4$. The converse is also true. R_m is the same for all users but it could be different if they had a different decoder, and therefore becoming constants c_j user-dependent.

Linear Model of Decoding Power

Now, we consider a linear model of decoding power. The problem is defined as:

$$\begin{aligned}
& \underset{\{R_i, p_i, B_i\}_{i=1}^K}{\text{maximize}} && \sum_{i=1}^K R_i + \mu \sum_{i=1}^K \left(\tilde{C}_i(t) - T_l \nu R_i - T_l P_c^{R_x} \right) && (3.25) \\
& \text{subject to} && C1 : \sum_{i=1}^K p_i + P_c^{T_x} \leq P_{max} \\
& && C2 : \sum_{i=1}^K B_i \leq W_T \\
& && C3 : -B_i \log \left(1 + \frac{p_i |g_i(t)|^2}{B_i N_0} \right) + R_i \leq 0 && i = 1, \dots, K, \\
& && C4 : R_{max,i} \geq R_i && i = 1, \dots, K, \\
& && C5 : R_i \geq \text{qos}_i && i = 1, \dots, K, \\
& && C6 : p_i \geq 0 && i = 1, \dots, K, \\
& && C7 : B_i \geq 0 && i = 1, \dots, K,
\end{aligned}$$

where constant ν was presented in §3.2.1 and is decoder specific and $R_{max,i} = \frac{\tilde{C}_i(t) - T_l P_c^{R_x}}{T_l \nu}$ assures that no more energy than the current available battery level is spent at the allocation. Based on KKT observation (see Appendix 3.H), we are able to provide the following lemma:

Lemma 3.7. *There exists a maximum value of weight μ , such that above this upper-bound the data-rate optimum solution is always zero. The value of the maximum μ is:*

$$\mu_{max} = \frac{1}{T_l \nu}. \quad (3.26)$$

Proof. See Appendix 3.K. ■

Lemma 3.7 provides an upper-bound on the value of μ . Hence the trade-off is only experienced when $0 \leq \mu \leq \mu_{max}$. One could notice that the only difference between the exponential model problem and the linear one is the objective function. By inspection, we could modify the objective of the linear model problem. If constant ν is not user dependent, then the objective can be rewritten as $\sum_{i=1}^K K \cdot R_i + \rho$, where $\rho = \sum_{i=1}^K \mu \tilde{C}_i(t) - T_l P_c^{R_x}$ and $K = 1 - T_l \nu$. Hence the maximization of the problem becomes the classical sum-rate problem where there are no constraints of energy. On the other hand, if constant ν is user dependent, the objective function can be arranged to be $\sum_{i=1}^K K_i \cdot R_i + \rho$ and now the problem is a weighted sum-rate problem which of course provides a different solution. The weighted sum-rate is a problem that has been studied in the literature [19]. It is common to relate the

weight associated to the data-rate as a certain QoS parameter. Users with higher weights will be allowed to have greater data-rates. Notice that in this case, the weights cannot be configured since they depend on the decoder specific constants of each user, which relates the energy to be spent by the decoder for a given data-rate. If constant ν_i of i -th user is small, it implies a good efficiency of the decoder and low energy to be spent when decoding. Thus, if ν_i is small, then K_i will be high, and the optimization problem will allow this user to have a greater data-rate due to its high weight since little energy is to be used by the receiver. The Pareto-optimal curve for a scenario with four users is shown in Fig. 3.14.

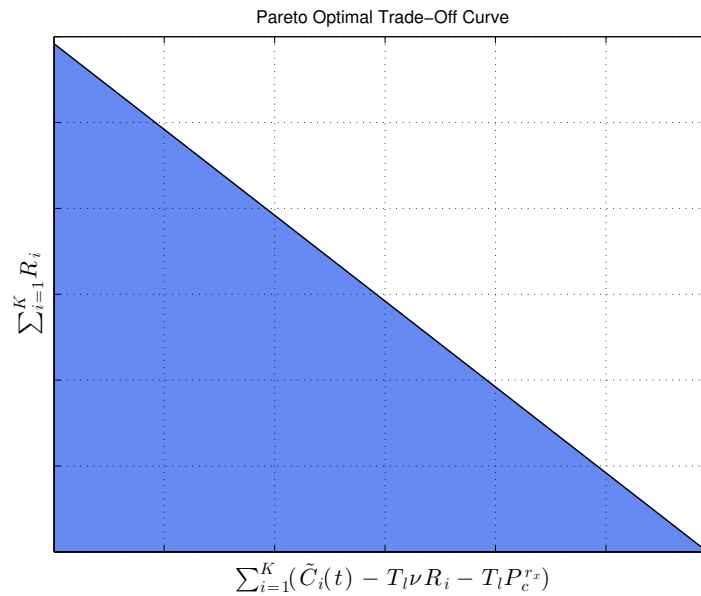


Figure 3.14: Trade-off between sum-rate and energy consumption

3.6.1 Sub-Optimal Case: Fixed Transmission Bandwidth

For the sub-optimal cases we are able to develop a semi-analytical solution for the problem from the KKT optimality conditions and we provide both algorithms that attain the optimum values.

Exponential Model of Decoding Power

The problem with exponential model is modeled as:

$$\begin{aligned}
& \underset{\{R_i, p_i\}_{i=1}^K}{\text{maximize}} && \sum_{i=1}^K R_i + \mu \sum_{i=1}^K \left(\tilde{C}_i(t) - T_l c_1 e^{c_4 R_i} - T_l P_c^{R_x} \right) && (3.27) \\
& \text{subject to} && C1 : \sum_{i=1}^K p_i + P_c^{T_x} \leq P_{max} \\
& && C2 : -B \log(1 + p_i \lambda_i) + R_i \leq 0, && i = 1, \dots, K, \\
& && C3 : R_{max,i} \geq R_i, && i = 1, \dots, K, \\
& && C4 : R_i \geq \text{qos}_i, && i = 1, \dots, K, \\
& && C5 : p_i \geq 0, && i = 1, \dots, K.
\end{aligned}$$

Lemma 3.5 and lemma 3.6 found for the optimal case can also be applied in this case. The power allocation for the i -th user is,

$$p_i^* = \left[\frac{(1 - \mu T_l c_1 c_4 e^{c_4 R_i^*} - \alpha_i^* + \gamma_i^*) B}{\sigma^* \ln(2)} - \frac{1}{\lambda_i} \right]^+, \quad (3.28)$$

where $f[x]^+ = \max(0, x)$, and α_i^*, γ_i^* , and σ^* are Lagrange multipliers. If the i -th user is not saturated in C3, i.e., $R_{max,i} > R_i^* \implies \alpha_i^* = 0$ by the complementary slackness. Besides, if $R_i^* > \text{qos}_i \implies \gamma_i^* = 0$. Thus, $p_i^* = \left[\frac{(1 - \mu T_l c_1 c_4 e^{c_4 R_i^*}) B}{\sigma^* \ln(2)} - \frac{1}{\lambda_i} \right]^+$, which is a water-filling-like solution with activation order given by $\frac{1}{\sigma^*} > \frac{\ln(2)}{\lambda_i (1 - \mu T_l c_1 c_4 e^{c_4 \text{qos}_i}) B}$. Moreover, if the i -th user is saturated, i.e., $R_{max,i} = R_i^*$, then $p_i^* = \frac{2^{\frac{R_{max,i}}{B}} - 1}{\lambda_i}$. By inspection, we are also able to find a saturation order, according to C3, that will help us develop an efficient algorithm that attains the optimum value. The condition for the i -th user to be saturated is $\frac{1}{\sigma^*} \geq \frac{\ln(2) 2^{\frac{R_{max,i}}{B}}}{(1 - \mu T_l c_1 c_4 e^{c_4 R_{max,i}}) \lambda_i B}$. The converse is also true. It is not so straightforward to solve this problem since the optimum value of power allocation depends on the optimum rate allocation, which also depends on the power. Notice also that the right hand side of the saturation order may be negative, since $1 - \mu T_l c_1 c_4 e^{c_4 R_{max}}$ could be negative for some value of R_{max} . The users with negative threshold will never reach saturation by R_{max} . The algorithm will first compute the saturation order, and will leave out the ones that are negative. Rate allocation will be computed using the fix-point method by introducing the optimum power (3.28) in the rate equation, resulting in (3.29), assuming they are not saturated and positive. In order to compute the optimum rate, we need to know the value of the Lagrange multiplier σ^* . Let us denote $\frac{1}{\sigma_i} = \frac{\ln(2) 2^{\frac{R_{max,i}}{B}}}{(1 - \mu T_l c_1 c_4 e^{c_4 R_{max,i}}) \lambda_i B}$. We first need to know in which interval the multiplier is, i.e., $\frac{1}{\sigma_i} > \frac{1}{\sigma^*} > \frac{1}{\sigma_j}, \forall i, j$ with $i \neq j$. Then, we proceed using fitting interval

technique applied to σ^* to find the proper value.

$$R_i^* = B \log \left(1 + \left[\frac{(1 - \mu T_l c_1 c_4 e^{c_4 R_i^*}) B}{\sigma^* \ln(2)} - \frac{1}{\lambda_i} \right]^+ \lambda_i \right) \quad (3.29)$$

Let us denote $s(i)$ as the index of the i -th saturated user and let also $c = \frac{B}{\sigma^* \ln(2)}$. Let us denote K to be the total number of users in the system.

The developed algorithm that attains the optimum value is presented below.

Algorithm 3: SR-SR Exponential model

- 1: **set** $\mathcal{D} = \{1, 2, 3, \dots, K\}$
- 2: $\mathcal{A} = \{\gamma_j \mid \gamma_j = \frac{2^{\frac{R_{max,j}}{B}}}{(1 - \mu T_l c_1 c_4 e^{c_4 R_{max,j}}) \lambda_j}, \forall j\} \rightarrow$ order increasingly
- 3: $\Omega = \{j \mid \gamma_j < 0, \forall j\}$
- 4: $\mathcal{A} \leftarrow \mathcal{A} - s(\Omega)$
- 5: $\sigma_1 = 0, \sigma_2 = 0$
- 6: **for** $k = 1$ to $|\mathcal{A}|$ **do**
- 7: set $\sigma = \frac{1}{\gamma_k}$
- 8: $R_i \leftarrow R_i = B \log \left(1 + \left[\frac{(1 - \mu T_l c_1 c_4 e^{c_4 R_i}) B}{\sigma \ln(2)} - \frac{1}{\lambda_i} \right]^+ \lambda_i \right), \forall i > k$
- 9: $p_i = \frac{2^{R_i} - 1}{\lambda_i}$
- 10: $p_j = \frac{2^{R_{max,j}} - 1}{\lambda_j}$ with $j \leq k$
- 11: **if** $(\sum_j p_j + \sum_i p_i) > P_{max}$ **then**
- 12: $\sigma_2 = \sigma$
- 13: go to 22
- 14: **end if**
- 15: **if** $(\sum_j p_j + \sum_i p_i) < P_{max}$ **then**
- 16: $\sigma_1 = \sigma$
- 17: **end if**
- 18: **if** $(\sum_j p_j + \sum_i p_i) = P_{max}$ **then**
- 19: $\sigma^* = \sigma$
- 20: go to 42
- 21: **end if**
- 22: **end for**
- 23: **if** $\sigma_1 = 0$ **then**
- 24: $P_r = P_{max}$
- 25: **else**
- 26: $P_r = P_{max} - \sum_j p_j$

```

27: end if
28:  $P_{ac} = 0$ 
29: while ( $|P_{ac} - P_r| > \epsilon$ ) do
30:    $\sigma_m = (\sigma_1 + \sigma)/2$ 
31:    $R_i \leftarrow R_i = B \log \left( 1 + \left[ \frac{(1-\mu T_l c_1 c_4 e^{c_4 R_i}) B}{\sigma_m \ln(2)} - \frac{1}{\lambda_i} \right]^+ \lambda_i \right), \forall i > k$ 
32:    $P_{ac} = \sum_i \frac{2^{R_i} - 1}{\lambda_i}$ 
33:   if  $P_{ac} > P_r$  then
34:      $\sigma_2 = \sigma_m$ 
35:   else
36:      $\sigma_1 = \sigma_m$ 
37:   end if
38: end do
39:  $\mathcal{D} \leftarrow \mathcal{D} - s(j)$  with  $j < k$ 
40: for all  $i \in \mathcal{D}$  do
41:    $R_i^* \leftarrow R_i = B \log \left( 1 + \left[ \frac{(1-\mu T_l c_1 c_4 e^{c_4 R_i}) B}{\sigma_m \ln(2)} - \frac{1}{\lambda_i} \right]^+ \lambda_i \right)$ 
42:    $p_i^* = \frac{2^{R_i^*} - 1}{\lambda_i}$ 
43: end for
44: end algorithm

```

Linear Model of Decoding Power

The problem with exponential model is modeled as:

$$\begin{aligned}
& \underset{\{R_i, p_i\}_{i=1}^K}{\text{maximize}} && \sum_{i=1}^K R_i + \mu \sum_{i=1}^K \left(\tilde{C}_i(t) - T_l \nu R_i - T_l P_c^{R_x} \right) && (3.30) \\
& \text{subject to} && C1 : \sum_{i=1}^K p_i + P_c^{T_x} \leq P_{max} \\
& && C2 : -B \log(1 + p_i \lambda_i) + R_i \leq 0 && i = 1, \dots, K, \\
& && C3 : R_{max,i} \geq R_i && i = 1, \dots, K, \\
& && C4 : R_i \geq \text{qos}_i && i = 1, \dots, K, \\
& && C5 : p_i \geq 0 && i = 1, \dots, K.
\end{aligned}$$

The power allocation for the i -th user is,

$$p_i^* = \left[\frac{(1 - \mu T_l \nu - \beta_i^* + \gamma_i^*)B}{\sigma^* \ln(2)} - \frac{1}{\lambda_i} \right]^+, \quad (3.31)$$

where $f[x]^+ = \max(0, x)$, and β_i^*, γ_i^* , and σ^* are Lagrange multipliers. If the i -th user is not saturated in C3, i.e., $R_{max,i} > R_i^* \implies \beta_i^* = 0$ by the complementary slackness. Besides, if $R_i^* > qoS_i \implies \gamma_i^* = 0$. Thus, $p_i^* = \left[\frac{(1 - \mu T_l \nu)B}{\sigma^* \ln(2)} - \frac{1}{\lambda_i} \right]^+$, which is a classical water-filling solution with activation order given by $\frac{1}{\sigma^*} > \frac{\ln(2)}{\lambda_i B}$. On the other hand, if user is saturated, i.e., $R_{max,i} = R_i^*$, then $p_i^* = \frac{2^{\frac{R_{max,i}}{B}} - 1}{\lambda_i}$. By inspection, we are also able to find a saturation order, according to C3, that will help us develop an efficient algorithm that attains the optimum value. The condition for the i -th user to be saturated is $\frac{1}{\sigma^*} \geq \frac{\ln(2)2^{\frac{R_{max,i}}{B}}}{(1 - \mu T_l \nu)\lambda_i B}$. The converse is also true, that is, if for the i -th user $\frac{1}{\sigma^*} \geq \frac{\ln(2)2^{\frac{R_{max,i}}{B}}}{(1 - \mu T_l \nu)\lambda_i B}$ holds, then the user is saturated.

Let us denote $s(i)$ as the index of the i -th saturated user and let also $c = \frac{B}{\sigma^* \ln(2)}$. The developed algorithm that attains the optimum value is presented below.

Algorithm 4: SR-SR linear model

- 1: **set** $\gamma_j = \frac{2^{\frac{R_{max,j}}{B}}}{(1 - \mu T_l \nu)\lambda_j B} \rightarrow$ order increasingly
 - 2: $\mathcal{A} = \{1, 2, \dots, K\}; k = 1$
 - 3: **solve** $c : \sum_{j \in \mathcal{A}} \left(c - \frac{1}{\lambda_j} \right)^+ = P_{max}$
 - 4: **if** $c \geq \gamma_k$ **then**
 - 5: $P_k = \frac{2^{\frac{R_{max,k}}{B}} - 1}{\lambda_k}$
 - 6: $P_{max} \leftarrow P_{max} - \sum_{j=1}^k P_k$
 - 7: $\mathcal{A} \leftarrow \mathcal{A} - \{s(k)\}$
 - 8: $k \leftarrow k + 1$
 - 9: **go to** 2
 - 10: **end if**
 - 11: **assign** $p_i^* = \min\left(c - \frac{1}{\lambda_i}, \gamma_k\right)$
 - 12: $R_i^* = B \log\left(1 + p_i^* \lambda_i\right)$
 - 13: **end algorithm**
-

3.7 Chapter Summary and Conclusions

In this chapter, RRA algorithms have been presented for a broadcast multi-user scenario in short distance networks, such as for example femtocells. For simplicity, the allocation was considered to be continuous, in terms of bandwidth, power, and thus data-rate. The nodes were considered battery-powered devices provided with energy harvesting sources. The key point was that the battery status of the users were considered in the allocation process, increasing the network lifetime.

Different resource allocation problems were formulated and solved, using commercial software packages for the case of optimal allocation, and we developed iterative algorithm to achieve the optimum in cases where the transmission bandwidth was considered fixed for all users.

Simulations showed that whenever the scheduler had information regarding the battery level of the users, it was able to allocate resources according to battery constraints, making the nodes live longer (in terms of battery), and thus, to increase the average sum-rate.

3.A Appendix: Proof of Lemma 3.1

We aim to show that $f(p_i, B_i) = -B_i \log\left(1 + \frac{p_i |g_i(t)|^2}{B_i N_0}\right)$ is jointly convex in p_i and B_i . In order to do that, we shall prove the second-order conditions which states that a function f is convex if and only if $\text{dom } f$ is convex and its Hessian is positive semidefinite [Boyd pag. 71]. Let x be the bandwidth B_i and y be the power p_i . Without loss of generality, we consider the logarithm to be the natural logarithm. Hence, we prove convexity of function $f(x, y) = -x \log\left(1 + \frac{y}{x}\right)$ on variables x and y . The Hessian of previous function can be verified to be positive semidefinite for $\forall x, y \geq 0$,

$$\nabla^2 f(x, y) = \begin{bmatrix} \frac{y^2}{x(x+y)^2} & -\frac{y}{(x+y)^2} \\ -\frac{y}{(x+y)^2} & \frac{x}{(x+y)^2} \end{bmatrix} \succeq 0, \quad (3.32)$$

A 2×2 matrix of the form $\begin{bmatrix} a & b \\ b & c \end{bmatrix}$ with $a > 0$ is positive semidefinite if and only if $b^2 - ac \geq 0$. Since the Hessian matrix presented before fulfills this property, it is positive semidefinite, or what is the same $f(p_i, B_i)$ is convex over B_i and p_i .

3.B Appendix: Proof of Lemma 3.2

In this section we prove that equation $R_i = B_i \log\left(1 + \frac{p_i |g_i(t)|^2}{B_i N_0}\right)$ is monotonically increasing in p_i and B_i . It is straightforward to see that it is monotonically increasing in p_i since the log function is indeed monotonically increasing. In contrast, it is not so straightforward to see the monotonicity in B_i . We will then prove so. Let x denote B_i and let transform the original function in a more suitable one being $f(x) = x \log\left(1 + \frac{\alpha}{x}\right)$. Without loss of generality we consider the logarithm to be a natural logarithm. We start the proof by working out what value the function takes when $x = 0$, that is $f(0)$:

$$\lim_{x \rightarrow 0} x \log\left(1 + \frac{\alpha}{x}\right) = \lim_{x \rightarrow 0} \frac{\log\left(1 + \frac{\alpha}{x}\right)}{\frac{1}{x}}, \quad (3.33)$$

applying L'Hôpital's rule it follows,

$$\lim_{x \rightarrow 0} \frac{\log\left(1 + \frac{\alpha}{x}\right)}{\frac{1}{x}} = \lim_{x \rightarrow 0} \frac{\frac{-\frac{\alpha}{x^2}}{1 + \frac{\alpha}{x}}}{-\frac{1}{x^2}} = \lim_{x \rightarrow 0} \frac{\alpha}{1 + \frac{\alpha}{x}} = \lim_{x \rightarrow 0} \frac{\alpha x}{x + \alpha} = 0. \quad (3.34)$$

Thus, function $f(x)$ starts at 0. In order to check if $f(x)$ is monotone increasing in x it is enough proving if the derivative of $f(x)$ is always positive, i.e.,

$$f'(x) = \log\left(1 + \frac{\alpha}{x}\right) - \frac{\alpha}{x + \alpha} \geq 0 \implies \log\left(1 + \frac{\alpha}{x}\right) \geq \frac{\alpha}{x + \alpha}. \quad (3.35)$$

In order to check if the second term of (3.35) is always fulfilled, we check the derivatives of both sides of the inequality,

$$\frac{\alpha}{x^2 + \alpha x} \geq \frac{\alpha}{(x + \alpha)^2}, \quad (3.36)$$

and because inequality is always attained for $x \geq 0$, this concludes the proof.

3.C Appendix: KKT Conditions of Problem (3.15)

Let us first denote the Lagrangian of the problem (3.15) as

$$\begin{aligned} \mathcal{L}\left(\sigma, \mu, \{R_i, p_i, B_i, \alpha_i, \beta_i, \gamma_i, \xi_i, \nu_i\}_{i=1}^K\right) = & - \sum_{i=1}^K R_i + \sigma \left(\sum_{i=1}^K (p_i + P_c^{tx} - P_{max}) \right) + \\ & + \mu \left(\sum_{i=1}^K B_i - W_T \right) + \sum_{i=1}^K \beta_i (R_i - R_{max,i}) + \\ & + \sum_{i=1}^K \alpha_i \left(R_i - B_i \log \left(1 + \frac{p_i |g_i(t)|^2}{B_i N_0} \right) \right) + \\ & + \sum_{i=1}^K \gamma_i (qos_i - R_i) - \sum_{i=1}^K \xi_i p_i - \\ & - \sum_{i=1}^K \nu_i B_i. \end{aligned} \quad (3.37)$$

Let R_i^*, p_i^*, B_i^* , and $\sigma^*, \mu^*, \alpha_i^*, \beta_i^*, \gamma_i^*, \xi^*, \nu^*$ be any primal and dual optimal points. Then, the KKT conditions of problem (3.15) are shown below:

$$-1 + \alpha_i^* + \beta_i^* - \gamma_i^* = 0 \quad \forall i, \quad (3.38)$$

$$\sigma^* - \frac{1}{\ln(2)} \frac{\alpha_i^* B_i^* |g_i(t)|^2}{B_i^* N_0 + p_i^* |g_i(t)|^2} - \xi_i^* = 0 \quad \forall i, \quad (3.39)$$

$$\mu^* - \alpha_i^* \log \left(1 + \frac{p_i^* |g_i(t)|^2}{B_i^* N_0} \right) + \frac{1}{\ln(2)} \frac{\alpha_i^* p_i^* |g_i(t)|^2}{B_i^* N_0 + p_i^* |g_i(t)|^2} - \nu_i^* = 0 \quad \forall i, \quad (3.40)$$

$$\sum_{i=1}^K p_i^* + P_c^{tx} - P_{max} \leq 0, \quad (3.41)$$

$$\sum_{i=1}^K B_i^* - W_T \leq 0, \quad (3.42)$$

$$R_i^* - B_i^* \log \left(1 + \frac{p_i^* |g_i(t)|^2}{B_i^* N_0} \right) \leq 0 \quad \forall i, \quad (3.43)$$

$$R_i^* - R_{max,i} \leq 0 \quad \forall i, \quad (3.44)$$

$$qos_i - R_i^* \leq 0 \quad \forall i, \quad (3.45)$$

$$-\tilde{p}_i^*, -B_i^* \leq 0 \quad \forall i, \quad (3.46)$$

$$\sigma^* \left(\sum_{i=1}^K p_i^* + P_c^{tx} - P_{max} \right) = 0, \quad (3.47)$$

$$\mu^* \left(\sum_{i=1}^K B_i^* - W_T \right) = 0, \quad (3.48)$$

$$\alpha_i^* \left(R_i^* - B_i^* \log \left(1 + \frac{p_i^* |g_i(t)|^2}{B_i^* N_0} \right) \right) = 0 \quad \forall i, \quad (3.49)$$

$$\beta_i^* (R_i^* - R_{max,i}) = 0 \quad \forall i, \quad (3.50)$$

$$\gamma_i^* (qos_i - R_i^*) = 0 \quad \forall i, \quad (3.51)$$

$$\xi_i^* p_i^* = 0 \quad \forall i, \quad (3.52)$$

$$\nu_i^* B_i^* = 0 \quad \forall i, \quad (3.53)$$

$$\sigma^* \geq 0, \mu^* \geq 0, \quad (3.54)$$

$$\alpha_i^* \geq 0, \beta_i^* \geq 0, \gamma_i^* \geq 0, \xi_i^* \geq 0, \nu_i^* \geq 0. \quad \forall i \quad (3.55)$$

Given the Lagrange multipliers and the optimal bandwidth allocation, we have that the optimal power allocation of the i -the user is

$$p_i^* = \left[\frac{\alpha_i^* B_i^*}{\sigma^* \ln(2)} - \frac{B_i^* N_0}{|g_i(t)|^2} \right]^+. \quad (3.56)$$

In a few special cases, the previous problem can be solved analytically. Usually, a semi-analytical solution using iterative methods can be applied to obtain the optimal variables. Unfortunately, in most of the times, a generic software package is needed to get the optimal solution of the problem. There are many commercial packages that provides with a set of algorithms able to solve convex problems. Among them, we find the package CVX [6], or the build-in function *fmincon* of the commercial software MATLAB [26]. Depending on the dimension of the problems, some packages are more suitable than others.

3.D Appendix: Proof of Lemma 3.3

In this section we prove the equivalence between problems (3.16) and (3.17). Remember that, we define this lemma in order to simplify the original problem and reduce one constraint so that one Lagrange multiplier is avoided. As a result, we transform the the QoS-constrained

problem into an equivalent unconstrained QoS problem. Let us start with the original problem:

$$\begin{aligned}
& \underset{\{R_i, p_i\}_{i=1}^K}{\text{maximize}} && \sum_{i=1}^K R_i && (3.57) \\
& \text{subject to} && C1 : \sum_{i=1}^K p_i + P_c^{tx} \leq P_{max} \\
& && C2 : -B \log(1 + p_i \lambda_i) + R_i \leq 0 \quad i = 1, \dots, K, \\
& && C3 : R_{max,i} \geq R_i \quad i = 1, \dots, K, \\
& && C4 : R_i \geq \text{qos}_i \quad i = 1, \dots, K, \\
& && C5 : p_i \geq 0 \quad i = 1, \dots, K.
\end{aligned}$$

Let us define $p_{min,i} = \frac{2^{\text{qos}_i} - 1}{\lambda_i}$. Thus, C4 can be eliminated and we incorporate a lower-bound on power p_i , such that C5 is rewritten as $p_i \geq p_{min,i}$. Then, introducing a new variable called $\tilde{p}_i = p_i - p_{min,i}$, C5 is modified as $\tilde{p}_i \geq 0$. Finally, making all the changes in variable p_i such that $p_i = \tilde{p}_i + p_{min,i}$, we obtain that $C2 = -B \log(1 + \tilde{p}_i \lambda_i + p_{min,i} \lambda_i) + R_i \leq 0$. By calling $\theta_i = 1 + p_{min,i} \lambda_i$ and $\tilde{P}_{max} = P_{max} - \sum_{i=1}^K p_{i,min}$, we end up with the following equivalent problem:

$$\begin{aligned}
& \underset{\{R_i, \tilde{p}_i\}_{i=1}^K}{\text{maximize}} && \sum_{i=1}^K R_i && (3.58) \\
& \text{subject to} && C1 : \sum_{i=1}^K \tilde{p}_i + P_c^{tx} \leq \tilde{P}_{max} \\
& && C2 : -B \log(\theta_i + \tilde{p}_i \lambda_i) + R_i \leq 0 \quad i = 1, \dots, K, \\
& && C3 : R_{max,i} \geq R_i \quad i = 1, \dots, K, \\
& && C4 : R_i \geq 0 \quad i = 1, \dots, K, \\
& && C5 : \tilde{p}_i \geq 0 \quad i = 1, \dots, K.
\end{aligned}$$

3.E Appendix: KKT Conditions of Problem (3.17)

Let us first denote the Lagrangian of the problem (3.17) as

$$\begin{aligned}
\mathcal{L}(\sigma, \{R_i, \tilde{p}_i, \alpha_i, \beta_i, \gamma_i\}_{i=1}^K) = & - \sum_{i=1}^K R_i + \sigma \left(\sum_{i=1}^K (\tilde{p}_i + P_c^{tx} - \tilde{P}_{max}) \right) + \sum_{i=1}^K \alpha_i (R_i - R_{max,i}) + \\
& + \sum_{i=1}^K \beta_i \left(R_i - B \log(\theta_i + \tilde{p}_i \lambda_i) \right) - \sum_{i=1}^K \gamma_i \tilde{p}_i - \sum_{i=1}^K \mu_i R_i. && (3.59)
\end{aligned}$$

Leaving out the last two terms of the Lagrangian, and considering later the fact that power and data-rate cannot be negative, the KKT conditions of the problem (3.17) are,

$$-1 + \alpha_i^* + \beta_i^* = 0 \quad \forall i, \quad (3.60)$$

$$\sigma^* - \frac{1}{\ln(2)} \frac{\beta_i^* \lambda_i B}{\theta_i + \tilde{p}_i^* \lambda_i} = 0 \quad \forall i, \quad (3.61)$$

$$\sum_{i=1}^K (\tilde{p}_i^* + P_c^{tx} - \tilde{P}_{max}) \leq 0, \quad (3.62)$$

$$R_i^* - R_{max,i} \leq 0 \quad \forall i, \quad (3.63)$$

$$R_i^* - B \log(\theta_i + \tilde{p}_i^* \lambda_i) \leq 0 \quad \forall i, \quad (3.64)$$

$$-\tilde{p}_i^*, -R_i^* \leq 0 \quad \forall i, \quad (3.65)$$

$$\sigma^* \left(\sum_{i=1}^K \tilde{p}_i^* + P_c^{tx} - \tilde{P}_{max} \right) = 0, \quad (3.66)$$

$$\alpha_i^* (R_i^* - R_{max,i}) = 0 \quad \forall i, \quad (3.67)$$

$$\beta_i^* (R_i^* - B \log(\theta_i + \tilde{p}_i^* \lambda_i)) = 0 \quad \forall i, \quad (3.68)$$

$$\sigma^* \geq 0, \quad (3.69)$$

$$\alpha_i^* \geq 0, \beta_i^* \geq 0 \quad \forall i. \quad (3.70)$$

From (3.61) we obtain that $\tilde{p}_i^* = \left[\frac{(1-\alpha_i^*)B}{\sigma^* \ln(2)} - \frac{\theta_i}{\lambda_i} \right]^+$, since $\beta_i = 1 - \alpha_i$ from (3.60) and where $f[x]^+ = \max(0, x)$ as power cannot be negative. From (3.66), if $\sum_{i=1}^K \tilde{p}_i^* + P_c^{tx} < \tilde{P}_{max} \implies \sigma^* = 0$ and we know all users are saturated. Hence, $R_i^* = R_{max,i}$ and then $\tilde{p}_i^* = \frac{R_{max,i} - \theta_i}{\lambda_i}$. Then it also implies from (3.61) that $\beta_i = 0 \implies \alpha_i = 1$ since we assume $\lambda_i > 0$ and $\tilde{p}_i^* > 0$. On the other hand, if $\sum_{i=1}^K \tilde{p}_i^* + P_c^{tx} = \tilde{P}_{max} \implies R_{max,i} \geq R_i^*$. This means some of the users may be saturated but it does not necessarily to be true. If $R_{max,i} > R_i^* \implies \alpha_i = 0$ and then $\tilde{p}_i^* = \left[\frac{B}{\sigma^* \ln(2)} - \frac{\theta_i}{\lambda_i} \right]^+$ and we end up with the classical water-filling solution with a saturation order given by $\frac{1}{\sigma^*} > \frac{\theta_i \ln(2)}{\lambda_i B}$. However, if $R_{max,i} = R_i^* \implies \alpha_i \geq 0$ then $\tilde{p}_i^* = \left(\frac{(1-\alpha_i^*)B}{\sigma^* \ln(2)} - \frac{\theta_i}{\lambda_i} \right)$ and $\tilde{p}_i^* = \frac{R_{max,i} - \theta_i}{\lambda_i}$. From both equations, we conclude that $\alpha_i^* = 1 - \frac{\sigma^* \ln(2) \frac{R_{max,i}}{B}}{\lambda_i B} \geq 0$. Hence, we can finally obtain the saturation order as $\frac{1}{\sigma^*} \geq \frac{\ln(2) \frac{R_{max,i}}{B}}{\lambda_i B}$.

3.F Appendix: Proof of Lemma 3.4

In this section we prove that if a user is not active, then it cannot be saturated. We order the users, making the first one be the user with highest $\frac{\theta_i}{\lambda_i}$ value, i.e., the last user be activated. We assume all the users are active except the first one. As a worst case, we will prove that this user will never be saturated, regardless of the value of $R_{max,i}$. Let us define $c = \frac{B}{\sigma^* \ln(2)}$. If user 1 is not active $\implies \tilde{P}_{max} < (N-1) \frac{\theta_1}{\lambda_1} - \sum_{i=2}^K \frac{\theta_i}{\lambda_i}$. Then, we

must also have that $\sum_{i=2}^K \left(c - \frac{\theta_i}{\lambda_i}\right) = \tilde{P}_{max}$. Thus, $c = \frac{1}{(N-1)} \left(\tilde{P}_{max} + \sum_{i=2}^K \frac{\theta_i}{\lambda_i}\right)$. Notice that in order to be saturated, $c \geq \frac{2^{\frac{R_{max,1}}{B}}}{\lambda_1}$. By combining previous equations, it yields that $\tilde{P}_{max} \geq (N-1) \frac{2^{\frac{R_{max,1}}{B}}}{\lambda_1} - \sum_{i=2}^K \frac{\theta_i}{\lambda_i}$ and this contradicts the condition of being not active since $2^{\frac{R_{max,1}}{B}} > \theta_1$, thus if a user is not active it can never be saturated.

3.G Appendix: KKT Conditions of Problem (3.22)

Let us first denote the Lagrangian as

$$\begin{aligned} \mathcal{L}(\sigma, \xi, \{R_i, p_i, B_i, \alpha_i, \beta_i, \lambda_i, \nu_i, \gamma_i\}_{i=1}^K) = & - \sum_{i=1}^K R_i - \mu \sum_{i=1}^K (C_i(t) - T_l c_1 e^{c_4 R_i} - T_l \cdot P_c^{R_x}) + \\ & + \sigma \left(\sum_{i=1}^K (p_i + P_c^{t_x} - P_{max}) \right) + \xi \left(\sum_{i=1}^K B_i - W_T \right) + \\ & + \sum_{i=1}^K \alpha_i (R_i - R_{max,i}) + \sum_{i=1}^K \lambda_i (\text{qos}_i - R_i) + \\ & + \sum_{i=1}^K \beta_i \left(R_i - B_i \log \left(1 + \frac{p_i^* |g_i(t)|^2}{B_i^* N_0} \right) \right) - \\ & - \sum_{i=1}^K \nu_i p_i - \sum_{i=1}^K \gamma_i B_i. \end{aligned} \quad (3.71)$$

The KKT conditions are the following:

$$-1 + \mu T_l c_1 c_4 e^{c_4 R_i} + \alpha_i^* + \beta_i^* - \lambda_i^* = 0 \quad \forall i, \quad (3.72)$$

$$\sigma^* - \frac{1}{\ln(2)} \frac{\beta_i^* B_i^* |g_i(t)|^2}{B_i^* N_0 + p_i^* |g_i(t)|^2} - \nu_i^* = 0 \quad \forall i, \quad (3.73)$$

$$\xi^* - \beta_i^* \log \left(1 + \frac{p_i^* |g_i(t)|^2}{B_i^* N_0} \right) + \frac{1}{\ln(2)} \frac{\beta_i^* p_i^* |g_i(t)|^2}{B_i^* N_0 + p_i^* |g_i(t)|^2} - \gamma_i^* = 0 \quad \forall i, \quad (3.74)$$

$$\sum_{i=1}^K p_i^* + P_c^{t_x} - P_{max} \leq 0, \quad (3.75)$$

$$\sum_{i=1}^K B_i^* - W_T \leq 0, \quad (3.76)$$

$$R_i^* - B_i^* \log \left(1 + \frac{p_i^* |g_i(t)|^2}{B_i^* N_0} \right) \leq 0 \quad \forall i, \quad (3.77)$$

$$R_i^* - R_{max,i} \leq 0 \quad \forall i, \quad (3.78)$$

$$\text{qos}_i - R_i^* \leq 0 \quad \forall i, \quad (3.79)$$

$$-p_i^*, -B_i^* \leq 0 \quad \forall i, \quad (3.80)$$

$$\sigma^* \left(\sum_{i=1}^K p_i^* + P_c^{tx} - P_{max} \right) = 0, \quad (3.81)$$

$$\xi^* \left(\sum_{i=1}^K B_i^* - W_T \right) = 0, \quad (3.82)$$

$$\beta_i^* \left(R_i^* - B_i^* \log \left(1 + \frac{p_i^* |g_i(t)|^2}{B_i^* N_0} \right) \right) = 0 \quad \forall i, \quad (3.83)$$

$$\alpha_i^* (R_i^* - R_{max,i}) = 0 \quad \forall i, \quad (3.84)$$

$$\lambda_i^* (\text{qos}_i - R_i^*) = 0 \quad \forall i, \quad (3.85)$$

$$\nu_i^* p_i^* = 0 \quad \forall i, \quad (3.86)$$

$$\gamma_i^* B_i^* = 0 \quad \forall i, \quad (3.87)$$

$$\sigma^* \geq 0, \xi^* \geq 0, \quad (3.88)$$

$$\alpha_i^* \geq 0, \beta_i^* \geq 0, \gamma_i^* \geq 0, \lambda_i^* \geq 0, \nu_i^* \geq 0 \quad \forall i. \quad (3.89)$$

3.H Appendix: KKT Conditions of Problem (3.25)

Let us first denote the Lagrangian as

$$\begin{aligned} \mathcal{L}(\sigma, \xi, \{R_i, p_i, B_i, \alpha_i, \beta_i, \lambda_i, \nu_i, \gamma_i\}_{i=1}^K) = & - \sum_{i=1}^K R_i - \mu \sum_{i=1}^K (C_i(t) - T_l \nu R_i - T_l \cdot P_c^{R_x}) + \\ & + \sigma \left(\sum_{i=1}^K (p_i + P_c^{tx} - P_{max}) \right) + \xi \left(\sum_{i=1}^K B_i - W_T \right) + \\ & + \sum_{i=1}^K \alpha_i (R_i - R_{max,i}) + \sum_{i=1}^K \lambda_i (\text{qos}_i - R_i) + \\ & + \sum_{i=1}^K \beta_i \left(R_i - B_i \log \left(1 + \frac{p_i^* |g_i(t)|^2}{B_i^* N_0} \right) \right) - \\ & - \sum_{i=1}^K \nu_i p_i - \sum_{i=1}^K \gamma_i B_i. \end{aligned} \quad (3.90)$$

The KKT conditions are the following:

$$-1 + \mu T_l \nu + \alpha_i^* + \beta_i^* - \lambda_i^* = 0 \quad \forall i, \quad (3.91)$$

$$\sigma^* - \frac{1}{\ln(2)} \frac{\beta_i^* B_i^* |g_i(t)|^2}{B_i^* N_0 + p_i^* |g_i(t)|^2} - \nu_i^* = 0 \quad \forall i, \quad (3.92)$$

$$\xi^* - \beta_i^* \log \left(1 + \frac{p_i^* |g_i(t)|^2}{B_i^* N_0} \right) + \frac{1}{\ln(2)} \frac{\beta_i^* p_i^* |g_i(t)|^2}{B_i^* N_0 + p_i^* |g_i(t)|^2} - \gamma_i^* = 0 \quad \forall i, \quad (3.93)$$

$$\sum_{i=1}^K p_i^* + P_c^{tx} - P_{max} \leq 0, \quad (3.94)$$

$$\sum_{i=1}^K B_i^* - W_T \leq 0, \quad (3.95)$$

$$R_i^* - B_i^* \log \left(1 + \frac{p_i^* |g_i(t)|^2}{B_i^* N_0} \right) \leq 0 \quad \forall i, \quad (3.96)$$

$$R_i^* - R_{max,i} \leq 0 \quad \forall i, \quad (3.97)$$

$$qos_i - R_i^* \leq 0 \quad \forall i, \quad (3.98)$$

$$-p_i^*, -B_i^* \leq 0 \quad \forall i, \quad (3.99)$$

$$\sigma^* \left(\sum_{i=1}^K p_i^* + P_c^{tx} - P_{max} \right) = 0, \quad (3.100)$$

$$\xi^* \left(\sum_{i=1}^K B_i^* - W_T \right) = 0, \quad (3.101)$$

$$\beta_i^* \left(R_i^* - B_i^* \log \left(1 + \frac{p_i^* |g_i(t)|^2}{B_i^* N_0} \right) \right) = 0 \quad \forall i, \quad (3.102)$$

$$\alpha_i^* (R_i^* - R_{max,i}) = 0 \quad \forall i, \quad (3.103)$$

$$\lambda_i^* (qos_i - R_i^*) = 0 \quad \forall i, \quad (3.104)$$

$$\nu_i^* p_i^* = 0 \quad \forall i, \quad (3.105)$$

$$\gamma_i^* B_i^* = 0 \quad \forall i, \quad (3.106)$$

$$\sigma^* \geq 0, \xi^* \geq 0, \quad (3.107)$$

$$\alpha_i^* \geq 0, \beta_i^* \geq 0, \gamma_i^* \geq 0, \lambda_i^* \geq 0, \nu_i^* \geq 0 \quad \forall i. \quad (3.108)$$

3.I Appendix: Proof of Lemma 3.5

From (3.91) we have that $\beta_i^* = 1 - \mu T_l c_1 c_4 e^{c_4 R_i} - \alpha_i^* + \lambda_i^* \geq 0$. Now, if $R_i^* > qos_i$ and $R_i^* < R_{max,i} \implies \alpha_i^* = 0, \lambda_i^* = 0$, and then $\beta_i^* = 1 - \mu T_l c_1 c_4 e^{c_4 R_i} \geq 0$. If μ increases, then for a given T_l, c_1, c_4 and R_i , β_i^* must decrease. But β_i^* cannot be negative. Therefore, when μ achieves a certain maximum value, $\beta_i^* = 0$. From that point, if μ increases, then $\lambda_i^* > 0$ in order to keep $\beta_i^* \geq 0$. Hence, at that point $R_i^* = qos_i$. If we consider $\beta_i^* = 0$, then we have $1 = \mu T_l c_1 c_4 e^{c_4 qos_i}$ that it produces $\mu_{max} = \frac{1}{T_l c_1 c_4 e^{c_4 qos_i}}$ and with this it concludes the proof.

3.J Appendix: Proof of Lemma 3.6

From (3.91) we have that $\beta_i^* = 1 - \mu T_l c_1 c_4 e^{c_4 R_i} - \alpha_i^* + \lambda_i^* \geq 0$. Now, if $R_i^* > qos_i$ and $R_i^* < R_{max,i} \implies \alpha_i^* = 0, \lambda_i^* = 0$, and then $\beta_i^* = 1 - \mu T_l c_1 c_4 e^{c_4 R_i} \geq 0$. For a fixed μ, T_l, c_1

and c_4 , if we increase $R_i^* \implies \beta_i^*$ decreases. Thus, there is a maximum R_i^* that makes $\beta_i^* = 0$, which is the same for all users considering that constants c_j are not user-dependent and can be expressed as $R_m = \frac{1}{c_4} \ln \left(\frac{1}{\mu T_l c_1 c_4} \right)$.

3.K Appendix: Proof of Lemma 3.7

From (3.72) we have that $\beta_i^* = 1 - \mu T_l \nu - \alpha_i^* + \lambda_i^* \geq 0$. Now, if $R_i^* > \text{qos}_i$ and $R_i^* < R_{\max,i} \implies \alpha_i^* = 0$, $\lambda_i^* = 0$, and then $\beta_i^* = 1 - \mu T_l \nu \geq 0$. Then, $\frac{1}{T_l \nu} \geq \mu$ and hence, $\mu_{\max} = \frac{1}{T_l \nu}$.

Chapter 4

Practical Energy Efficient Resource Allocation with Energy Harvesting Nodes over Frequency-Selective Channels

4.1 Introduction

Resource allocation in frequency-selective channels started to be developed for Asynchronous Digital Subscriber Line (ADSL) systems. The first works in the literature dealt with the problem of assigning bits and power to sub-carriers in systems based on Discrete Multi Tone (DMT) modulations [29]. With the introduction of OFDM in wireless communications, there was a need for developing allocation algorithms but now dealing with the features of radio channels. In the last decade, a lot of effort has been put to obtain accurate models for RRA algorithms. As it was presented in Chapter 2, in general, assignment problems with frequency-selective channels are combinatorial integer programming, which is a class of non convex problems. Besides, it is proved that these problems are NP-complete [23]. As a consequence, most of the works found in the literature deal with finding sub-optimal algorithms that approach the optimum [31], [37], [20]. Real-time approaches can also be found by using low-complexity algorithms [49], [8].

Generally, the community classifies all the approaches into two groups:

- Rate adaptive schemes.
- Margin adaptive schemes.

Rate adaptive schemes provide strategies that have as a target to optimize a certain data-rate function. The classical rate adaptive scheme is the maximization of the sum-rate with power constraints [27]. The allocation problem can be stated as

$$\begin{aligned}
& \underset{\{p_n\}, \{\rho_{k,n}\}}{\text{maximize}} && \sum_{k=1}^K \sum_{n=1}^N \log \left(1 + \frac{p_n |g_{k,n}(t)|^2}{N_0} \right) \rho_{k,n} && (4.1) \\
& \text{subject to} && C1 : \sum_{k=1}^K \rho_{k,n} \leq 1 \quad \forall n \\
& && C2 : \sum_{n=1}^N p_n \leq P_{max} \\
& && C3 : \rho_{k,n} \in \{0, 1\} \quad \forall k, n, && (4.2)
\end{aligned}$$

where K and N are the number of users and the number of subcarriers, k and n represents the user index and the subcarrier index respectively, p_n is the subcarrier power, N_0 is the noise power, $g_{k,n}$ is the channel gain, P_{max} is the maximum transmit power and, $\rho_{k,n}$ is called the univocal assignment of the subcarrier to a specific user which is defined as

$$\rho_{k,n} = \begin{cases} 1 & \text{if } c_{k,n} \neq 0. \\ 0 & \text{if } c_{k,n} = 0. \end{cases} \quad (4.3)$$

The solution to this problem is to assign each sub-carrier to the user that maximizes the channel gain of that particular sub-carrier, and then perform water-filling over all the allocated sub-carriers [27]. Other examples of rate adaptive schemes are the maximization of the minimum user data-rates [41] or the maximum sum-rate with proportional rate constraints [53].

As far as the margin adaptive schemes are concerned, they refer to strategies where the objective function of the optimization deals with a certain power function. Here again, we have that the classical margin adaptive scheme is the minimization of the power with data-

rate constraints [8]. The allocation problem can be modeled as

$$\begin{aligned}
 & \underset{\{r_{k,n}\}, \{\rho_{k,n}\}}{\text{minimize}} && \sum_{k=1}^K \sum_{n=1}^N (2^{r_{k,n}} - 1) \frac{N_0}{|g_{k,n}(t)|^2} \rho_{k,n} && (4.4) \\
 & \text{subject to} && C1 : \sum_{k=1}^K \rho_{k,n} \leq 1 \quad \forall n \\
 & && C2 : \sum_{n=1}^N r_{k,n} \rho_{k,n} \geq r_{min,k} \\
 & && C3 : \rho_{k,n} \in \{0, 1\} \quad \forall k, n,
 \end{aligned}
 \tag{4.5}$$

where K and N are the number of users and the number of subcarriers, k and n represents the user index and the subcarrier index respectively, $r_{k,n}$ is the data-rate, N_0 is the noise power, $g_{k,n}$ is the channel gain, $r_{min,k}$ is the minimum data-rate (QoS parameter) and, $\rho_{k,n}$ is the univocal assignment of the subcarrier to a specific user. The objective function is obtained isolating the power from the Shannon's bit-rate formula.

The solution to this problem assigns the sub-carriers to the users and the rate on each sub-carrier. This problem is in general very difficult to solve. Many works can be found approaching different ways of solving the problem. For example, in [8], authors propose a solution based on the integer relaxation of the variable ρ , making the problem convex. However, due to the relaxation, the solution is suboptimal.

The optimal solution to the previous problems was found based on the dual domain (see §2.1.4). In [52], authors propose an iterative algorithm. However, the complexity associated with this approach is prohibitively for real applications.

In this chapter, we propose solutions to allocation problems based on rate adaptive, margin adaptive, and a new group that we call energy adaptive schemes, where the energy constraints are introduced.

4.2 System Model

In this chapter we follow the same system model that was presented in Chapter 3. We assume a broadcast transmission where nodes are battery-powered devices equipped with energy harvesting sources. We take into consideration the current battery status of the nodes in the design. Models for power consumption of the RF subsystems and the baseband signal

processing algorithms were presented in previous chapters. The main difference introduced in this chapter is that channels are no longer flat-fading but frequency-selective. This means that each sub-carrier may experience a different channel gain. We consider the frequency separation among sub-carriers to be smaller than the coherence bandwidth of the channel, making the subchannels to be flat-fading for each independent sub-carrier. Two different realizations of a frequency-selective channel with parameters given by Appendix 4.A are shown in Fig. 4.1. Moreover, we have included another realistic degree: we no longer consider

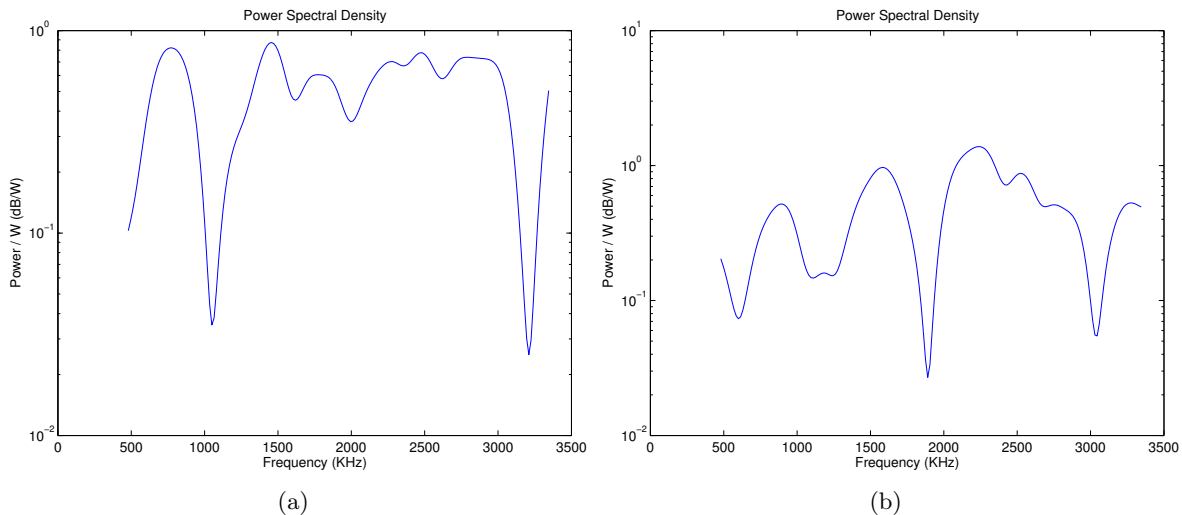


Figure 4.1: Power spectral density of two realizations of Rayleigh frequency-selective channels used in this chapter.

a continuous bit assignment as in previous chapter, but we consider a discrete bit assignment from a possible set of different modulation schemes. This implies that the power allocated to each sub-carrier is also discrete. As a consequence, we do not work with the *Shannon* formula as a bound for the data rate any more, but we introduce a realistic power-rate function given by the probability of error (i.e., BER). From [39], we have that the required power at reception using $c_{k,n}$ bits per symbol for the k -th user at the n -th sub-carrier, guaranteeing a certain BER is

$$P_{k,n}(c_{k,n}) = \frac{N_{0,k,n}}{3} \left[Q^{-1} \left(\frac{BER_{k,n}}{4} \right) \right]^2 (2^{c_{k,n}} - 1), \quad (4.6)$$

where $Q(x) = \frac{1}{\sqrt{2\pi}} \int_x^\infty e^{-t^2/2} dt$, N_0 is the noise power per sub-carrier. This is more restrictive than necessary, since we require that all subcarriers of a given user must fulfill the BER requirement, where, in real systems, the BER is required to be the average of all the subcarriers. If, on the other hand, an averaged BER is considered, it couples the problem in the frequency domain among all the subcarriers, making the allocation problem too difficult to be solved. For the sake of simplicity, we consider that the BER requirement and the noise power are the same for all subcarriers and users, and thus, we drop the subindexes associated to the power-rate function presented before. Given all that, the transmitted power at the BS

can be modeled as

$$P_T = \sum_{n=1}^N \sum_{k=1}^K \frac{P(c_{k,n})}{|g_{k,n}(t)|^2} \rho_{k,n} + P_c^{tx}, \quad (4.7)$$

where $|g_{k,n}(t)|^2$ is the channel power of the k -th user at the n -th sub-carrier computed as shown in Appendix 4.A.

We consider in all the algorithms presented in this thesis that the subcarriers are assigned to a single user during one slot, i.e., we do not allow subcarrier time-sharing between users, since it is proved in [27] that single assignment is optimum.

4.3 Energy Adaptive Schemes with Battery Constraints

In this section we propose a novel allocation algorithm that deals with the new class of allocation algorithms that we call *energy adaptive schemes*. As happens with the two classical approaches, now, the objective function is a function that explicitly includes energy related to the allocation procedure. This section is, indeed, the extension to the problem (3.19) presented in previous chapter, including all the new constraints commented in §4.2. Therefore, the new problem can be stated as

$$\begin{aligned} & \underset{\{c_{k,n}\}, \{\rho_{k,n}\}}{\text{maximize}} && \min_{k=1, \dots, K} \left(\tilde{C}_k(t) - T_l c_1 e^{c_4 \sum_{n=1}^N \frac{c_{k,n}}{t_{OFDM}} \rho_{k,n}} - T_l P_c^{Rx} \right) && (4.8) \\ & \text{subject to} && C1 : \sum_{n=1}^N \sum_{k=1}^K \frac{P(c_{k,n})}{|g_{k,n}(t)|^2} \rho_{k,n} + P_c^{tx} \leq P_{max} \\ & && C2 : \sum_{i=k}^K \rho_{k,n} = 1, && n = 1, \dots, N, \\ & && C3 : R_{max,k} \geq \sum_{n=1}^N \frac{c_{k,n}}{t_{OFDM}} \rho_{k,n}, && k = 1, \dots, K, \end{aligned}$$

where $R_{max,k} = \frac{1}{c_4} \ln \left(\frac{\tilde{C}_k(t) - T_l P_c^{Rx}}{T_l c_1} \right)$ and t_{OFDM} is the duration of the OFDM symbol. Notice the differences between problems (3.19)-(4.8). Now, we have integrity condition in the modulation type (it is not continuous as before) represented by means of the variable $c_{k,n}$, and also the integrity in the subcarrier allocation expressed through the variable $\rho_{k,n}$. The rest is very similar to the former problem.

In order to find the optimal solution of this problem, we should proceed in a combinatorial manner. Since the number of all possible combinations increases exponentially with the number of subcarriers, the complexity of the optimal solution is impracticable. In these

situations, the idea is to find an iterative algorithm, that is suboptimal in a general sense, but closely approaches to the optimal solution, and in some cases it coincides with it. Of course, the complexity associated with the iterative approach should be reduced compared with the combinatorial, otherwise still becomes unrealizable in any real scenario. Besides, it is desired a linear complexity increment when the number of subcarriers is increased. Generally, *greedy* algorithms are implemented to solve this kind of algorithms. The idea of the greedy assignment makes the algorithms very simple and in some situations they approach the optimal solution decently.

As happened before, this optimization problem has infinite number of solutions. The reasons were exposed in the corresponding section. Here again, we design the algorithm such that we obtain the solution that maximizes the sum-rate at the same time that meets the requirements of the objective function. As a consequence, the greedy algorithm presented in this section only provides one solution to the problem (4.8).

Given all that, we propose a greedy algorithm that iteratively assigns subcarriers and bits to the given set of users. The algorithm is as follows:

Algorithm 5: Energy adaptive scheme algorithm

```

1: set  $\mathcal{A} = \{1, 2, 3, \dots, N\}$ 
2:    $\mathcal{B} = \{1, 2, 3, \dots, K\}$ 
3:    $\mathcal{A}_k = \emptyset \quad \forall k$ 
4:    $c_{k,n} = 0 \quad \forall k, n$ 
5:    $\rho_{k,n} = 0 \quad \forall k, n$ 
6:    $P_{k,n} = 0 \quad \forall k, n$ 
7:    $\Delta P_{k,n} = \frac{P(1)}{|g_{k,n}(t)|^2} \quad \forall k, n$ 
8: while  $\left( \sum_{k=1}^K \sum_{n=1}^N P_{k,n} \leq P_{max} - P_c^{tx} \quad \text{and} \quad \mathcal{B} \neq \emptyset \right)$  do
9:    $\tilde{k} = \arg \max_{k \in \mathcal{B}} \tilde{C}_k(t) - T_l c_1 e^{c_4 \sum_{n=1}^N \frac{c_{k,n}}{t_{OFDM}} \rho_{k,n}} - T_l P_c^{R_x}$ 
10:   $\tilde{n} = \arg \min_{n \in \mathcal{A} \cup \mathcal{A}_{\tilde{k}}} \Delta P_{\tilde{k},n}$ 
11:   $c_{\tilde{k},\tilde{n}} \leftarrow c_{\tilde{k},\tilde{n}} + 1$ 
12:   $P_{\tilde{k},\tilde{n}} = \frac{P(c_{\tilde{k},\tilde{n}})}{|g_{\tilde{k},\tilde{n}}(t)|^2}$ 
13:   $\Delta P_{\tilde{k},\tilde{n}} = \frac{P(c_{\tilde{k},\tilde{n}}+1) - P(c_{\tilde{k},\tilde{n}})}{|g_{\tilde{k},\tilde{n}}(t)|^2}$ 
14:  if  $(\tilde{n} \in \mathcal{A})$  then
15:     $\mathcal{A}_{\tilde{k}} \leftarrow \mathcal{A}_{\tilde{k}} \cup \{\tilde{n}\}$ 
16:     $\mathcal{A} \leftarrow \mathcal{A} - \{\tilde{n}\}$ 
17:     $\rho_{\tilde{k},\tilde{n}} = 1$ 
18:  end if
19:  if  $\left( \sum_{n=1}^N \frac{c_{\tilde{k},n}}{t_{OFDM}} \rho_{\tilde{k},n} == R_{max,\tilde{k}} \right)$  then
20:     $\mathcal{B} \leftarrow \mathcal{B} - \{\tilde{k}\}$ 
21:  end if
22: end do
23: end algorithm

```

The algorithm selects the available user that maximizes the objective at each iteration and then, it selects the subcarrier that requires least power to assign a new bit to it. Due to this fact, we claim that the solution tries to maximize the sum rate. When searching subcarriers, the set must be bounded to the set of available subcarriers (not assigned yet) plus the already assigned subcarriers to the user. Then, it performs some updates, and if the user has achieved its maximum rate according to the available energy, it is moved out of the set of available users. In further sections, simulation results showing the performance and behavior of the algorithm will be presented.

4.4 Rate Adaptive Schemes with Battery Constraints

In this section, we deal with the resource allocation under rate adaptive schemes. This is a classical RRA problem that has been studied since long ago. The maximization of the sum-rate, the maximization of the minimum bit-rate, or the maximization of the weighted sum-rate are examples of rate adaptive schemes. Among all possible rate adaptive schemes, in particular, the maximization of the sum rate is considered in this section as a RRA policy. If no battery constraints are added, the solution to this problem is quite simple and was presented in §4.1. Therefore, for this particular case where the maximization of the sum rate with power constraint is considered, a greedy approach is shown to be optimum [27]. However, if the battery constraint is included in the design, there is no longer a simple procedure to find the solution, nor a greedy procedure that yields the optimal allocation.

The maximization of the sum rate with power and battery constraint can be expressed as

$$\begin{aligned}
 & \underset{\{c_{k,n}\}, \{\rho_{k,n}\}}{\text{maximize}} && \sum_{k=1}^K \sum_{n=1}^N \frac{c_{k,n}}{t_{OFDM}} \rho_{k,n} && (4.9) \\
 & \text{subject to} && C1: \sum_{n=1}^N \sum_{k=1}^K \frac{P(c_{k,n})}{|g_{k,n}(t)|^2} \rho_{k,n} + P_c^{tx} \leq P_{max} \\
 & && C2: \sum_{i=k}^K \rho_{k,n} = 1, && n = 1, \dots, N, \\
 & && C3: R_{max,k} \geq \sum_{n=1}^N \frac{c_{k,n}}{t_{OFDM}} \rho_{k,n}, && k = 1, \dots, K,
 \end{aligned}$$

where $R_{max,k} = \frac{1}{c_4} \ln \left(\frac{\tilde{C}_k(t) - T_l P_c^{Rx}}{T_l c_1} \right)$ and the rest of parameters were defined before. The reader may notice the similarities of this problem compared with the problem (3.15). They are, in fact, equivalent in the sense that both problems maximizes the sum-rate and have battery and transmission power constraints. However, the new formulation involves integrity in the assignment process, so the resolution of the problem is completely different.

The addition of the battery constraint through R_{max} complicates the search considerably. However, we present a greedy approach that provides a solution that is close to the optimal one. Two different approaches are presented in next sections. First, a suboptimal allocation is considered where only one modulation type is allowable. This simplification reduces notably the complexity of the algorithm as it will be shown. This algorithm is intended for scenarios where the computational cost is an issue. Then, a totally adaptive RRA algorithm is developed where number of bits loaded per subcarrier is optimized. Simulation results will be presented in future sections.

4.4.1 Single Modulation Type

For complexity reasons, we develop a greedy algorithm where only one modulation type is allowable. In such a case, all the subcarriers are only allowed to have the same number of bits, e.g., 4 bits in case that 16-QAM modulation is selected. As a consequence, the resulting algorithm only performs subcarrier allocation and does not consider bit allocation. The algorithm is simpler, and thus, has low complexity, but it performs worse in terms of sum-rate with respect to the case where the number of bits per carrier is also variable and can be optimized. The proposed greedy RRA algorithm with single modulation type is as follows:

Algorithm 6: Rate adaptive scheme with fixed modulation

```

1: set  $\mathcal{A} = \{1, 2, 3, \dots, N\}$ 
2:    $\mathcal{B} = \{1, 2, 3, \dots, K\}$ 
3:    $\Delta P_{k,n} = \frac{P^{(4)}}{|g_{k,n}(t)|^2} \forall k, n$ 
4:    $P_{k,n} = 0 \forall k, n$ 
5:    $N_k = \lfloor \frac{R_{max,ktOFDM}}{ModLevel} \rfloor \forall k$ 
6: while  $(\sum_{k=1}^K \sum_{n=1}^N P_{k,n} \leq P_{max} - P_c^{tx} \text{ and } \mathcal{B} \neq \emptyset \text{ and } \mathcal{A} \neq \emptyset)$  do
7:    $\tilde{k}, \tilde{n} = \arg \min_{n \in \mathcal{A}, k \in \mathcal{B}} \Delta P_{k,n}$ 
8:    $\rho_{\tilde{k}, \tilde{n}} = 1$ 
9:    $\mathcal{A} \leftarrow \mathcal{A} - \{\tilde{n}\}$ 
10:   $P_{\tilde{k}, \tilde{n}} = \Delta P_{\tilde{k}, \tilde{n}}$ 
11:  if  $(\sum_{n=1}^N \rho_{\tilde{k}, n} == N_{\tilde{k}})$  then
12:     $\mathcal{B} \leftarrow \mathcal{B} - \{\tilde{k}\}$ 
13:  end if
14: end do
15: end algorithm

```

In order to maximize the bit rate, the algorithm must assign the power to the least expensive subcarriers, so that more subcarriers can be assigned and as a result higher sum-rate can be obtained. This is exactly what the algorithm performs. At each iteration, it looks for the subcarrier that requires least power to be assigned the corresponding bits in all users. Then, the selected subcarrier is assigned to the corresponding user. Some updates follow and, finally, the user is disabled if it has achieved the maximum bit rate.

4.4.2 Adaptive Modulation

We saw in the previous section a simple algorithm to assign subcarriers to the users based on a greedy approach. The modulation type was fixed for all subcarriers and as a consequence bit allocation was not performed. In this section we go one step further, and we include bit allocation combined with subcarrier allocation, i.e., each subcarrier may be assigned a different number of bits. However, there exists a constraint on the maximum allowable number of bits per subcarrier. As in real systems, link adaptation is performed over a finite set of modulation types. Due to all this, the algorithm fully exploits all the degrees of freedom and maximizes the objective function.

Due to the nature of the greedy allocation, in a few cases, the algorithm yields to a solution which is far above the optimal one. This is because the greedy procedure assigns resources to the best user at each particular moment without considering future assignments. However, users have a constraint on a maximum bit-rate. Therefore, we could have the situation where the algorithm assigns most of the subcarriers to a given user, making these subcarriers non-eligible for the rest of users. This is not a problem if the user takes good profit of them, but it may happen that the scheduler only assigns one bit per subcarrier and then the user reaches saturation leading to a solution that is far from the optimum. In order to avoid this situation, we develop an algorithm that swaps bits from different subcarriers of a given user in order to leave unselected subcarriers. Of course this swapping procedure may have a cost in the available power, but it allows the scheduler to keep assigning other subcarriers which turns out to increase the sum-rate.

Besides, in order to obtain a fast convergence, we impose a maximum subcarrier assignment to each user based on the maximum bit-rate constraint. This reduces the flexibility of the solution but makes it a little worst (in terms of suboptimality). As always, there exists a trade-off between speed of convergence and better solution. From experimental results, we concluded that the maximum number of subcarriers to be assigned was 1.2 times the number of subcarriers that the scheduler would assign if all subcarriers were to have the maximum constellation size.

The proposed algorithm for this section is as follows:

Algorithm 7: Rate adaptive scheme

```

1: set  $\mathcal{A} = \{1, 2, 3, \dots, N\}$ 
2:    $\mathcal{B} = \{1, 2, 3, \dots, K\}$ 
3:    $\mathcal{A}_k = \emptyset \quad \forall k$ 
4:    $\mathcal{D}_k = \emptyset \quad \forall k$ 
5:    $\mathcal{C}_k = \mathcal{A} \cup \mathcal{A}_k \quad \forall k$ 
6:    $\Delta P_{k,n} = \frac{P(1)}{|g_{k,n}(t)|^2} \quad \forall k, n$ 
7:    $P_{k,n} = 0 \quad \forall k, n$ 
8:    $c_n = 0 \quad \forall n$ 
9:    $\rho_{k,n} = 0 \quad \forall k, n$ 
10:   $N_k = \lfloor \frac{1.2R_{max,k}t_{OFDM}}{MaxModLevel} \rfloor \quad \forall k$ 
11: while  $(\sum_{k=1}^K \sum_{n=1}^N P_{k,n} \leq P_{max} - P_c^{tx} \quad \text{and} \quad \mathcal{B} \neq \emptyset)$  do
12:    $\tilde{k}, \tilde{n} = \arg \min_{k \in \mathcal{B}, n \in \mathcal{C}_k} \Delta P_{k,n}$ 
13:   if  $(\rho_{\tilde{k}, \tilde{n}} == 0)$  then
14:      $\rho_{\tilde{k}, \tilde{n}} = 1$ 
15:      $\mathcal{A} \leftarrow \mathcal{A} - \{\tilde{n}\}$ 
16:      $\mathcal{A}_{\tilde{k}} \leftarrow \mathcal{A}_{\tilde{k}} \cup \{\tilde{n}\}$ 
17:     if  $(|\mathcal{A}_{\tilde{k}}| + |\mathcal{D}_{\tilde{k}}| \leq N_{max}^{\tilde{k}})$  then
18:        $\mathcal{C}_{\tilde{k}} \leftarrow \mathcal{A} \cup \mathcal{A}_{\tilde{k}}$ 
19:     else
20:        $\mathcal{C}_{\tilde{k}} \leftarrow \mathcal{A}_{\tilde{k}}$ 
21:     end if
22:   end if
23:    $c_{\tilde{n}} \leftarrow c_{\tilde{n}} + 1$ 
24:   if  $(c_{\tilde{n}} == MaxModLevel)$  then
25:      $\mathcal{D}_{\tilde{k}} \leftarrow \mathcal{D}_{\tilde{k}} \cup \{\tilde{n}\}$ 
26:      $\mathcal{A}_{\tilde{k}} \leftarrow \mathcal{A}_{\tilde{k}} - \{\tilde{n}\}$ 
27:   end if
28:    $P_{\tilde{k}, \tilde{n}} = \frac{P(c_{\tilde{n}})}{|g_{\tilde{k}, \tilde{n}}(t)|^2}$ 
29:    $\Delta P_{\tilde{k}, \tilde{n}} = \frac{P(c_{\tilde{n}}+1) - P(c_{\tilde{n}})}{|g_{\tilde{k}, \tilde{n}}(t)|^2}$ 
30:    $R_{max, \tilde{k}} \leftarrow R_{max, \tilde{k}} - 1$ 
31:   if  $(R_{max, \tilde{k}} == 0)$  then
32:      $\mathcal{B} \leftarrow \mathcal{B} - \{\tilde{k}\}$ 
33:   end if
34:   if  $(\mathcal{A} = \emptyset)$  then
35:     if  $(\mathcal{A}_k = \emptyset, \forall k \in \mathcal{B})$  then
36:       swappPossible  $\leftarrow$  run swapping algorithm

```

```

37:         if (swappPossible ==0) then
38:             go to 43
39:         end if
40:     end if
41: end if
42: end do
43: end algorithm

```

Due to its simplicity and similarity with the previous algorithm, we consider that no extra explanation is needed. Just to clarify, notice that the swapping algorithm is only called if some power remains unused and if the available users have no subcarrier assigned to them. Under this situation, the algorithm would not be able to continue since there is no available subcarriers. However, there is still power to be assigned. Thus, a possible strategy should be to sacrifice some power by moving bits from one subcarrier to another within a user. A more complete swapping would be to move bits from different subcarriers and different users, but in a system with a considerable number of subcarriers and users, this search becomes prohibitively in terms of time and computational cost. Therefore, we consider only the case where the swapping of bits is done within a user.

The swapping algorithm works as follows. First, it finds the subcarrier that has least number of bits assigned. Then, it looks for the user assigned to this subcarrier. Later, for the given user, it computes the power cost of adding the bits of the selected subcarrier to another subcarrier that will yield to a least power cost operation. If this power is affordable, then it proceeds with the swapping. If the cost of power was too high, then it moves to the next subcarrier with least bits uploaded.

In the case where the swapping was not possible, then, the main RRA algorithm ends. At this point, we consider the solution to be the best possible solution under this greedy approach.

The proposed swapping algorithm is shown below.

4.5 Simulation Results

In this section we present simulation results related to the previous RRA problems. From now on, we will refer as greedy-SREE to problem (4.9) (with two version: single and adaptive

modulation), and greedy-maximinEE to problem (4.8).

Algorithm 8: Swapping algorithm

```

1: set  $\mathcal{S} = \{1, 2, 3, \dots, N\}$ 
2:   swappPossible = 0
3: while ( $\mathcal{S} \neq \emptyset$ ) do
4:    $n^* = \arg \min_{n \in \mathcal{S}} c_n$ 
5:    $k^* = \arg_k \rho_{k,n^*} = 1$ 
6:    $\hat{n} = \arg \min_{n \in \mathcal{A}_{k^*} \cap n^*, c_n + c_{n^*} \leq \text{MaxModLevel}} \frac{P(c_n + c_{n^*}) - P(c_n)}{|g_{k^*,n}(t)|^2}$ 
7:   if ( $\sum_{k=1}^K \sum_{n=1}^N P_{k,n} - P_{k^*,n^*} + \frac{P(c_{\hat{n}} + c_{n^*})}{|g_{k^*,\hat{n}}(t)|^2} \leq P_{max} - P_c^{tx}$ ) then
8:      $c_{\hat{n}} \leftarrow c_{\hat{n}} + c_{n^*}$ 
9:      $c_{n^*} = 0$ 
10:     $P_{k^*,n^*} = 0$ 
11:     $P_{k^*,\hat{n}} = \frac{P(c_{\hat{n}})}{|g_{k^*,\hat{n}}(t)|^2}$ 
12:     $\mathcal{A} \leftarrow \mathcal{A} \cup \{n^*\}$ 
13:     $\mathcal{A}_{k^*} \leftarrow \mathcal{A}_{k^*} - \{n^*\}$ 
14:    swappPossible = 1
15:    go to 20
16:  else
17:     $\mathcal{S} \leftarrow \mathcal{S} - \{n^*\}$ 
18:  end if
19: end do
20: end algorithm

```

Table 4.2 depicts all the simulation parameters considered in the model. The values of the parameters concerning the RF blocks were extracted from [CUI]. We consider an exponential model for energy consumption of baseband signal processing algorithms where all users have the same algorithms implemented, although similar results could have been obtained following other consumption models. Additionally, simulations using a different value of the parameter α are shown. Initial level of batteries are assigned randomly between a minimum value, 1000 mAh, and a maximum value, 15000 mAh. This means that some users may have the same initial battery. Besides, we assume the maximum capacity level C_{max}^k is two times the initial value, thus, users start the reception with half of its total battery capacity.

Let us start with the simulation results concerning the greedy-maximinEE. The simulations were performed with 50 users in the system and 500 channel realizations. Fig. 4.2 depicts the evolution of the battery of 10 random users. As it is expected, and due to the nature of the maximin problem, all users will tend to finish with the same battery level.

Table 4.2: Simulation parameters

Parameter	Value
Central frequency	2 GHz
Number of sub-carriers	192
Sub-carrier spacing Δf	15 KHz
FFT points	256
Cyclic prefix length	64 samples
Number of filter taps	64
Delay Spread	0.5 μs
Standard deviation shadowing σ	8 dB
Noise figure ν	9 dB
Frame duration	10 ms
Time-slot duration T_l	0.5 ms
BER	10^{-3}
Maximum BS transmission power	1 W
P_{mix}	30 mW
$P_{filt} = P_{filtr}$	2.5 mW
P_{LNA}	20 mW
P_{syn}	50 mW
P_{IFA}	3 mW
$P_{ADC} = P_{DAC}$	60 mW
Energy packet size E	100 mAh
Battery capacity level	$1000 \leq C_{max}^k \leq 15000$ [mAh]
Channel model	Rayleigh frequency-selective
Noise power N_0	$-174 \text{ dBm} + 10 \log_{10}(\Delta f) + \nu$
Decoder constant c_1	200000
Decoder constant c_4	4.83e-6
Energy allocation parameter α	0.1 and 0.01
Mobile terminal speed	static
Number of channel realizations	500

This is so since, at the beginning of the frame, the users with the greatest level of battery are served with more resources. When the time evolves, this problem tends to stabilize all battery levels, since the users first selected will let other users obtain more resources.

Fig. 4.3 shows the evolution of the sum-rate of the greedy-maximinEE approach when the number of users increases. The saturation experienced in this approach when the number of users is high is a feature of all these practical algorithms. This is so due to the nature of the finite-size constellation design and it will be noticeable in the other approaches as well.

Now we focus on the rate adaptive scheme. Fig. 4.4 provides a simple but powerful representation of the behavior of the fully adaptive greedy-SREE. The figure shows a single channel realization with 4 users and 50 subcarriers in the system. The maximum constellation

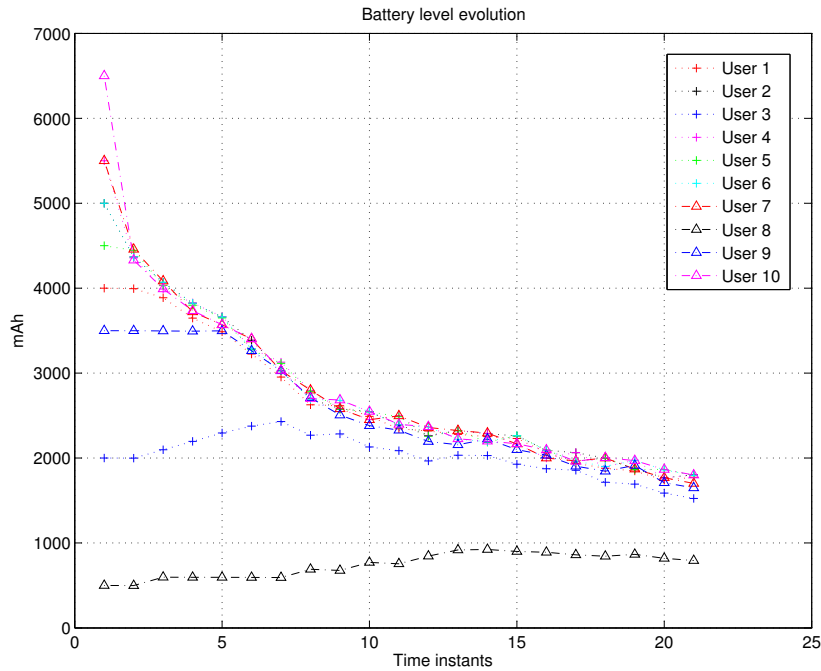


Figure 4.2: Battery evolution of the maximin problem.

size corresponds to 5 bits per subcarrier, that is, 32-QAM. For clarity, it is also expressed the maximum number of subcarriers and bits due to battery constraints. As it is observed, whenever the user has a good channel gain in the corresponding frequency band, subcarriers are assigned. The number of bits depends on the remaining power and the level of the channel gain. For example, user 1 (starting from the top) has the best last subcarriers, so they are assigned to it. However, the channel gain is quite low, thus, only one bit to each subcarrier is assigned, even though it has more bits available. This must be so due to power constraints. Second user has the best first subcarriers and their channel gain is high. As a consequence, the maximum number of bits (19 in this case) were distributed among the 4 assigned subcarriers.

The behavior of the single modulation greedy-SREE is similar to the adaptive one. However, the number of bits per subcarrier is fixed and the results are more intuitive. If a user has good channel gain, a specific subcarrier will be assigned with a fixed number of bits.

Fig. 4.5 shows the evolution of the sum rate and the percentage of battery usage averaged among all users. It can be observed that the fully adaptive approach outperforms the single modulation scheme in both modes of operations ($\alpha = 0.1$ and $\alpha = 0.01$). Notice that the loss in sum rate by using the single modulation type allocation is not very high. Therefore, in real time applications it would be acceptable to assign equal number of bits for all subcarriers. In terms of energy savings, Fig. 4.5(b), in general sense, we have that the higher the number of users, the lower average battery usage we have. This is due to the fact that if there is a

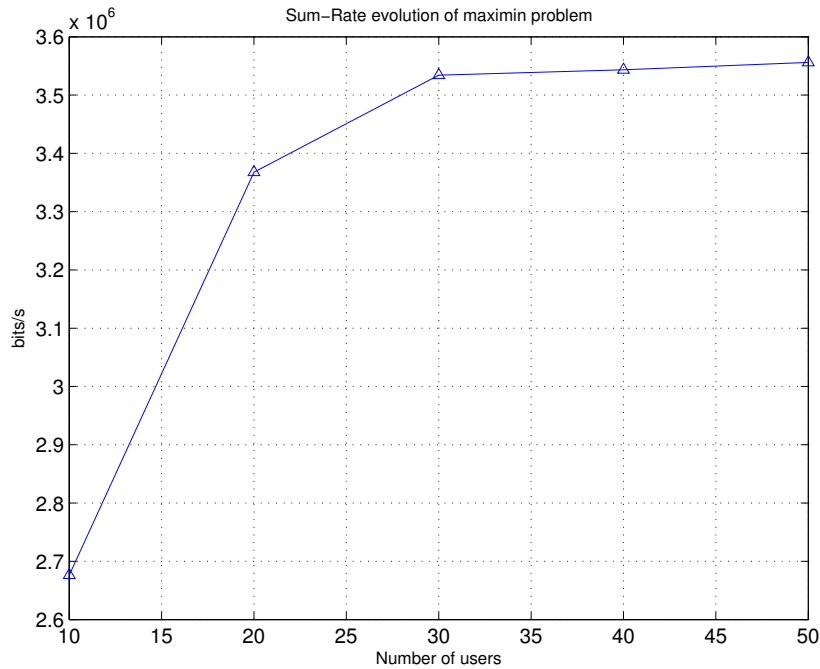


Figure 4.3: Sum-rate evolution of the maximin problem.

high number of users in the system, at least some of them would be served with very little resources or even with no resources, since the objective is to maximize the sum rate. This is the case of users placed far from the BS. Notice, however, that the behavior matches the results found in the previous chapter.

The following two figures, Fig. 4.6 and Fig. 4.7, depicts the battery evolution of the single and adaptive modulation greedy-SREE schemes. The results are similar than the ones obtained in the previous chapter. If the number of users is high, the battery level tends to keep stable for some users and decrease a little for others. It depends on how they contribute to the sum rate and also on the harvesting source. In general, if there are few users in the system, the battery spent by receivers can be controlled using the parameter α as it can be observed from the figures. There exists a small difference in energy savings between the single and fully adaptive scheme. The latter makes the users consume a small fraction more than the single scheme. This phenomenon is more significant when α is set to 0.1. It can be appreciated carefully in some figures.

The following two tables, Table 4.3 and Table 4.4, show the execution time comparison between the greedy approaches presented in the rate adaptive schemes and the optimal procedure¹. The last ones has been computed trying all the possible combinations. They have been generated with 4 users, and for the case of adaptive greedy-SREE, 3 different types of

¹The execution time depends on the computer used for the simulations, but the results are only intended for comparison purposes.

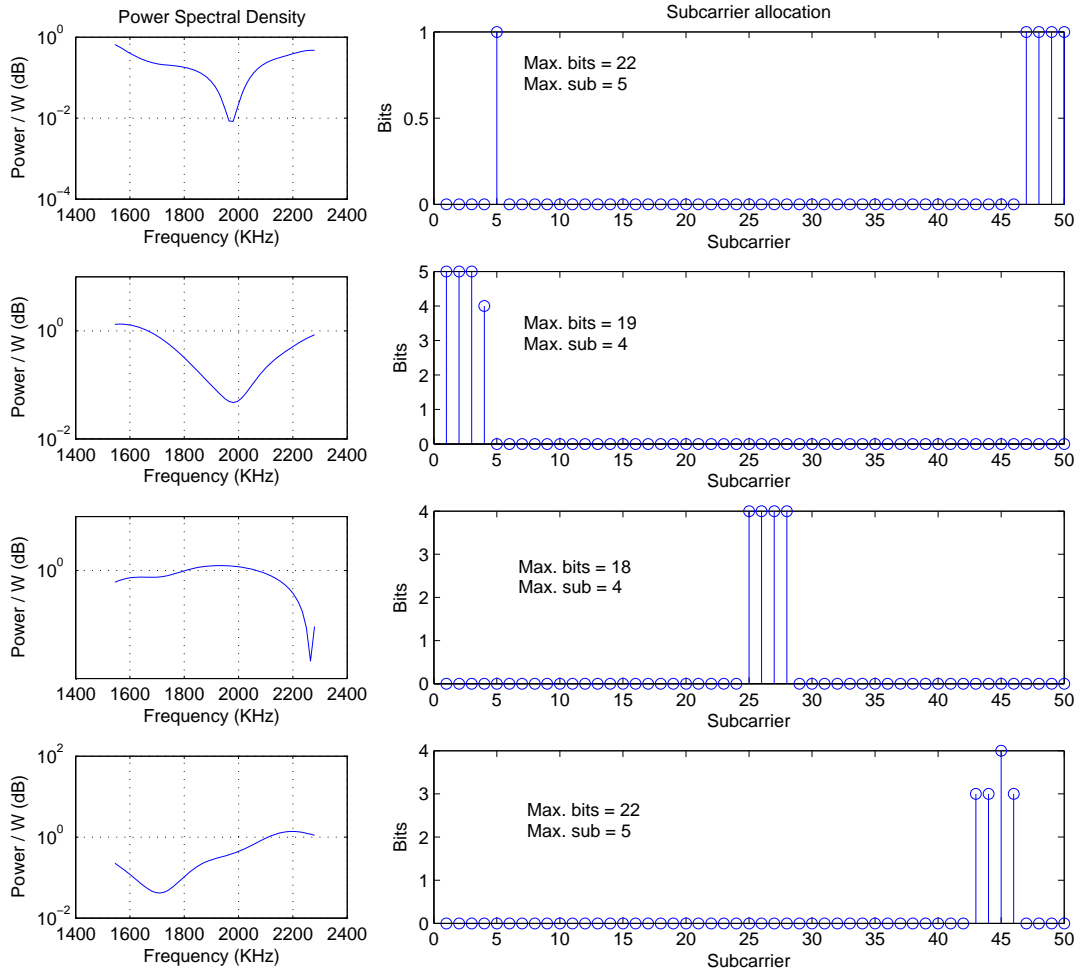


Figure 4.4: Example of resource allocation of the adaptive modulation greedy algorithm.

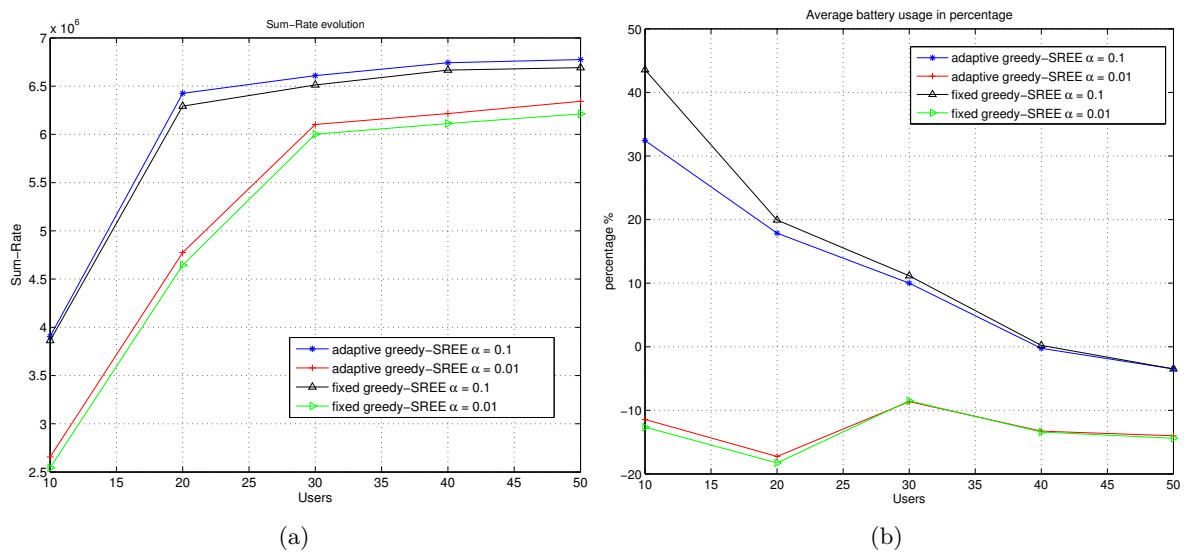


Figure 4.5: (a) Sum rate evolution. (b) Average percentage of battery level spent by users (a negative percentage means a gain in battery level).

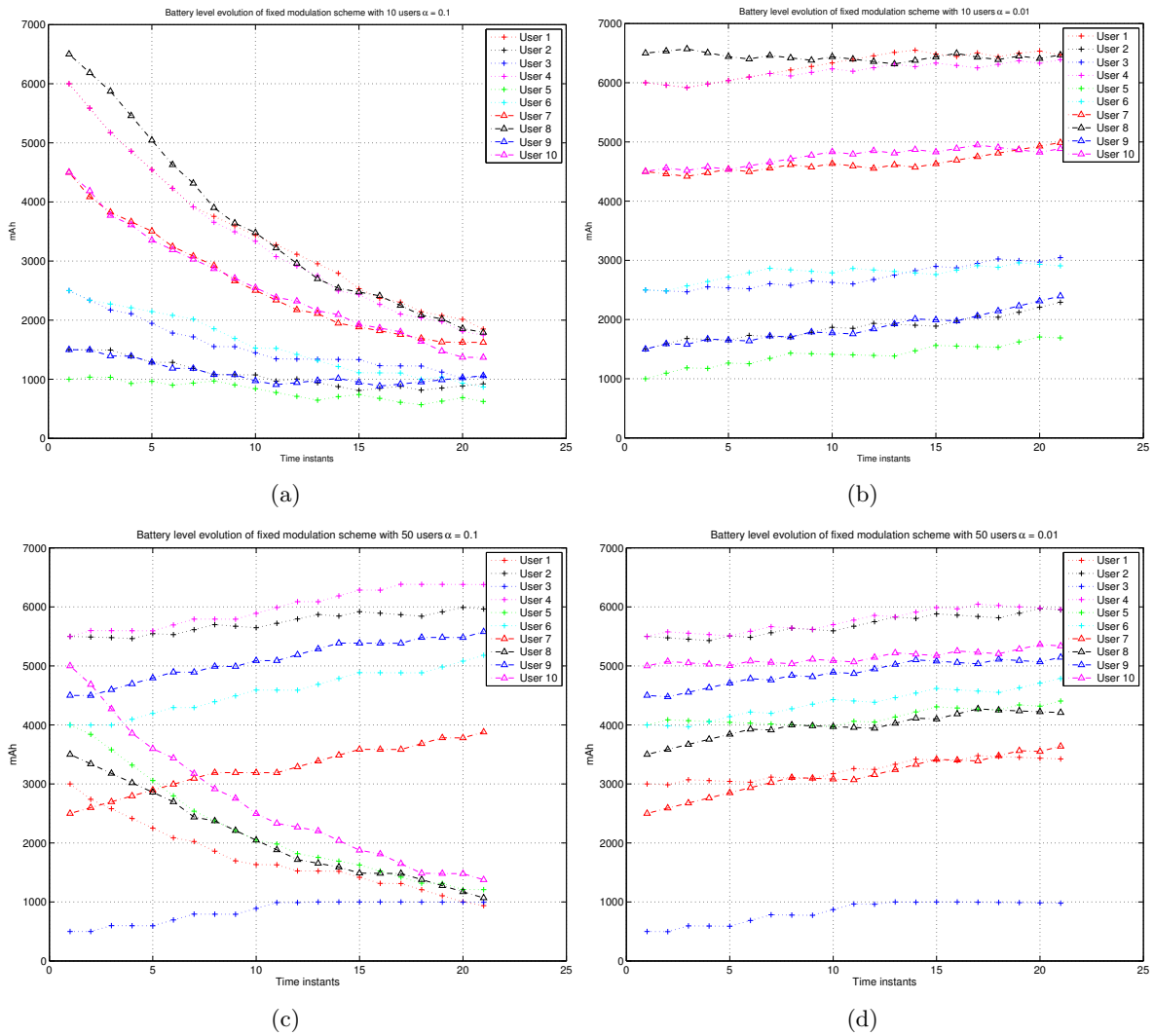


Figure 4.6: Battery evolution of single modulation greedy-SREE scheme (a) System with 10 users and $\alpha = 0.1$. (b) System with 10 users and $\alpha = 0.01$. (c) System with 50 users and $\alpha = 0.1$. Only ten random users are depicted. (d) System with 50 users and $\alpha = 0.01$. Only ten random users are depicted.

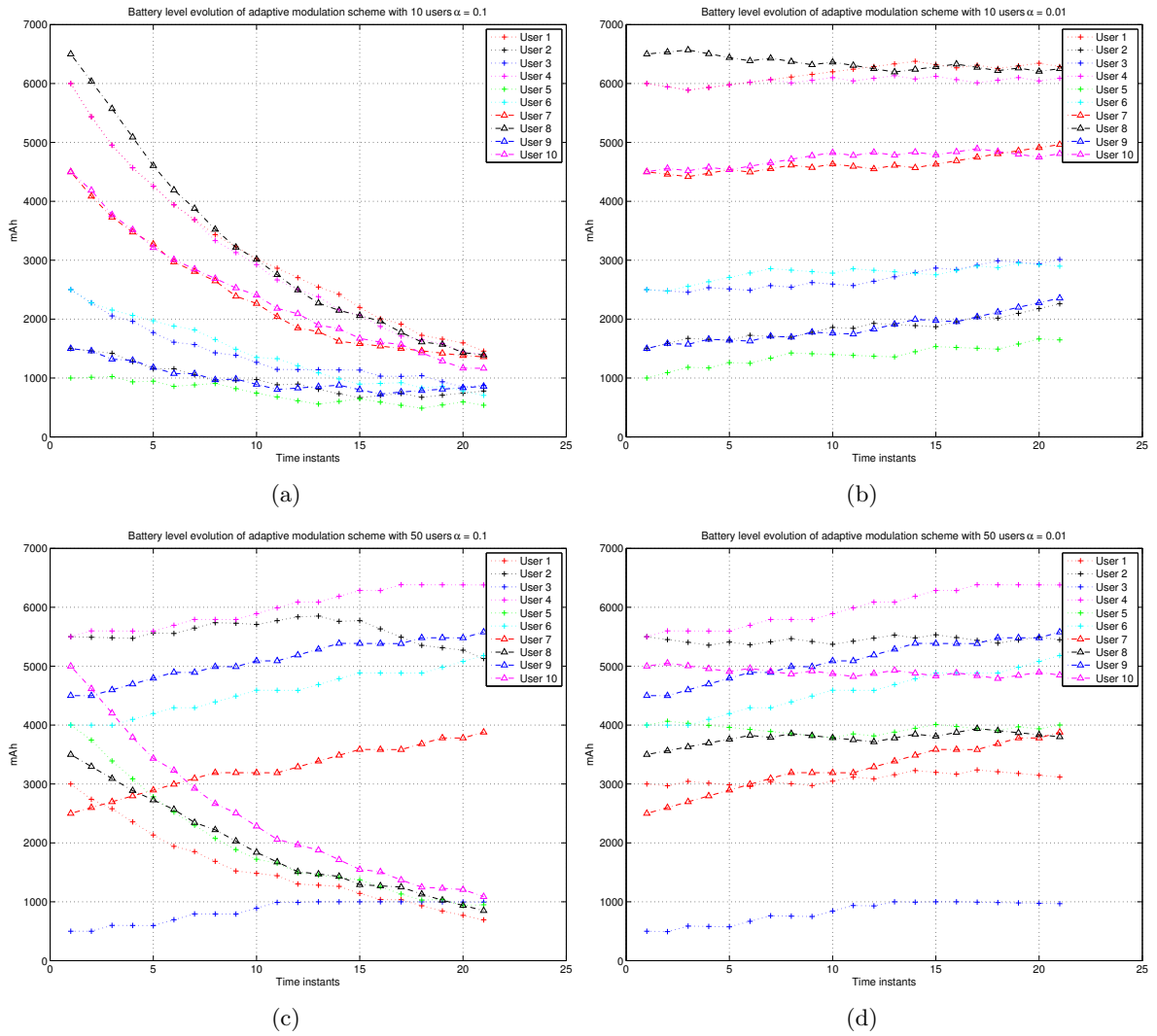


Figure 4.7: Battery evolution of adaptive modulation greedy-SREE scheme (a) System with 10 users and $\alpha = 0.1$. (b) System with 10 users and $\alpha = 0.01$. (c) System with 50 users and $\alpha = 0.1$. Only ten random users are depicted. (d) System with 50 users and $\alpha = 0.01$. Only ten random users are depicted.

modulations were considered.

Table 4.3: Time of execution of optimum and greedy algorithms with single modulation

# subcarriers	# combinations	time (optimum)	time (greedy)
2	25	10 ms	130 μ s
4	625	330 ms	200 μ s
6	15625	10 sec	270 μ s
8	390625	4.5 min	340 μ s
10	9.7×10^6	132 min	410 μ s
100	5×10^{100}	37 days	3.8 ms

Table 4.4: Time of execution of optimum and greedy algorithms with adaptive modulation

# subcarriers	# combinations	time (optimum)	time (greedy)
2	169	90 ms	3.2 ms
4	28561	20 sec	3.4 ms
6	4826809	80 min	3.7 ms
8	8×10^8	12 days	4.1 ms
10	1.4×10^{11}	7.5 years	4.3 ms
100	13×10^{100}	70000 years	14.1 ms

As it can be observed, the difference in execution time between the optimal and greedy approaches is extremely high. In the case of adaptive greedy-SREE, in a system with only 4 users and 10 subcarriers, the scheduler will last 7.5 years before finding the solution. It is, thus, inevitable to develop suboptimal strategies that computes the solution in a reasonable time.

4.6 Chapter Summary and Conclusions

In this chapter, practical greedy-like RRA algorithms have been presented for a broadcast multi-user scenario in short-distance networks. The allocation consisted in bit loading, power allocation and subcarrier assignment. Nodes were considered to be battery-powered devices provided with energy harvesting sources. This chapter was an extension of the previous chapter, now including realistic and practical features on the allocation, such as for example finite constellation size.

Two different resource allocation problems were considered. First, an energy adaptive scheme was addressed. In this case, the objective function was the maximization of the minimum residual battery level after the allocation. Then, two rate adaptive schemes were presented. A simplified version using single modulation was derived. This simplification yielded to a simple subcarrier assignment algorithm that performs very well as it was shown

in simulation results. An adaptive modulation resource allocation was also developed. For this case, an extension algorithm that swaps bits within a user was implemented in order to approach the optimum in some cases.

Simulations results showed similar results to the ones obtained in the previous chapter. For the maximin formulation, we had that all users tend to end up with the same battery level. For the rate adaptive schemes, we found that by controlling the amount of available energy for the allocation we were able to increase the network lifetime, letting users with low battery level use low resources and increase its level through the harvesting procedure.

4.A Appendix: System and Simulation Modeling

This appendix presents the system modeling that was considered in the formulation of the RRA techniques proposed in this chapter. The appendix is organized as follows. §4.A.1 presents how the users are distributed along the cell. Propagation models of the wireless channel are described in §4.A.2. Finally, §4.A.3 shows the procedure to calculate channel gain for each user at each sub-carrier.

4.A.1 User Distribution

In the downlink scenario proposed in this thesis, the users are uniformly distributed over the circular coverage area of the BS, as depicted in Fig. 4.8. In this particular example, 100 users are distributed through the cell and the BS is placed at the center of it. For the sake of simplicity, sectors will not be considered in this thesis. The radius of the cell is chosen to be 50 meters, which corresponds to range between picocell and femtocell deployment architecture.

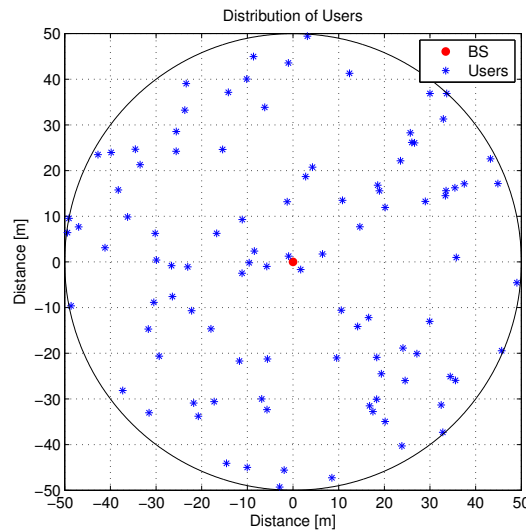


Figure 4.8: Uniformly distributed users

4.A.2 Propagation

Path Loss

The path loss follows the model proposed in [46] for a test scenario in urban and suburban areas. Considering a 2 GHz carrier frequency and a mean BS antenna height of 15 m, the

equation of the path loss L_j^{path} in dB as a function of the distance d between the BS and the j -th user in km is presented as follows:

$$L_j^{\text{path}} = 128.1 + 37.6 \log_{10} d. \quad (4.10)$$

The theoretical path loss given by (4.10) is plotted in Fig. 4.9(a).

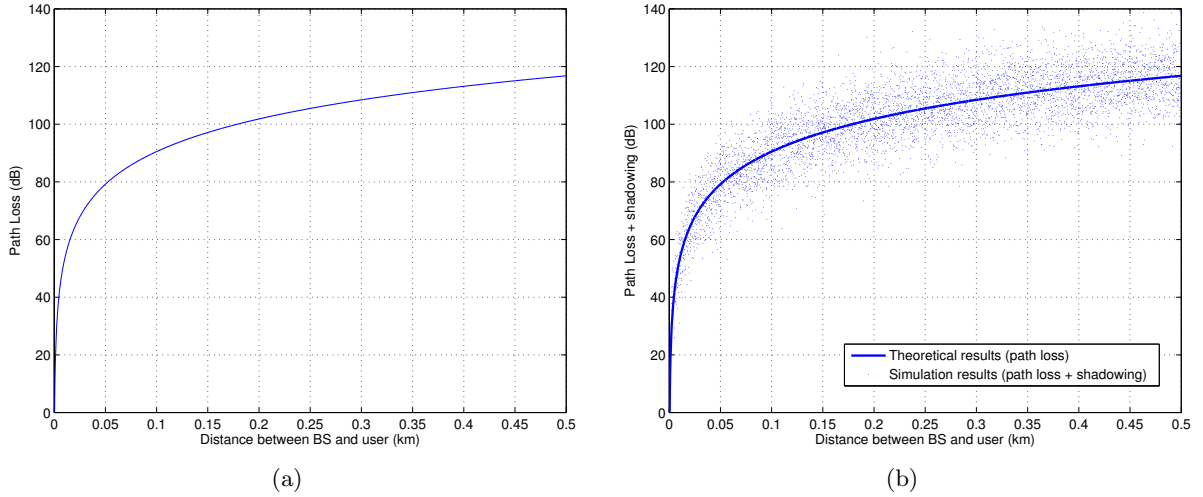


Figure 4.9: (a) Path loss. (b) Path loss + shadowing.

Large-Scale Fading

The modeling of the large-scale fading used in this thesis is the well-known zero-mean log-normal shadowing fading model characterized by a given standard deviation [ref]. Assuming that the standard deviation is σ dB, we have that the shadowing fading with respect to the j -th user is defined as $L_j^{\text{shadow}} \sim N(0, \sigma^2)$ (in dB), being $N(0, \sigma^2)$ a normal random variable with zero mean and a standard deviation equal to σ .

Fig. 4.9(b) shows how the path gain composed of path loss and shadowing deviates from the theoretical path loss model. These simulation samples were taken using a log-normally distributed shadowing with standard deviation of 8 dB.

Small-Scale Fading

In this thesis, we assume that the small-scale fading (fast fading) follows a Rayleigh distribution. Rayleigh fading is a reasonable model when there are many objects in the environment

and there is no dominant propagation along a Line of Sight (LOS) between the transmitter and receiver. For LOS models, Rician distributions should be considered.

If the number of scatterers is sufficiently high, the central limit theorem can be invoked and the channel impulse response can be modeled as a Gaussian process irrespective of the distribution of the individual components. There are multiple ways to generate the Rayleigh fading. The approach followed in this thesis is by means of an exponential Power Delay Profile (PDP). The PDP relates the power intensity between channel coefficients as a function of time delay, being the time delay the difference in travel time between multipath arrivals. The mathematical expression of the exponential PDP with K multipath arrivals is

$$PDP(\tau) = \frac{e^{-\frac{\tau}{\mu}}}{\sum_{k=1}^K e^{-\frac{\tau_k}{\mu}}}, \quad (4.11)$$

where μ is the Delay Spread (DS) of the multipath channel [22]. In the remainder of this appendix, we represent the fast fading gain of the j -th user in the k -th sub-carrier as $L_{j,k}^{\text{fast}}$ (in dB).

4.A.3 Channel Gain Calculation

Taking into account the propagation losses described in previous section, we are able to compute the channel coefficients that appear in the system model. The idea is to obtain the α coefficients that are user and sub-carrier-dependent. Thus, for the j -th user at the k -th sub-carrier, the channel gain in dB can be expressed as

$$|g_{j,k}(t)|_{\text{dB}}^2 = -L_j^{\text{path}} - L_j^{\text{shadow}} + L_{j,k}^{\text{fast}}, \quad (4.12)$$

and in linear magnitudes we have that

$$|g_{j,k}(t)|^2 = 10^{(-L_j^{\text{path}} - L_j^{\text{shadow}} + L_{j,k}^{\text{fast}})/10}. \quad (4.13)$$

Chapter 5

Conclusions and Future Work

5.1 Conclusions

This thesis has considered the radio resource allocation design in a broadcast scenario in short-distance networks with battery-powered nodes provided with energy harvesting sources.

A motivation and introduction of the thesis was presented in Chapter 1, jointly with an outline of the work.

Chapter 2 presented a brief description of the main convex optimization theory tools used along the thesis. Besides, an overview of the classical resource allocation mechanisms, describing the most commonly techniques used, was presented.

Chapter 3 was devoted to the design of radio resource allocation algorithms for efficient battery management of wireless nodes. Models of RF circuitry and baseband signal processing power consumption were presented. We concluded that only the signal processing techniques are bit-rate dependent. For simplicity, only the power spent by decoders was considered. Two different models, linear and exponential models, associated with the dependency on the bit-rate were taken for the signal processing and baseband stages. Moreover, it was assumed that nodes were provided with a energy harvesting source able to collect energy from the environment. Battery status level and harvesting information were given to the base station to allocate resources in a more efficient way. Simulations were carried out considering flat-fading channels and the information rate provided by the Shannon's formula. As a consequence, continuous power, bandwidth and rate allocation were implemented. We developed an iterative algorithm for a suboptimal case where all the transmission bandwidths

were fixed. It showed good performance compared with the optimum approach and it was much faster in terms of convergence speed. Looking at the battery level evolution, we were able to control the user lifetime by means of assigning more or less resources to users with good battery status. Comparing the presented algorithm with the traditional approaches, it showed a gain in both average bit-rate and a longer network lifetime by far.

Chapter 4 extended the formulation presented in previous chapter. The main difference was that finite-size constellations and frequency-selective channels were included in the design. The latter condition made the subcarrier assignment univocal to the users. Greedy-like dynamic subcarrier allocation, bit loading and power adaptation algorithms were developed for different radio resource allocation policies. Terminals kept the same configuration as before, and battery status information was available to the base station as well. As a consequence, simulation results were considerably similar to the results obtained in previous chapter, but now, the allocation was more realistic and practical for implementation.

5.2 Future Work

There are several lines of research that can extend the work carried out in this thesis:

- Introduction of MIMO technology in both sides of communications, since MIMO technology has emerged as one potential technique for future wireless communication system.
- To consider the whole design of the multiple parallel relay channel, from the source node to the intermediate relays and then from the relays to the destination node, in order to minimize the battery usage of the relays.
- In mobile networks, cooperation between base stations may be considered in order to maximize the network lifetime.
- Incorporating the information of the battery status in the feedback channel is a must for the allocation. As a consequence, new design strategies should include it, as a single parameter, or jointly with the channel state information.

Bibliography

- [1] A. Perez A. Pascual, D. Palomar and M.A. Lagunas. A robust maximin approach for mimo communications with imperfect channel state information based on convex optimization. *IEEE Trans. on Signal Processing*, 54(1):346–360, 2006.
- [2] Tomasin S. Erkip E. Bakanoglu, K. Resource allocation for the parallel relay channel with multiple relays. *IEEE Trans. on Wireless Communications*, 22(6):792–802, 2011.
- [3] E. V. Belmega and S. Lasaulce. Energy-efficient precoding for multiple-antenna terminals. *IEEE Trans. on Signal Processing*, 59(1):329–340, 2011.
- [4] Lasaulce S. Debbah M. Belmega, E. A survey on energy-efficient communications. In *IEEE International Symposium on Personal, Indoor and Mobile Radio Communications*, pages 289–294, 2010.
- [5] J. A. C. Bingham. Multicarrier modulation for data transmission: an idea whose time has come. 28(5):5–14, 1990.
- [6] S. Boyd. cvx software package. <http://cvxr.com/cvx/download/>.
- [7] S. Boyd and L. Vandenbergue. *Convex optimization*. Cambridge, first edition, 2004.
- [8] K. Letaief C. Wong, R. Cheng and R. Murch. Multiuser ofdm with adaptive subcarrier, bit and power allocation. *IEEE Journal on Selected Areas in Communications*, 17(10):1747–1758, 1999.
- [9] Andrwes J. Chandrasekhar, V. Femtocell networks: a survey. *IEEE Communications Magazine*, september:59–67, 2008.
- [10] L. J. Cimini. Data transmission by frequency-division multiplexing using the discrete fourier transform. 33(7):665–675, 1985.
- [11] Goldsmith A. Bahai A. Cui, S. Power estimation for viterbi decoders. In *Report, Stanford University*, 2003.

- [12] Goldsmith A. Bahai A. Cui, S. Joint modulation and multiple access optimization under energy constraints. In *IEEE Globecom*, 2004.
- [13] Goldsmith Bahai A. Cui, S. Energy-constrained modulation optimization. *IEEE Trans. on Wireless Communications*, 4(5):2349–2360, 2005.
- [14] Goldsmith Lall S. Cui, S. Cross-layer energy and delay optimization in small-scale sensor networks. *IEEE Trans. on Wireless Communications*, 6(10):3688–3699, 2007.
- [15] J.M. Cioffi D. Palomar and M.A. Lagunas. Joint tx-rx beamforming design for multi-carrier mimo channels: a unified framework for convex optimization. *IEEE Trans. on Signal Processing*, 51(9):2381–2401, 2003.
- [16] M. Ehrgott. *Multicriteria optimization*. Springer Verlag, 2005.
- [17] A. Zappone et al. Energy-efficient non-cooperative resource allocation in multi-cell ofdma systems with multiple base station antennas. In *IEEE Online Conference on Green Communications*, pages 82–87, 2011.
- [18] C. Xiong et al. Energy-efficient resource allocation in ofdma networks. In *IEEE Globecom*, 2011.
- [19] K. Eriksson et al. Globally optimal resource allocation for achieving maximum weighted sum rate. In *IEEE Globecom*, pages 1–6, 2010.
- [20] P. C. Weeraddana et al. Adaptive subcarrier and power allocation for ofdma systems. In *Wireless Days*, pages 1–5. IEEE, 2008.
- [21] H. V. Poor F. Meshkati and S. C. Schwartz. Energy-efficient resource allocation in wireless networks: an overview of game theoretic approaches. *IEEE Signal Processing Magazine*, may:58–68, 2007.
- [22] A. Goldsmith. *Wireless communications*. Cambridge University Press, 2005.
- [23] J. Gross and M. Bohge. Dynamic mechanisms in ofdm wireless systems: a survey on mathematical and system engineering contributions. In *Report, Technical University Berlin*, 2006.
- [24] Woyach K. Sahai A. Grover, P. Towards a communication-theoretic understanding of system-level power consumption.
- [25] Zhang R. Ho, C. Optimal energy allocation for wireless communications with energy harvesting constraints. *IEEE Trans. on Signal Processing*, To be published.
- [26] Mathworks Inc. Matlab. <http://www.mathworks.es/products/matlab/>.

- [27] J. Jang and K. B. Lee. Transmit power adaptation for multiuser ofdm systems. *IEEE Journal on Selected Areas in Communications*, 21(2):171–178, 2003.
- [28] C. Jiang and L. J. Cimini. Energy-efficient multiuser mimo beamforming. In *IEEE Annual Conference on Information Sciences and Systems*, pages 1–5, 2011.
- [29] P. Chow K. Sistanizadeh and J. Cioffi. Multi-tone transmission for asymmetric digital subscriber lines. In *IEEE International Communication Conference*, pages 756–760, 1993.
- [30] Kwak J. Kim, R. Wimax femtocell: requirements, challenges and solutions. *IEEE Communications Magazine*, september:84–91, 2009.
- [31] D. Kivanc and H. Liu. Subcarrier allocation and power control for ofdma. In *Conference on Signals, Systems and Computers*, pages 147–151, 2000.
- [32] Sofoklis A. Kyriazakos and George T. Karetsos. *Practical radio resource management in wireless systems*. Artech House, 2004.
- [33] G. et al. Li. Energy-efficient wireless communications: tutorial, survey and open issues. *IEEE Wireless Communications*, december:28–35, 2009.
- [34] Himayat N. Li Y. Miao, G. Energy-efficient transmission in frequency-selective channels. In *IEEE Globecom*, 2008.
- [35] Himayat N. Li Y. Bormann D. Miao, G. Energy-efficient design in wireless ofdma. In *IEEE International Communication Conference*, pages 3307–3312, 2008.
- [36] Himayat N. Li Y. Talwar S. Miao, G. Energy-efficient transmission in frequency-selective channels. In *IEEE International Communication Conference*, 2008.
- [37] M. Moretti. A novel dynamic subcarrier assignment scheme for multiuser ofdma systems. In *IEEE Vehicular Technology Conference*, pages 2109–2113. IEEE, 2006.
- [38] R. Prasad. *OFDM for wireless communications systems*. Artech House, 2004.
- [39] J. Proakis. *Digital communications*. McGraw-Hill, fifth edition, 2008.
- [40] I. Santamaria R. Eickhoff, R. Kraemer and L. Gonzalez. Developing energy-efficient mimo radios. *IEEE Vehicular Technology Magazine*, march:329–340, 2009.
- [41] W. Rhee and J. M. Cioffi. Increase in capacity of multiuser ofdm system using dynamic subchannel allocation. In *IEEE Vehicular Technology Conference*, pages 1085–1089, 2000.

- [42] H. Rohling and R. Grunheid. Performance comparison of different multiple access schemes for the downlink of an ofdm communication system. In *IEEE Vehicular Technology Conference*, pages 1365–1369, 1997.
- [43] Fettweis G. Rost, P. On the transmission-computation-energy tradeoff in wireless and fixed networks. In *IEEE Globecom 2010 workshop en Green Communications*, pages 1934–1939, 2010.
- [44] A. Goldsmith S. Cui and A. Bahai. Energy-efficiency of mimo and cooperative mimo techniques in sensor networks. *IEEE Journal on Selected Areas in Communications*, 22(6):1089–1098, 2004.
- [45] L. Cuthbert T. Zhang, S. Zhao and Y. Chen. Energy-efficient cooperative relay selection scheme in mimo relay cellular networks. In *IEEE International Conference on Communication Systems*, pages 269–273, 2010.
- [46] UMTS. Selection procedures for the choice of radio transmission technologies of the umts. In *Tech. Rep. TR 101 112 V3.2.0 - UMTS 30.03, Universal Mobile Telecommunications System (UMTS), Sophia Antipolis, France*, 1998.
- [47] S. Verdu. On channel capacity per unit cost. *IEEE Trans. on Information Theory*, 36(5).
- [48] S. B. Weinstein and P. M. Ebert. Data transmission by frequency-division multiplexing using the discrete fourier transform. 19(5):628–634, 1971.
- [49] J.-W. Chen Y.-F. Chen and C. P. Li. A real-time joint subcarrier, bit, and power allocation scheme for multiuser ofdm-based systems. In *IEEE Vehicular Technology Conference*, pages 1826–1830. IEEE, 2004.
- [50] L. Yang Y. Hu, Y. Huang and J. Zhou. Energy-efficient resource allocation in multi-user ofdma systems. In *IEEE International Conference on Wireless Communications and Signal Processing*, pages 1–5, 2011.
- [51] Ozel O. Ulukus S. Yang, J. Broadcasting with an energy harvesting rechargeable transmitter. *IEEE Trans. on Wireless Communications*, 11(2):571–583, 2012.
- [52] W. Yu and R. Lui. Dual methods for nonconvex spectrum optimization of multicarrier systems. *IEEE Trans. on Communications*, 54(7):1310–1322, 2006.
- [53] G. Andrews Z. Shen and B. L. Evans. Optimal power allocation in multiuser ofdm systems. In *IEEE Globecom*, pages 337–341, 2003.